Response to Bernd Souw Attachment to the February 11, 2004 Office Action in U.S. 09/009,837

For the convenience of the Examiner, this Response will retain the references numbers and validation points consistent with those given in the attached document entitled "**Lower-Energy Hydrogen Experimental Data**."

Applicant has published over 50 articles in reputable, peer-reviewed journals and has submitted over 100 which Applicant is confident will eventually be published materially in their present form. These articles detail studies that experimentally confirm a novel reaction of atomic hydrogen, which produces hydrogen in fractional quantum states that are at lower energies than the traditional "ground" ($n = 1$) state, a chemically generated or assisted plasma (rt-plasma), and novel hydride compounds, including:

extreme ultraviolet (EUV) spectroscopy[1],
characteristic emission from catalysis and the hydride ion products[2],
lower-energy hydrogen emission[3],
plasma formation[4],
Balmer α line broadening[5],
population inversion of hydrogen lines[6],
elevated electron temperature[7],
anomalous plasma afterglow duration[8],
power generation[9],
excessive light emission[10],
analysis of chemical compounds[11], and

---

[1] Reference Nos. 11-16, 20, 24, 27-29, 31-36, 39, 42, 43, 46-47, 50-52, 54, 55, 57, 59, 63, 65-68, 70-76, 78, 79, 81, 83, 85, 86, 89, 91-93, 95-96, 98, 101, 104

[2] Reference Nos. 24, 27, 32, 39, 42, 46, 51, 52, 55, 57, 68, 72, 73, 81, 89, 91

[3] Reference Nos. 14, 28, 29, 33-36, 50, 63, 67, 70, 71, 73, 75, 76, 78, 79, 86, 87, 90, 92, 93, 98, 101, 104

[4] Reference Nos. 11-13, 15, 16, 20, 24, 27, 32, 39, 42, 46, 47, 51, 52, 54, 55, 57, 72, 81, 89, 91-93

[5] Reference Nos. 16, 20, 30, 33-37, 39, 42, 43, 49, 51, 52, 54, 55, 57, 63-65, 68, 69, 71-74, 81-85, 88, 89, 91-93, 95-97, 105

[6] Reference Nos. 39, 46, 51, 54, 55, 57, 59, 65, 66, 68, 74, 83, 85, 89, 91

[7] Reference Nos. 34-37, 43, 49, 63, 67, 73

[8] Reference Nos. 12, 13, 47, 81

[9] Reference Nos. 30, 31, 33, 35, 36, 39, 43, 50, 63, 71-73, 76, 77, 81, 84, 89, 92, 93, 98

[10] Reference Nos. 11, 16, 20, 23, 31, 37, 43, 52, 72

[11] Reference Nos. 6-10, 19, 25, 38, 41, 44, 45, 60-62, 64, 69, 75, 81, 82, 87, 88, 90, 92-94, 98, 100, 101, 104

direct plasma to electric power conversion[12]

Exemplary studies include:

1.) the observation of intense extreme ultraviolet (EUV) emission at low temperatures (e.g. $\approx 10^3\ K$) from atomic hydrogen and only those atomized elements or gaseous ions which provide a net enthalpy of reaction of approximately $m \cdot 27.2\ eV$ via the ionization of t electrons to a continuum energy level where t and m are each an integer (e.g. K and Cs atoms and Rb^+ and Sr^+ ions ionize at integer multiples of the potential energy of atomic hydrogen and caused emission; whereas, the chemically similar atoms, Na, Mg, and Ba, do not ionize at integer multiples of the potential energy of atomic hydrogen and caused no emission)[13],

2.) the observation of novel EUV emission lines from microwave and glow discharges of helium with 2% hydrogen with energies of $q \cdot 13.6\ eV$ where $q = 1,2,3,4,6,7,8,9,11,12$ or these lines inelastically scattered by helium atoms in the excitation of $He\ (1s^2)$ to $He\ (1s^1 2p^1)$ that were identified as hydrogen transitions to electronic energy levels below the "ground" state corresponding to fractional quantum numbers[14],

3.) the observation of novel EUV emission lines from microwave and glow discharges of helium with 2% hydrogen at 44.2 nm and 40.5 nm with energies of $q \cdot 13.6 + \left(\frac{1}{n_f^2} - \frac{1}{n_i^2}\right) X 13.6\ eV$ where $q = 2$ and $n_f = 2,4$ $n_i = \infty$ that corresponded to multipole coupling to give two-photon emission from a continuum excited state atom and an atom undergoing fractional Rydberg state transition[15],

4.) the identification of transitions of atomic hydrogen to lower energy levels corresponding to lower-energy hydrogen atoms in the extreme ultraviolet emission spectrum from interstellar medium and the sun[16],

---

[12] Reference Nos. 18, 26, 40, 48, 56, 68

[13] Reference Nos. 11-13, 15, 16, 20, 24, 27, 32, 39, 42, 46, 47, 51, 52, 54, 55, 57, 72, 81, 89, 91-93

[14] Reference Nos. 28, 33-36, 50, 63, 67, 71, 73, 75, 76, 78, 86, 87, 90

[15] Reference Nos. 36, 71, 73

[16] Reference Nos. 1, 5, 17, 28, 29

5.) the observation that the novel EUV series of lines with energies of $q \cdot 13.6\ eV$ was observed with an Evenson microwave cell, only the peak corresponding to $q = 2$ was observed with an RF cell, and none of the peaks were observed with a glow discharge cell[17],

6.) the observation that in a comparison of Evenson, McCarroll, cylindrical, and Beenakker microwave cavity plasmas, the novel EUV series of lines with energies of $q \cdot 13.6\ eV$ was only observed for Evenson-cavity helium-hydrogen plasmas[18],

7.) the EUV spectroscopic observation of lines for a hydrogen-K catalyst plasma by the Institut für Niedertemperatur-Plasmaphysik e.V. that could be assigned to transitions of atomic hydrogen to lower energy levels corresponding to fractional principal quantum numbers and the emission from the excitation of the corresponding hydride ions[19],

8.) the recent analysis of mobility and spectroscopy data of individual electrons in liquid helium which shows direct experimental confirmation that electrons may have fractional principal quantum energy levels[20],

9.) the observation of novel EUV emission lines from microwave discharges of argon or helium with 10% hydrogen that matched those predicted for the reaction $H(1/4)+H^{+} \rightarrow H_2(1/4)^{+}$ having an energy spacing of 2^2 times the transition-state vibrational energy of H_2^{+} with the series ending on the bond energy of $H_2(1/4)^{+}$[21],

10.) the result that the novel vibrational series for the reaction $H(1/4)+H^{+} \rightarrow H_2(1/4)^{+}$ was only observed for catalyst plasmas of helium, neon, and argon mixed with hydrogen, but not with noncatalyst xenon or krypton mixed plasmas[22],

11.) the observation that based on the intensities of the peaks, the catalyst and the plasma source dependence of the reaction rate to form $H_2(1/4)^{+}$ is $Ar^{+} > He^{+} > Ne^{+}$

---

[17] Reference Nos. 71, 73
[18] Reference No. 76
[19] Reference No. 14
[20] Reference Nos. 17, 53
[21] Reference Nos. 29, 70, 73, 79, 92, 93, 98, 101, 104
[22] Reference Nos. 29, 70, 73, 79, 92, 93, 101

and microwave > glow discharge >> RF, respectively[23],

12.) the observation that the microwave plasma source dependence of the reaction rate to form $H_2(1/4)^+$ is Evenson microwave > McCarroll, cylindrical, Beenakker[24],

13.) the observation of rotational lines in the 145-300 nm region from atmospheric pressure 15 keV electron-beam excited argon-hydrogen plasmas where the unprecedented energy spacing of 4^2 times that of hydrogen established the internuclear distance as 1/4 that of H_2 and identified $H_2(1/4)$[25],

14.) the observation of a series of vibration-rotational bands in the 60-67 nm region, a high-energy region for which vibration-rotational spectra are ordinarily unknown, emitted from low-pressure helium-hydrogen (99/1%) microwave plasmas that matched the predicted energy spacing of the vibrational energy of H_2 about the bond energy of $H_2(1/2)$ corresponding to the reaction $2H(1/2) \rightarrow H_2(1/2)$[26],

15.) the observation of EUV plasma emission spectra in the region 60 *nm* to 100 *nm* that matched the predicted emission lines $E_{D\,H_2}$ due to the reaction $2H(1/2) \rightarrow H_2(1/2)$ with vibronic coupling at energies of $E_{D+vib} = 17.913 \pm \left(\frac{\upsilon^*}{3}\right) 0.515902\ eV$ to longer wavelengths for $\upsilon^* = 2$ to $\upsilon^* = 32$ and to shorter wavelengths for $\upsilon^* = 1$ to $\upsilon^* = 16$ to within the spectrometer resolution of about $\pm 0.05\%$[27],

16.) the observation that in addition to members of the series of novel emission lines with energies of $q \cdot 13.6\ eV$ or $E_{D+vib} = 17.913 \pm \left(\frac{\upsilon^*}{3}\right) 0.515902\ eV$ an additional intense peak was observed from a scaled-up Evenson cell at 41.6 *nm* with an energy of 29.81 *eV* that matched $q \cdot 13.6\ eV$ with $q = 4$ less 24.58741 *eV* corresponding to inelastic scattering of these photons by helium atoms due to ionization of *He* to He^+[28],

---

[23] Reference No. 70
[24] Reference No. 79
[25] Reference No. 98, 101, 104
[26] Reference No. 99
[27] Reference Nos. 50, 75, 76, 78, 86, 87, 90
[28] Reference No. 86

17.) the observation that in a comparison of Evenson, McCarroll, cylindrical, and Beenakker microwave cavity plasmas, the novel series of spectral lines due to the reaction $2H(1/2) \rightarrow H_2(1/2)$ with vibronic coupling at energies of $E_{D+vib} = 17.913 \pm \left(\frac{\upsilon^*}{3}\right) 0.515902\ eV$ was only observed for Evenson-cavity helium-hydrogen and neon-hydrogen plasmas[29],

18.) the observation by gas chromatography that hydrogen was consumed by the helium-hydrogen plasmas which showed the novel EUV series of lines with energies of $q \cdot 13.6\ eV$, the novel series of spectral lines due to the reaction $2H(1/2) \rightarrow H_2(1/2)$ with vibronic coupling at energies of $E_{D+vib} = 17.913 \pm \left(\frac{\upsilon^*}{3}\right) 0.515902\ eV$, extraordinary H Balmer line broadening corresponding to 180 - 210 eV, and excess power of 21.9 W in 3 cm^3[30],

19.) the observation of the dominant He^+ emission and an intensification of the plasma emission observed when He^+ was present with atomic hydrogen demonstrated the role of He^+ as a catalyst[31],

20.) the observation of continuum state emission of Cs^{2+} and Ar^{2+} at 53.3 nm and 45.6 nm, respectively, with the absence of the other corresponding Rydberg series of lines from these species which confirmed the resonant nonradiative energy transfer of 27.2 eV from atomic hydrogen to the either Cs or Ar^+ catalyst[32],

21.) the spectroscopic observation of the predicted hydride ion $H^-(1/2)$ of hydrogen catalysis by either Cs or Ar^+ catalyst at 407 nm corresponding to its predicted binding energy of 3.05 eV[33],

22.) the observation of characteristic emission from K^{3+} which confirmed the resonant nonradiative energy transfer of $3 \cdot 27.2\ eV$ from atomic hydrogen to atomic K[34],

---

[29] Reference No. 76
[30] Reference No. 76
[31] Reference Nos. 36, 73
[32] Reference Nos. 24, 39, 51, 54, 55, 57, 91
[33] Reference No. 24
[34] Reference Nos. 27, 39, 42, 46, 51, 54, 55, 57, 81, 89, 91

23.) the spectroscopic observation of the predicted $H^-(1/4)$ ion of hydrogen catalysis by K catalyst at 110 nm corresponding to its predicted binding energy of 11.2 eV[35],

24.) the observation of characteristic emission from Rb^{2+} which confirmed the resonant nonradiative energy transfer of 27.2 eV from atomic hydrogen to Rb^+[36],

25.) the spectroscopic observation of the predicted $H^-(1/2)$ ion of hydrogen catalysis by Rb^+ catalyst at 407 nm corresponding to its predicted binding energy of 3.05 eV[37],

26.) the observation of $H^-(1/2)$, the hydride ion catalyst product of K^+ / K^+ or Rb^+, at its predicted binding energy of 3.0468 eV by high resolution visible spectroscopy as a continuum threshold at 4068.2 Å and a series of structured peaks separated from the binding energy by an integer multiple of the fine structure of $H(1/2)$ starting at 4071 Å that matched predicted free-free transitions[38],

27.) the observation that the high resolution visible K^+ / K^+ or $Rb^+ - H_2$ plasma emission spectra in the region of 3995 to 4060 Å matched the predicted bound-free hyperfine structure lines E_{HF} of $H^-(1/2)$ calculated from the electron g factor as $E_{HF} = j^2 3.00213\, X 10^{-5} + 3.0563\ eV$ (j is an integer) for $j = 1$ to $j = 39$ (3.0563 eV to 3.1012 eV—the hydride binding energy peak plus one and five times the spin-pairing energy, respectively) to within a 1 part per 10^4[39],

28.) Rb^+ or $2K^+$ catalysts formed a plasma having strong VUV emission with a stationary inverted Lyman population with an overpopulation sufficient for lasing, and emission from $H^-(1/2)$ was observed at 4071 Å corresponding to its predicted binding energy of 3.0468 eV with the fine structure and its predicted bound-free hyperfine structure lines $E_{HF} = j^2 3.00213\, X 10^{-5} + 3.0563\ eV$ (j is an integer) that matched for $j = 1$ to $j = 37$ to within a 1 part per 10^4[40],

---

[35] Reference Nos. 27, 42, 81

[36] Reference Nos. 32, 39, 42, 46, 51, 54, 55, 57, 81, 89, 91

[37] Reference No. 32

[38] Reference Nos. 39, 42, 46, 57, 81, 89, 91

[39] Reference Nos. 39, 42, 46, 57, 81, 89, 91

[40] Reference Nos. 39, 42, 46, 51, 54, 55, 57, 81, 89, 91

29.) the observation of stationary inverted H Balmer and Lyman populations from a low pressure water-vapor microwave discharge plasma with an overpopulation sufficient for lasing at wavelengths over a wide range from micron to blue wherein molecular oxygen served as the catalyst as supported by O^{2+} emission and H Balmer line broadening of 55 eV compared to 1 eV for hydrogen alone[41],

30.) the observation of H Balmer line broadening of 55 eV compared to 1 eV for hydrogen alone at distances up to 5 cm from the coupler[42],

31.) the observation that with a microwave input power of 9 $W \cdot cm^{-3}$, a collisional radiative model showed that the hydrogen excited state population distribution was consistent with an $n = 1 \rightarrow 5,6$ pumping power of an unprecedented 200 $W \cdot cm^{-3}$ permissive of gas laser efficiencies orders of magnitude those of conventional visible gas lasers and direct generation of electrical power using photovoltaic conversion of the spontaneous or stimulated water vapor plasma emission[43];

32.) the observation of stimulation of the stationary inverted H Balmer population from a low pressure water-vapor microwave discharge plasma by back illumination with an infrared source that showed depopulation of the $n = 5$ state[44],

33.) the observation of stationary inverted H Balmer and Lyman populations from a low pressure water-vapor microwave discharge plasma with an overpopulation sufficient for lasing was observed for Evenson microwave plasmas, but not for RF or discharge plasmas[45],

34.) the observation of stationary inverted H Balmer and Lyman populations from a low pressure water-vapor microwave discharge plasma with an overpopulation sufficient for lasing that was dependent on the microwave plasma source with the highest inversion from Evenson microwave plasmas[46],

---

41 Reference Nos. 59, 65, 66, 68, 74, 83, 85
42 Reference No. 74
43 Reference Nos. 68, 83, 85
44 Reference Nos. 59, 65, 68, 85
45 Reference Nos. 59, 65, 66, 68, 73, 83, 85
46 Reference No. 83

35.) the observation of stationary inverted H Balmer and Lyman populations from a low pressure water-vapor microwave discharge plasma with an overpopulation sufficient for lasing that was dependent on the pressure of the Evenson microwave plasma[47],

36.) the observation of stationary inverted H Balmer populations from a low pressure water-vapor microwave discharge plasma with an overpopulation sufficient for lasing at distances up to 5 cm from the coupler[48],

37.) the observation that the requirement for the natural hydrogen-oxygen stoichiometry of the Evenson water plasma was stringent in that a deviation by over 2% excess of either gas caused a reversal of the H inversion in water vapor plasmas[49],

38.) the observation of a typical slow H population for a water-vapor plasma maintained in a GEC-type cell that was independent of time, and a new phenomenon, an extraordinary fast population that increased from zero to a significant portion of the Balmer α emission with time under no-flow conditions wherein the peak width and energy increased with time up to a 0.7 nm half-width corresponding to an average hydrogen atom energy of 200 eV[50],

39.) the observation of a substantial fast H population (~20% at 40 eV) for a water-vapor plasmas maintained in a GEC-type cell that was independent of position including regions were the electric field was orders of magnitude to low to explain the extraordinarily high Doppler energies[51],

40.) the observation of fast H population (40-50 eV) for a He/H_2 (95/5%), Ar/H_2 (95/5%), and H_2 plasmas maintained in a GEC-type cell that was independent of position including regions were the electric field was orders of magnitude to low to explain the extraordinarily high Doppler energies[52],

---

[47] Reference Nos. 59, 68, 73, 83, 85
[48] Reference No. 74
[49] Reference Nos. 59, 68, 83, 85
[50] Reference No. 95
[51] Reference No. 96
[52] Reference Nos. 92, 93, 97, 105

41.) the observation by the Institut für Niedertemperatur-Plasmaphysik e.V. of an anomalous plasma and plasma afterglow duration formed with hydrogen-potassium mixtures[53],

42.) the observation of anomalous afterglow durations of plasmas formed by catalysts providing a net enthalpy of reaction within thermal energies of $m \cdot 27.28\ eV$[54],

43.) the formation of a chemically generated hydrogen plasma with the observation of Lyman series in the EUV that represents an energy release about 10 times that of hydrogen combustion which is greater than that of any possible known chemical reaction[55],

44.) the observation of line emission by the Institut für Niedertemperatur-Plasmaphysik e.V. with a 4° grazing incidence EUV spectrometer that was 100 times more energetic than the combustion of hydrogen[56],

45.) the excessive increase in the Lyman emission upon the addition of helium or argon catalyst to a hydrogen plasma[57],

46.) the observation of the characteristic emission from Sr^+ and Sr^{3+} that confirmed the resonant nonradiative energy transfer of $2 \cdot 27.2\ eV$ from atomic hydrogen to Sr^+[58],

47.) the observation of anomalous plasmas formed with Sr and Ar^+ catalysts at 1% of the theoretical or prior known voltage requirement with a light output per unit power input up to 8600 times that of the control standard light source[59],

48.) the observation that the optically measured output power of gas cells for

---

[53] Reference Nos. 13, 47, 81
[54] Reference Nos. 12, 13, 47, 81
[55] Reference Nos. 11-13, 15, 16, 20, 24, 27, 32, 39, 42, 46, 47, 51, 52, 54, 55, 57, 72, 81, 89, 91
[56] Reference No. 14
[57] Reference Nos. 20, 31, 37, 43
[58] Reference Nos. 16, 52
[59] Reference Nos. 11, 16, 20, 23, 52, 72

power supplied to the glow discharge increased by over two orders of magnitude depending on the presence of less than 1% partial pressure of certain catalysts in hydrogen gas or argon-hydrogen gas mixtures, and an excess thermal balance of 42 W was measured for the 97% argon and 3% hydrogen mixture versus argon plasma alone[60],

49.) the observation that glow discharge plasmas of the catalyst-hydrogen mixtures of strontium-hydrogen, helium-hydrogen, argon-hydrogen, strontium-helium-hydrogen, and strontium-argon-hydrogen showed significant Balmer α line broadening corresponding to an average hydrogen atom temperature of 25 - 45 eV; whereas, plasmas of the noncatalyst-hydrogen mixtures of pure hydrogen, krypton-hydrogen, xenon-hydrogen, and magnesium-hydrogen showed no excessive broadening corresponding to an average hydrogen atom temperature of ≈ 3 eV[61],

50.) the observation that microwave helium-hydrogen and argon-hydrogen plasmas having catalyst Ar^+ or He^+ showed extraordinary Balmer α line broadening due to hydrogen catalysis corresponding to an average hydrogen atom temperature of 110 - 130 eV and 180 - 210 eV, respectively; whereas, plasmas of pure hydrogen, neon-hydrogen, krypton-hydrogen, and xenon-hydrogen showed no excessive broadening corresponding to an average hydrogen atom temperature of ≈ 3 eV[62],

51.) the observation that microwave helium-hydrogen and argon-hydrogen plasmas showed average electron temperatures that were high, $30,500 \pm 5\%$ K and $13,700 \pm 5\%$ K, respectively; whereas, the corresponding temperatures of helium and argon alone were only $7400 \pm 5\%$ K and $5700 \pm 5\%$ K, respectively[63],

52.) the observation of significant Balmer α line broadening of 17, 9, 11, 14, *and* 24 eV from rt-plasmas of incandescently heated hydrogen with K^+ / K^+, Rb^+, cesium, strontium, and strontium with Ar^+ catalysts, respectively, wherein the results could not be explained by Stark or thermal broadening or electric field acceleration of charged species since the measured field of the incandescent heater was extremely weak, 1 V/cm, corresponding to a broadening of much less than 1 eV[64],

---

[60] Reference No. 22

[61] Reference Nos. 16, 20, 30, 52, 72

[62] Reference Nos. 33-37, 43, 49, 60, 63, 64, 69, 71, 73, 74, 82, 84, 88

[63] Reference Nos. 34-37, 43, 49, 63, 67, 73

[64] Reference Nos. 39, 42, 46, 51, 52, 54, 55, 57, 72, 81, 89, 91

53.) calorimetric measurement of excess power of 20 mW/cc on rt-plasmas formed by heating hydrogen with K^+ / K^+ and Ar^+ as catalysts[65],

54.) the observation of rt-plasmas formed with strontium and argon at 1% of the theoretical or prior known voltage requirement with a light output per unit power input up to 8600 times that of the control standard light source as well as an excess power of 20 mW/cm from rt-plasmas formed by Ar^+ as the catalyst in an incandescent-filament cell[66],

55.) the Calvet calorimetry measurement of an energy balance of over $-151{,}000\ kJ/mole\ H_2$ with the addition of 3% hydrogen to a plasma of argon having the catalyst Ar^+ compared to the enthalpy of combustion of hydrogen of $-241.8\ kJ/mole\ H_2$; whereas, under identical conditions no change in the Calvet voltage was observed when hydrogen was added to a plasma of noncatalyst xenon[67],

56.) the observation that the power output exceeded the power supplied to hydrogen glow discharge plasmas by 35-184 W depending on the presence of catalysts from helium or argon and less than 1% partial pressure of strontium metal in noble gas-hydrogen mixtures; whereas, the chemically similar noncatalyst krypton had no effect on the power balance[68],

57.) the observation that with the addition of 3% flowing hydrogen to an argon microwave plasma with a constant input power of 40 W, the gas temperature increased from 400°C to over 750°C; whereas, the 400°C temperature of a xenon plasma run under identical conditions was essentially unchanged with the addition of hydrogen[69],

58.) observations of power such as that where the addition of 10% hydrogen to a helium microwave plasma maintained with a constant microwave input power of 40 W, the thermal output power was measured to be at least 280 W corresponding to a reactor temperature rise from room temperature to 1200°C within 150 seconds, a power density

---

[65] Reference Nos. 39, 81, 89
[66] Reference No. 72
[67] Reference No. 31
[68] Reference No. 30
[69] Reference No. 43

of 28 MW/m^3, and an energy balance of at least $-4\ X10^5\ kJ/mole\ H_2$ compared to the enthalpy of combustion of hydrogen of $-241.8\ kJ/mole\ H_2$[70],

59.) the observation of $306 \pm 5\ W$ of excess power generated in 45 cm^3 by a compound-hollow-cathode-glow discharge of a neon-hydrogen (99.5/0.5%) mixture corresponding to a power density of 6.8 MW/m^3 and an energy balance of at least $-1\ X10^6\ kJ/mole\ H_2$ compared to the enthalpy of combustion of hydrogen of $-241.8\ kJ/mole\ H_2$[71],

60.) the observation that for an input of 37.7 W, the total plasma power of the neon-hydrogen plasma measured by water bath calorimetry was 60.7 W corresponding to 23.0 W of excess power in 3 cm^3[72],

61.) the observation of intense He^+ emission and a total plasma power of a helium-hydrogen plasma measured by water bath calorimetry of 30.0 W for an input of 8.1 W, corresponding to 21.9 W of excess power in 3 cm^3 wherein the excess power density and energy balance were high, 7.3 W/cm^3 and $-2.9\ X10^4\ kJ/mole\ H_2$, respectively[73],

62.) in the comparison of helium-hydrogen plasmas sources, the observation that i.) with an input power of 24.8± 1 W, the total plasma power of the Evenson microwave helium-hydrogen plasma measured by water bath calorimetry was 49.1 ± 1 W corresponding to 24.3 ± 1 W of excess power in 3 cm^3 corresponding to a high excess power density and energy balance of 8.1 W/cm^3 and over $-3\ X10^4\ kJ/mole\ H_2$, respectively, ii.) with an input of 500 W, a total power of 623 W was generated in a 45 cm^3 compound-hollow-cathode-glow discharge, iii.) less than 10% excess power was observed from inductively coupled RF helium-hydrogen plasmas, and iv.) no measurable heat was observed from MKS/Astex microwave helium-hydrogen plasmas that corresponded to the absence of H Balmer line broadening[74],

63.) the observation of energy balances of helium-hydrogen microwave plasmas

---

[70] Reference Nos. 34, 35
[71] Reference Nos. 50, 78
[72] Reference No. 76
[73] Reference Nos. 36, 63, 71, 73
[74] Reference Nos. 84, 98, 104

of over 100 times the combustion of hydrogen and power densities greater than 10 W/cm^3 measured by water bath calorimetry[75],

64.) at the load matching condition of 600 Ω, the direct plasmadynamic conversion (PDC) of open circuit voltages of 11.5 V and ~200 mW of electrical power with a 0.125 in diameter by 3/4 in long plasmadynamic electrode and a 140 G applied field corresponding to an extracted power density of ~1.61 W/cm^3 and an efficiency of ~18.8%[76],

65.) at the load matching condition of 250 Ω, the direct plasmadynamic conversion (PDC) of open circuit voltages of 21.8 V and 1.87 W of electrical power with a 0.125 in diameter by 3/4 in long plasmadynamic electrode and a 140 G applied field corresponding to an extracted power density of 3.6 W/cm^3 and an efficiency of 42%[77],

66.) the projection that the generation of electricity using magnetohydrodynamic (MHD) conversion of the plasma particle energy of small to mid-size chemically assisted microwave or glow discharge plasma (ca-plasma) power sources in the range of a few hundred Watts to several 10's of kW for microdistributed commercial applications appears feasible at 50% efficiency or better with a simple compact design[78],

67.) the differential scanning calorimetry (DSC) measurement of minimum heats of formation of *KHI* by the catalytic reaction of *K* with atomic hydrogen and *KI* that were over −2000 $kJ/mole\,H_2$ compared to the enthalpy of combustion of hydrogen of −241.8 $kJ/mole\,H_2$[79],

68.) the isolation of novel hydrogen compounds as products of the reaction of atomic hydrogen with atoms and ions which formed an anomalous plasma as reported in the EUV studies[80],

69.) the synthesis and identification of a novel diamond-like carbon film

---

[75] Reference Nos. 34-36, 50, 63, 71, 73, 76-78, 84. 92, 93, 101
[76] Reference No. 48
[77] Reference No. 56
[78] Reference No. 40
[79] Reference No. 25
[80] Reference Nos. 6-10, 19, 25, 38, 41, 44, 45, 60-62, 75, 81, 87, 90, 92, 93, 100, 101

terminated with $CH(1/p)$ (H^*DLC) comprising high binding energy hydride ions was synthesized for the first time from solid carbon by a microwave plasma reaction of a mixture of 10-30% hydrogen and 90-70% helium wherein He^+ served as a catalyst with atomic hydrogen to form the highly stable hydride ions and an energetic plasma[81],

70.) the synthesis of polycrystalline diamond films on silicon substrates without diamond seeding by a very low power microwave plasma reaction of a mixture of helium-hydrogen-methane (48.2/48.2/3.6%) wherein He^+ served as a catalyst with atomic hydrogen to form an energetic plasma with an average hydrogen atom temperature of $180-210\ eV$ versus $\approx 3\ eV$ for pure hydrogen and bombardment of the carbon surface by highly energetic hydrogen formed by the catalysis reaction may play a role in the formation of diamond[82],

71.) the synthesis of polycrystalline diamond films on silicon substrates without diamond seeding by a very low power microwave plasma reaction of a mixture of argon-hydrogen-methane (17.5/80/2.5%) wherein Ar^+ served as a catalyst with atomic hydrogen to form an energetic plasma with an average hydrogen atom temperature of $110-130\ eV$ versus $\approx 3\ eV$ for pure hydrogen and bombardment of the carbon surface by highly energetic hydrogen formed by the catalysis reaction may play a role in the formation of diamond[83],

72.) the identification of a novel highly stable surface coating $SiH(1/p)$ by time of flight secondary ion mass spectroscopy that showed SiH^+ in the positive spectrum and H^- dominant in the negative spectrum and by X-ray photoelectron spectroscopy which showed that the H content of the SiH coatings was hydride ions, $H^-(1/4)$, $H^-(1/9)$, and $H^-(1/11)$ corresponding to peaks at 11, 43, and 55 eV, respectively, and showed that the surface was remarkably stable to air[84],

73.) the isolation of novel inorganic hydride compounds such as $KH\,KHCO_3$ and KH following each of the electrolysis and plasma electrolysis of a K_2CO_3 electrolyte which comprised high binding energy hydride ions that were stable in water with their identification by methods such as (i) ToF-SIMS on $KH\,KHCO_3$ which showed inorganic

---

[81] Reference No. 60
[82] Reference Nos. 64, 69, 88
[83] Reference Nos. 82, 88
[84] Reference Nos. 45, 61, 100

hydride clusters $K[KH\,KHCO_3]_n^+$ and a negative ToF-SIMS dominated by hydride ion, (ii) X-ray photoelectron spectroscopy which showed novel peaks corresponding to high binding energy hydride ions, and (iii) ^1H nuclear magnetic resonance spectroscopy which showed upfield shifted peaks corresponding to more diamagnetic, high-binding-energy hydride ions[85],

74.) the identification of $LiHCl$ comprising a high binding energy hydride ion by time of flight secondary ion mass spectroscopy which showed a dominant H^- in the negative ion spectrum, X-ray photoelectron spectroscopy which showed $H^-(1/4)$ as a new peak at its predicted binding energy of 11 eV, ^1H nuclear magnetic resonance spectroscopy which showed an extraordinary upfield shifted peak of -15.4 ppm corresponding to the novel hydride ion, and powder X-ray diffraction which showed novel peaks[86],

75.) the identification of novel hydride compounds by a number of analytical methods such as (i) time of flight secondary ion mass spectroscopy which showed a dominant hydride ion in the negative ion spectrum, (ii) X-ray photoelectron spectroscopy which showed novel hydride peaks and significant shifts of the core levels of the primary elements bound to the novel hydride ions, (iii) ^1H nuclear magnetic resonance spectroscopy (NMR) which showed extraordinary upfield chemical shifts compared to the NMR of the corresponding ordinary hydrides, and (iv) thermal decomposition with analysis by gas chromatography, and mass spectroscopy which identified the compounds as hydrides[87],

76.) the NMR identification of novel hydride compounds MH^*X wherein M is the alkali or alkaline earth metal, X, is a halide, and H^* comprises a novel high binding energy hydride ion identified by a large distinct upfield resonance[88],

77.) the replication of the NMR results of the identification of novel hydride compounds by large distinct upfield resonances at Spectral Data Services, University of Massachusetts Amherst, University of Delaware, Grace Davison, and National Research

---

[85] Reference Nos. 6-7, 9, 38, 41

[86] Reference Nos. 44, 62

[87] Reference Nos. 6-10, 19, 25, 38, 41, 44, 45, 60-62, 75, 81, 87, 90, 92, 93, 100

[88] Reference Nos. 10, 19, 41, 44, 62, 81

Council of Canada[89],

78.) the NMR identification of novel hydride compounds MH^* and MH_2^* wherein M is the alkali or alkaline earth metal and H^* comprises a novel high binding energy hydride ion identified by a large distinct upfield resonance that proves the hydride ion is different from the hydride ion of the corresponding known compound of the same composition[90],

79.) the observation that the ^1H MAS NMR spectrum of novel compound KH^*Cl relative to external tetramethylsilane (TMS) showed a large distinct upfield resonance at -4.4 corresponding to an absolute resonance shift of -35.9 ppm that matched the theoretical prediction of $p = 4$, and the novel peak of KH^*I at -1.5 ppm relative to TMS corresponding to an absolute resonance shift of -33.0 ppm matched the theoretical prediction of $p = 2$[91],

80.) the observation that the predicted catalyst reactions, position of the upfield-shifted NMR peaks, and spectroscopic data for $H^-(1/2)$ and $H^-(1/4)$ were found to be in agreement[92],

81.) the isolation of fraction-principal-quantum-level molecular hydrogen $H_2(1/p)$ gas by liquefaction using an ultrahigh-vacuum, liquid nitrogen cryotrap, and the observations of novel peaks by cryogenic gas chromatography, a higher ionization energy than H_2 by mass spectroscopy, a substantial change in the EUV emission spectrum with deuterium substitution in a region where no hydrogen emission has ever been observed, and upfield shifted NMR peaks at 0.21, 2.18 and 3.47 ppm compared to that of H_2 at 4.63 ppm[93],

82.) the observation of ^1H NMR singlet peaks upfield of H_2 with a predicted integer spacing of 0.64 ppm at 3.47, 3.02, 2.18, 1.25, 0.85, and 0.22 ppm identified as the consecutive series $H_2(1/2)$, $H_2(1/3)$, $H_2(1/4)$, $H_2(1/5)$, $H_2(1/6)$, and $H_2(1/7)$, respectively, and $H_2(1/10)$ at -1.8 ppm wherein $H_2(1/p)$ gas was isolated by liquefaction

---

[89] Reference Nos. 19, 81
[90] Reference Nos. 19, 81
[91] Reference No. 81
[92] Reference No. 81
[93] Reference Nos. 75, 87, 90, 92, 93, 94, 101

at liquid nitrogen temperature, by decomposition of compounds found to contain the corresponding hydride ions $H^-(1/p)$, and by permeation through a hollow nickel cathode[94].

83.) the observation of excess enthalpy from a K_2CO_3 electrolytic cell of a factor of two times that of the resistive power dissipation and ^1H NMR singlet peaks upfield of H_2 with a predicted integer spacing of 0.64 ppm at 3.49, 2.17, 1.25, 0.86, and 0.21 ppm which matched the consecutive series $H_2(1/2)$, $H_2(1/4)$, $H_2(1/5)$, $H_2(1/6)$, and $H_2(1/7)$, respectively, and a higher ionizing molecular hydrogen recorded on the electrolysis gases collected in a hollow nickel cathode[95].

The hydrino spectrum has been published in top-tier peer reviewed journals such as:

67. R. L. Mills, P. Ray, "Extreme Ultraviolet Spectroscopy of Helium-Hydrogen Plasma", J. Phys. D, Applied Physics, Vol. 36, (2003), pp. 1535-1542.
50. R. L. Mills, P. Ray, J. Dong, M. Nansteel, B. Dhandapani, J. He, "Spectral Emission of Fractional-Principal-Quantum-Energy-Level Atomic and Molecular Hydrogen", Vibrational Spectroscopy, Vol. 31, No. 2, (2003), pp. 195-213.
33. R. L. Mills, P. Ray, B. Dhandapani, M. Nansteel, X. Chen, J. He, "New Power Source from Fractional Quantum Energy Levels of Atomic Hydrogen that Surpasses Internal Combustion", J Mol. Struct., Vol. 643, No. 1-3, (2002), pp. 43-54.

In reference 50, all possible alternative assignments including exotic ones were eliminated as the source of the novel series of peaks with energies of $q \cdot 13.6\ eV$ where $q = 1,2,3,4,6,7,8,9,11,12$ or these lines inelastically scattered by helium atoms in the excitation of $He\ (1s^2)$ to $He\ (1s^1 2p^1)$ that were identified as hydrogen transitions to electronic energy levels below the "ground" state corresponding to fractional quantum numbers **(hydrino lines)**.

The Examiner does not present any alternative explanation for the cited data.

Broadening was observed in glow discharge, RF discharge, and filament cells (rt-plasma) as well as microwave cells. Thus, the broadening is not dependent on the particular plasma source. Only those mixed plasma which contained a catalyst and hydrogen demonstrated

---

[94] Reference Nos. 98, 101, 103, 104

[95] Reference Nos. 103, 104

broadening. Balmer α line broadening is reported in references[96]. Standard broadening mechanisms were considered and eliminated including pressure broadening, resonance broadening, and microwave field broadening. Applicant confirmed that Doppler broadening due to thermal motion was the dominant source to the extent that other sources may be neglected when each source was considered. In general, the experimental profile is a convolution of two Doppler profiles, an instrumental profile, the natural (lifetime) profile, Stark profiles, van der Waals profiles, a resonance profile, and fine structure. The contribution from each source was determined to be below the limit of detection as shown in

49. R. L. Mills, P. Ray, E. Dayalan, B. Dhandapani, J. He, "Comparison of Excessive Balmer α Line Broadening of Inductively and Capacitively Coupled RF, Microwave, and Glow Discharge Hydrogen Plasmas with Certain Catalysts", IEEE Transactions on Plasma Science, Vol. 31, No. (2003), pp. 338-355.
43. R. L. Mills, P. Ray, "Substantial Changes in the Characteristics of a Microwave Plasma Due to Combining Argon and Hydrogen", New Journal of Physics, www.njp.org, Vol. 4, (2002), pp. 22.1-22.17.
37. R. L. Mills, P. Ray, B. Dhandapani, R. M. Mayo, J. He, "Comparison of Excessive Balmer α Line Broadening of Glow Discharge and Microwave Hydrogen Plasmas with Certain Catalysts", J. of Applied Physics, Vol. 92, No. 12, (2002), pp. 7008-7022.

In addition, only those plasma which contained a catalyst with hydrogen demonstrated other unique features such as the formation of a chemically generated hydrogen plasma (rt-plasma), novel spectral lines corresponding to lower-energy hydrogen states, and inverted hydrogen populations as discussed in:

84. R. L. Mills, P. Ray, J. Dong, M. Nansteel, R. M. Mayo, B. Dhandapani, X. Chen, "Comparison of Balmer α Line Broadening and Power Balances of Helium-Hydrogen Plasma Sources", Plasma Sources Science and Technology, submitted.
74. R. L. Mills, P. C. Ray, R. M. Mayo, M. Nansteel, B. Dhandapani, J. Phillips, "Spectroscopic Study of Unique Line Broadening and Inversion in Low Pressure Microwave Generated Water Plasmas", Physics of Plasmas, submitted.

Additional data confirming the novel claimed reaction of atomic hydrogen to results in extraordinary H energy as measured by the broadening of the Balmer α line are:

---

[96] Reference Nos. 16, 20, 30, 33-37, 39, 42-43, 49, 51-52, 54-55, 57, 63-65, 68-69, 71-74, 81-85, 88-89, 91, 92, 93

16.) the observation by gas chromatography that hydrogen was consumed by the helium-hydrogen plasmas which showed the novel EUV series of lines with energies of $q \cdot 13.6\ eV$, the novel series of spectral lines due to the reaction $2H(1/2) \rightarrow H_2(1/2)$ with vibronic coupling at energies of $E_{D+vib} = 17.913 \pm \left(\frac{\upsilon^*}{3}\right) 0.515902\ eV$, extraordinary H Balmer line broadening corresponding to 180 - 210 eV, and excess power of 21.9 W in 3 cm^3[97],

27.) the observation of stationary inverted H Balmer and Lyman populations from a low pressure water-vapor microwave discharge plasma with an overpopulation sufficient for lasing at wavelengths over a wide range from micron to blue wherein molecular oxygen served as the catalyst as supported by O^{2+} emission and H Balmer line broadening of 55 eV compared to 1 eV for hydrogen alone[98],

28.) the observation of H Balmer line broadening of 55 eV compared to 1 eV for hydrogen alone at distances up to 5 cm from the coupler[99],

44.) the observation that glow discharge plasmas of the catalyst-hydrogen mixtures of strontium-hydrogen, helium-hydrogen, argon-hydrogen, strontium-helium-hydrogen, and strontium-argon-hydrogen showed significant Balmer α line broadening corresponding to an average hydrogen atom temperature of 25 - 45 eV; whereas, plasmas of the noncatalyst-hydrogen mixtures of pure hydrogen, krypton-hydrogen, xenon-hydrogen, and magnesium-hydrogen showed no excessive broadening corresponding to an average hydrogen atom temperature of $\approx 3\ eV$[100],

45.) the observation that microwave helium-hydrogen and argon-hydrogen plasmas having catalyst Ar^+ or He^+ showed extraordinary Balmer α line broadening due to hydrogen catalysis corresponding to an average hydrogen atom temperature of 110 - 130 eV and 180 - 210 eV, respectively; whereas, plasmas of pure hydrogen, neon-hydrogen, krypton-hydrogen, and xenon-hydrogen showed no excessive broadening corresponding to an average hydrogen atom temperature of $\approx 3\ eV$[101], and

---

[97] Reference No. 76
[98] Reference Nos. 59, 65-66, 68, 74, 83, 85
[99] Reference No. 74
[100] Reference Nos. 16, 20, 30, 52, 72
[101] Reference Nos. 33-37, 43, 49, 60, 63-64, 69, 71, 73-74, 82, 84, 88, 92, 93

47.) the observation of significant Balmer α line broadening of 17, 9, 11, 14, *and* 24 *eV* from rt-plasmas of incandescently heated hydrogen with K^+ / K^+, Rb^+, cesium, strontium, and strontium with Ar^+ catalysts, respectively, wherein the results could not be explained by Stark or thermal broadening or electric field acceleration of charged species since the measured field of the incandescent heater was extremely weak, 1 V/cm, corresponding to a broadening of much less than 1 *eV*[102].

Applicant has correctly used Maxwell's equations to solve the atom and predict the new states of hydrogen. Applicant's use of first principles to solve problems on scales spanning 85 orders of magnitude is unprecedented and can not be matched with QM. Classical Quantum Mechanics (CQM) solves problems to greater accuracy than quantum mechanics (QM) and further solves problems which remain unsolvable by QM such as the basis of gravity, fundamental particles, and the acceleration of the expansion of the cosmos, all predicted accurately by Applicant's CQM.

As a specific example, problems that are intractable for QM can easily be solved by CQM such as the particle masses given in the Leptons section, the Proton and Neutron section, and the Quarks section of Ref. [1]:

RELATIONS BETWEEN FUNDAMENTAL PARTICLES

The relations between the lepton masses and neutron to electron mass ratio which are independent of the definition of the imaginary time ruler *ti* including the contribution of the fields due to charge production are given in terms of the dimensionless fine structure constant α only:

$$\frac{m_\mu}{m_e} = \left(\frac{\alpha^{-2}}{2\pi}\right)^{\frac{2}{3}} \frac{\left(1+2\pi\frac{\alpha^2}{2}\right)}{\left(1+\frac{\alpha}{2}\right)} = 206.76828 \qquad (206.76827)$$

$$\frac{m_\tau}{m_\mu} = \left(\frac{\alpha^{-1}}{2}\right)^{\frac{2}{3}} \frac{\left(1+\frac{\alpha}{2}\right)}{\left(1-4\pi\alpha^2\right)} = 16.817 \qquad (16.817)$$

---

[102] Reference Nos. 39, 42, 46, 51-52, 54-55, 57, 72, 81, 89, 91

$$\frac{m_\tau}{m_e} = \left(\frac{\alpha^{-3}}{4\pi}\right)^{\frac{2}{3}} \frac{\left(1+2\pi\frac{\alpha^2}{2}\right)}{\left(1-4\pi\alpha^2\right)} = 3477.2 \qquad (3477.3)$$

$$\frac{m_N}{m_e} = \frac{12\pi^2}{1-\alpha}\sqrt{\frac{\sqrt{3}}{\alpha}} \frac{\left(1+2\pi\frac{\alpha^2}{2}\right)}{\left(1-2\pi\frac{\alpha^2}{2}\right)} = 1838.67 \qquad (1838.68)$$

The success of Applicant's theory is summarized in a book review given by Landvogt.[103]

Some well-known facts were previously pointed out in detail by the Applicant[104]—QM is postulated, purely mathematical, and can have no basis in realty. It only works because it tolerates renormalization and fictitious adjustable terms and parameters that are not physical and lack internal consistency. Considering the requirement of internal consistency and the adherence to physical laws, QM has never correctly solved a physical problem. It has many inescapable and intractable problems as documented in the following articles and references contained therein:

94. R. L. Mills, "The Nature of the Chemical Bond Revisited and an Alternative Maxwellian Approach", J. Phys. D, submitted.
80. R. L. Mills, The Fallacy of Feynman's Argument on the Stability of the Hydrogen Atom According to Quantum Mechanics, Foundations of Physics, submitted.
58. R. L. Mills, "Classical Quantum Mechanics", Physics Essays, submitted.
53. R. Mills, "A Maxwellian Approach to Quantum Mechanics Explains the Nature of Free Electrons in Superfluid Helium", Theoretical Chemistry Accounts, submitted.
22. R. Mills, "The Grand Unified Theory of Classical Quantum Mechanics", Global Foundation, Inc. Orbis Scientiae entitled *The Role of Attractive and Repulsive Gravitational Forces in Cosmic Acceleration of Particles The Origin of the Cosmic Gamma Ray Bursts*, (29th Conference on High Energy Physics and Cosmology Since 1964) Dr. Behram N. Kursunoglu, Chairman, December 14-17, 2000, Lago Mar Resort, Fort Lauderdale, FL, Kluwer Academic/Plenum Publishers, New York, pp. 243-258.

---

[103] G. Landvogt, "The Grand Unified Theory of Classical Quantum Mechanics", International Journal of Hydrogen Energy, Vol. 28, No. 10, (2003), pp. 1155

[104] Reference Nos. 1, 5, 17, 21, 22, 53, 58, 80, 94

21. R. Mills, "The Grand Unified Theory of Classical Quantum Mechanics", Int. J. Hydrogen Energy, Vol. 27, No. 5, (2002), pp. 565-590.
17. R. Mills, "The Nature of Free Electrons in Superfluid Helium--a Test of Quantum Mechanics and a Basis to Review its Foundations and Make a Comparison to Classical Theory", Int. J. Hydrogen Energy, Vol. 26, No. 10, (2001), pp. 1059-1096.
5. R. Mills, "The Hydrogen Atom Revisited", Int. J. of Hydrogen Energy, Vol. 25, Issue 12, December, (2000), pp. 1171-1183.
1. R. Mills, *The Grand Unified Theory of Classical Quantum Mechanics*, September 2001 Edition, BlackLight Power, Inc., Cranbury, New Jersey, Distributed by Amazon.com; July 2003 Edition posted at www.blacklightpower.com.

Ironically, Dirac originally attempted to solve the bound electron physically with stability with respect to radiation according to Maxwell's equations with the further constraints that it was relativistically invariant and gave rise to electron spin [1. P. Pearle, Foundations of Physics, "Absence of radiationless motions of relativistically rigid classical electron", Vol. 7, Nos. 11/12, (1977), pp. 931-945.]. He was unsuccessful and resorted to the current mathematical-probability-wave model that has many problems as discussed in Appendix II: Quantum Electrodynamics (QED) is Purely Mathematical and Has No Basis in Reality of Ref. [1]. From Weisskopf [V. F. Weisskopf, Reviews of Modern Physics, Vol. 21, No. 2, (1949), pp. 305-315], "Dirac's quantum electrodynamics gave a more consistent derivation of the results of the correspondence principle, but it also brought about a number of new and serious difficulties." Quantum electrodynamics; 1.) does not explain nonradiation of bound electrons; 2.) contains an internal inconsistency with special relativity regarding the classical electron radius—the electron mass corresponding to its electric energy is infinite; 3.) it admits solutions of negative rest mass and negative kinetic energy; 4.) the interaction of the electron with the predicted zero-point field fluctuations leads to infinite kinetic energy and infinite electron mass; 5.) Dirac used the unacceptable states of negative mass for the description of the vacuum; yet, infinities still arise.

Dirac's postulated relativistic wave equation also leads to the inescapable results that it gives rise to the Klein Paradox and a cosmological constant that is at least 120 orders of magnitude larger than the best observational limit as discussed in Chp. 1, Appendix II of Ref. [1] and previously[105].

QM does not provide a basis for a "ground state" of the hydrogen atom beyond an

---

[105] Reference Nos. 5, 17, 21, 33, 53, 58, 80, 94

arbitrary definition as discussed previously:

80. R. L. Mills, The Fallacy of Feynman's Argument on the Stability of the Hydrogen Atom According to Quantum Mechanics, Foundations of Physics, submitted.
1. R. Mills, *The Grand Unified Theory of Classical Quantum Mechanics*, September 2001 Edition, BlackLight Power, Inc., Cranbury, New Jersey, Distributed by Amazon.com; January 2003 Edition posted at www.blacklightpower.com; Chps. 35-37.

Furthermore, Applicant has more than met the burden of experimental evidence to support his claimed invention as given in the document entitled "**Lower-Energy Hydrogen Experimental Data**," attached. Over 50 articles are published in peer reviewed scientific journals and over 90 articles are submitted:

List of journals where Applicant's articles have been published:

Applied Physics Letters
Chemistry of Materials
Electrochimica Acta
Fusion Technology
IEEE Transactions on Plasma Science
International Journal of Hydrogen Energy
Journal of Applied Physics
Journal of Molecular Structure
Journal of Plasma Physics
Journal of Quantitative Spectroscopy and Radiative Transfer,
Journal of Physics D: Applied Physics
Journal of New Materials for Electrochemical Systems
New Journal of Physics
Plasma Sources Science and Technology
Solar Energy Materials & Solar Cells
Thermochimica Acta
Vibrational Spectroscopy

List of journals where Applicant's articles have been submitted and are being reviewed:

Acta Physica Polonica A
AIAA Journal
Annales De La Fondation Louis DeBroglie
Brazilian Journal of Physics
Canadian Journal of Physics
Central European Journal of Physics
Contributions to Plasma Physics
Current Applied Physics
Doklady Chemistry
European Journal of Physics D
European Physical Journal: Applied Physics
Europhysics Letters
Foundations of Physics
Frizika A
International Journal of Theoretical Physics
Journal of Applied Physics
Journal of Applied Spectroscopy
Journal of Electroanalytical Chemistry
Journal of Material Science
Journal of the Physical Society of Japan
Journal of Physical Chemistry A
Journal of Physical Chemistry B
Journal of Plasma Physics
Journal of Quantitative Spectroscopy and Radiative Transfer
Journal of Vacuum Science & Technology A
Materials Characterization
Materials Chemistry and Physics
Materials Science
New Journal of Chemistry
Physica B
Physics Essays
Physics of Plasmas
Spectrochemica Acta Part B: Atomic Spectroscopy
Technical Physics
Thin Sold Films
Vacuum

Applicant's experimental data has been published in peer reviewed journal articles as given in the attached document entitled "**Lower-Energy Hydrogen Experimental Data.**" Over 50 articles are published in peer reviewed scientific journals and over 100 articles are submitted.

Applicant's use of the terminology Rydberg states is justified and appears in peer reviewed journal articles. From Ref. [67], R. L. Mills, P. Ray, "Extreme Ultraviolet Spectroscopy of Helium-Hydrogen Plasma", J. Phys. D, Applied Physics, Vol. 36, (2003), pp. 1535-1542:

Key Words: helium-hydrogen plasma, catalysis, energetic atomic hydrogen, **novel extended Rydberg series**

The elimination of known explanations indicate a new result. Since the novel peaks were only observed with helium and hydrogen present, new hydrogen, helium, or helium-hydrogen species are possibilities. It is well known that empirically the excited energy states of atomic hydrogen are given by **Rydberg** equation (Eq. (2a) for $n > 1$ in Eq. (2b)).

$$E_n = -\frac{e^2}{n^2 8\pi\varepsilon_o a_H} = -\frac{13.598\ eV}{n^2} \tag{2a}$$

$$n = 1,2,3,\ldots \tag{2b}$$

The $n = 1$ state is the "ground" state for "pure" photon transitions (i.e. the $n = 1$ state can absorb a photon and go to an excited electronic state, but it cannot release a photon and go to a lower-energy electronic state). However, an electron transition from the ground state to a lower-energy state may be possible by a resonant nonradiative energy transfer such as multipole coupling or a resonant collision mechanism. Processes such as hydrogen molecular bond formation that occur without photons and that require collisions are common[106]. Also, some commercial phosphors are based on resonant nonradiative energy transfer involving multipole coupling[107].

We propose that atomic hydrogen may undergo a catalytic reaction with certain atoms and ions such as He^+ which singly or multiply ionize at integer multiples of the potential energy of atomic hydrogen, $m \cdot 27.2\ eV$ wherein m is an integer. The theory was given previously[108]. The reaction involves a nonradiative energy transfer to form a hydrogen atom that is lower in energy than unreacted atomic hydrogen that corresponds to a fractional principal quantum number. That is

---

[106] Reference No. 47
[107] Reference No. 48
[108] Reference No. 49

$$n = \frac{1}{2}, \frac{1}{3}, \frac{1}{4}, ..., \frac{1}{p}; \quad p \text{ is an integer; } p \leq 137 \tag{2c}$$

replaces the well known parameter n = integer in the **Rydberg** equation for hydrogen excited states. **Thus, the Rydberg states are extended to lower levels as depicted in Figure 9.** The $n = 1$ state of hydrogen and the $n = \frac{1}{\text{integer}}$ states of hydrogen are nonradiative, but a transition between two nonradiative states is possible via a nonradiative energy transfer, say $n = 1$ to $n = 1/2$. Thus, a catalyst provides a net positive enthalpy of reaction of $m \cdot 27.2\ eV$ (i.e. it resonantly accepts the nonradiative energy transfer from hydrogen atoms and releases the energy to the surroundings to affect electronic transitions to fractional quantum energy levels). As a consequence of the nonradiative energy transfer, the hydrogen atom becomes unstable and emits further energy until it achieves a lower-energy nonradiative state having a principal energy level given by Eqs. (2a) and (2c).

The novel peaks fit two empirical relationships. In order of energy, the set comprising the peaks at 91.2 *nm*, 45.6 *nm*, 30.4 *nm*, 13.03 *nm*, 10.13 *nm*, and 8.29 *nm* correspond to energies of $q \cdot 13.6\ eV$ where $q = 1,2,3,7,9,11$. In order of energy, the set comprising the peaks at 37.4 *nm*, 20.5 *nm*, and 14.15 *nm* correspond to energies of $q \cdot 13.6 - 21.21\ eV$ where $q = 4,6,8$. These lines can be explained as electronic transitions to **fractional Rydberg states** of atomic hydrogen given by Eqs. (2a) and (2c) wherein the catalytic system involves helium ions because the second ionization energy of helium is 54.417 eV, which is equivalent to $2 \cdot 27.2\ eV$. In this case, 54.417 eV is transferred nonradiatively from atomic hydrogen to He^+ which is resonantly ionized. The electron decays to the $n = 1/3$ state with the further release of 54.417 eV which may be emitted as a photon. The catalysis reaction is

$$54.417\ eV + He^+ + H[a_H] \rightarrow He^{2+} + e^- + H\left[\frac{a_H}{3}\right] + 108.8\ eV \tag{3}$$

$$He^{2+} + e^- \rightarrow He^+ + 54.417\ eV \tag{4}$$

And, the overall reaction is

$$H[a_H] \rightarrow H\left[\frac{a_H}{3}\right] + 54.4\ eV + 54.4\ eV \tag{5}$$

Since the products of the catalysis reaction have binding energies of $m \cdot 27.2\ eV$, they may further serve as catalysts. Thus, further catalytic transitions may occur: $n = \frac{1}{3} \rightarrow \frac{1}{4}$, $\frac{1}{4} \rightarrow \frac{1}{5}$, and so on.

Electronic transitions to Rydberg states given by Eqs. (2a) and (2c) catalyzed by the resonant nonradiative transfer of $m \cdot 27.2\ eV$ would give rise to a series of emission lines of energies $q \cdot 13.6\ eV$ where q is an integer. It is further proposed that the photons that arise from hydrogen transitions may undergo inelastic helium scattering. That is, the catalytic

reaction

$$H\left[a_H\right] \xrightarrow{He^+} H\left[\frac{a_H}{3}\right] + 54.4\ eV + 54.4\ eV \tag{6}$$

yields $54.4\ eV$ by Eq. (4) and a photon of $54.4\ eV$ ($22.8\ nm$). Once emitted, the photon may be absorbed or scattered. When this photon strikes $He\,(1s^2)$, $21.2\ eV$ may be absorbed in the excitation to $He\,(1s^1 2p^1)$. This leaves a $33.19\ eV$ ($37.4\ nm$) photon peak and a $21.21\ eV$ ($58.4\ nm$) photon from $He\,(1s^1 2p^1)$. Thus, for helium the inelastic scattered peak of $54.4\ eV$ photons from Eq. (3) is given by

$$E = 54.4\ eV - 21.21\ eV = 33.19\ eV\ (37.4\ nm) \tag{7}$$

A novel peak shown in Figures 2-4 was observed at $37.4\ nm$. Furthermore, the intensity of the $58.4\ nm$ peak corresponding to the spectra shown in Figure 4 was about 60,000 photons/sec. Thus, the transition $He\,(1s^2) \rightarrow He\,(1s^1 2p^1)$ dominated the inelastic scattering of EUV peaks. The general reaction is

$$photon\ (h\nu) + He\,(1s^2) \rightarrow He\,(1s^1 2p^1) + photon\ (h\nu - 21.21\ eV) \tag{8}$$

The two empirical series may be combined—one directly from Eqs. (2a, 2c) and the other indirectly with Eq. (8). The energies for the novel lines in order of energy are $13.6\ eV$, $27.2\ eV$, $40.8\ eV$, $54.4\ eV$, $81.6\ eV$, $95.2\ eV$, $108.8\ eV$, $122.4\ eV$ and $149.6\ eV$. The corresponding peaks are $91.2\ nm$, $45.6\ nm$, $30.4\ nm$, $37.4\ nm$, $20.5\ nm$, $13.03\ nm$, $14.15\ nm$, $10.13\ nm$, and $8.29\ nm$, respectively. Thus, the identified novel lines correspond to energies of $q \cdot 13.6\ eV$, $q = 1,2,3,7,9,11.$ or $q \cdot 13.6\ eV$, $q = 4,6,8$ less $21.2\ eV$ corresponding to inelastic scattering of these photons by helium atoms due to excitation of $He\,(1s^2)$ to $He\,(1s^1 2p^1)$. The values of q observed are consistent with those expected based on Eq. (5) and the subsequent autocatalyzed reactions as discussed previously[109]. The broad satellite peak at $44.2\ nm$ show in Figure 2-4 is consistent with the reaction mechanism of a nonradiative transfer to a catalyst followed by emission. **There is remarkable agreement between the data and the proposed transitions to fractional Rydberg states** and these lines inelastically scattered by helium according to Eq. (8). All other peaks could be assigned to He I, He II, second order lines, or atomic or molecular hydrogen emission. No known lines of helium or hydrogen explain the $q \cdot 13.6\ eV$ related set of peaks.

These data confirm the products of the claimed reaction such as 1.) power, 2.) plasma from the energetic reaction, 3.) fast H arising from the energy transfer from H undergoing a transition to a lower-energy state to the subsequent fast H acting as a colliding body to conserve

---

[109] Reference No. 50

energy and momentum, and 4.) novel compounds including new hydride compounds.

Based on the data presented in the cited Attachments, there is ample basis to propose commercial applications. The data has its characteristics such as plasma formation[110], population inversion of hydrogen lines[111], power generation[112], excessive light emission[113], and novel chemical compounds [114] independent of the underlying hydrino hypothesis as does direct plasma to electric power conversion[115]. Furthermore, the scientific hypothesis based on Maxwell's equations is valid and using the flawed QM as basis for discounting the claimed Invention is erroneous. The inescapable problems of QM including its inability to provide a physical basis for the "ground" state of atomic hydrogen are discussed in:

94. R. L. Mills, "The Nature of the Chemical Bond Revisited and an Alternative Maxwellian Approach", J. Phys. D, submitted.
80. R. L. Mills, The Fallacy of Feynman's Argument on the Stability of the Hydrogen Atom According to Quantum Mechanics, Foundations of Physics, submitted.
58. R. L. Mills, "Classical Quantum Mechanics", Physics Essays, submitted.
53. R. Mills, "A Maxwellian Approach to Quantum Mechanics Explains the Nature of Free Electrons in Superfluid Helium", Theoretical Chemistry Accounts, submitted.
22. R. Mills, "The Grand Unified Theory of Classical Quantum Mechanics", Global Foundation, Inc. Orbis Scientiae entitled *The Role of Attractive and Repulsive Gravitational Forces in Cosmic Acceleration of Particles The Origin of the Cosmic Gamma Ray Bursts*, (29th Conference on High Energy Physics and Cosmology Since 1964) Dr. Behram N. Kursunoglu, Chairman, December 14-17, 2000, Lago Mar Resort, Fort Lauderdale, FL, Kluwer Academic/Plenum Publishers, New York, pp. 243-258.
21. R. Mills, "The Grand Unified Theory of Classical Quantum Mechanics", Int. J. Hydrogen Energy, Vol. 27, No. 5, (2002), pp. 565-590.
17. R. Mills, "The Nature of Free Electrons in Superfluid Helium--a Test of Quantum Mechanics and a Basis to Review its Foundations and Make a Comparison to Classical Theory", Int. J. Hydrogen Energy, Vol. 26, No. 10, (2001), pp. 1059-1096.
5. R. Mills, "The Hydrogen Atom Revisited", Int. J. of Hydrogen Energy, Vol. 25, Issue 12,

---

[110] Reference Nos. 11-13, 15-16, 20, 24, 27, 32, 39, 42, 46-47, 51-52, 54-55, 57, 72, 81, 89, 91-93
[111] Reference Nos. 39, 46, 51, 54, 55, 57, 59, 65-66, 68, 74, 83, 85, 89, 91
[112] Reference Nos. 30-31, 33, 35-36, 39, 43, 50, 63, 71-73, 76-77, 81, 84, 89, 92, 93
[113] Reference Nos. 11, 16, 20, 23, 31, 37, 43, 52, 72
[114] Reference Nos. 6-10, 19, 25, 38, 41, 44-45, 60-62, 64, 69, 75, 81-82, 87-88, 90, 92, 93, 94
[115] Reference Nos. 18, 26, 40, 48, 56, 68

December, (2000), pp. 1171-1183.

1. R. Mills, *The Grand Unified Theory of Classical Quantum Mechanics*, September 2001 Edition, BlackLight Power, Inc., Cranbury, New Jersey, Distributed by Amazon.com; July 2003 Edition posted at www.blacklightpower.com.

e.) The Examiner cites Applicants paper:

28. R. Mills, P. Ray, "Spectral Emission of Fractional Quantum Energy Levels of Atomic Hydrogen from a Helium-Hydrogen Plasma and the Implications for Dark Matter", Int. J. Hydrogen Energy, (2002), Vol. 27, No. 3, pp. 301-322.

as failing to identify the 304 Å line as the He II line. The Examiner shows carelessness and has erred since the Applicant has assigned the 304 Å to He II. Table 1 of gives:

304	304	$He^+(n=2) \rightarrow He^+(n=1) + 40.8\ eV$ [b]	7, 8, 9, 10, 12

In the legend appears:

[b] In Figures 7, 8, 9, 10, and 12, the peak corresponding to $He^+(n=3) \rightarrow He^+(n=1) + 48.35\ eV$ (256 Å) was absent which makes this assignment difficult.

Furthermore, in Sec. IIIA appears:

> It is also proposed that the 304 Å peak shown in Figures 7, 8, 9, 10 and 12 was not entirely due to the He II transition. Conspicuously absent was the 256 *Å* (48.3 *eV*) line of He II shown in Figures 6 and 8 which implies only a minor He II transition contribution to the 304 Å peak.

The solar spectrum is not the same as the spectrum of a pure helium-hydrogen (98/2%) plasma. The Sun is known to contain the elements even beyond iron (See Table 4.2 of Stix, M., The Sun, Springer-Verlag, Berlin, (1991)). Based on the Examiner's errors and using the same

standard as the Examiner applies to Applicant, his scientific credibility is compromised on **all** of his arguments.

The Examiner is confused. As given in **Appendix #2**, the Applicant does not claim resonance broadening, rather the source of Balmer line broadening is Doppler broadening. The resonance ionization involves the catalyst as given for the He^+ in **Appendix #b**. The catalyst reaction involves a nonradiative, resonant energy transfer of $m \cdot 27.2\ eV$ to a catalyst followed the remaining energy between the initial and final states being released as a photon or transferred to a body such as H to form fast H. The resulting broadening is Doppler.

Hydrogen does not emit below 80 nm, the emission region of the novel series of peaks with energies of $q \cdot 13.6\ eV$ where $q = 1,2,3,4,6,7,8,9,11,12$ or these lines inelastically scattered by helium atoms in the excitation of $He\ (1s^2)$ to $He\ (1s^1 2p^1)$. These lines having wavelengths shorter than those of the Lyman lines were identified as hydrogen transitions to electronic energy levels below the "ground" state corresponding to fractional quantum numbers **(hydrino lines). See Appendix #1.** In the case of hydrogen Lyman emission due to plasma formation[116], there is **no** EUV emission in the controls. The formation of a plasma at low temperature with low or no electric field requirement is a first and quite unexpected. The plasma formation only occurs for those systems where catalyst is present. The predicted catalyst emission is observed. The predicted novel hydride ion emission is observed, and novel chemical compounds are formed. The plasma (rt-plasma) was independently replicated and alternative explanations were eliminated by top plasma physicists[117]. The Examiner has offered no plausible alternative explanation as to why a very energetic plasma should form with the heating of trace amounts of an inorganic compound and low pressure hydrogen gas.

Data clearly showing that the predicted catalytic hydrogen reaction occurs in these plasma includes:

1.) the observation of intense extreme ultraviolet (EUV) emission at low temperatures (e.g. $\approx 10^3\ K$) from atomic hydrogen and only those atomized elements or gaseous ions which provide a net enthalpy of reaction of approximately $m \cdot 27.2\ eV$ via the ionization of t electrons to a continuum energy level where t and m are each an integer (e.g. K, Cs, and Sr atoms and Rb^+ ion ionize at integer multiples of the potential energy of atomic hydrogen and

---

[116] Reference Nos. 11-13, 15-16, 20, 24, 27, 32, 39, 42, 46-47, 51-52, 54-55, 57, 72, 81, 89, 91-93
[117] Reference No. 47

caused emission; whereas, the chemically similar atoms, Na, Mg, and Ba, do not ionize at integer multiples of the potential energy of atomic hydrogen and caused no emission)[118],

2.) the observation of novel EUV emission lines from microwave and glow discharges of helium with 2% hydrogen with energies of $q \cdot 13.6\ eV$ where $q = 1,2,3,4,6,7,8,9,11,12$ or these lines inelastically scattered by helium atoms in the excitation of $He\ (1s^2)$ to $He\ (1s^1 2p^1)$ that were identified as hydrogen transitions to electronic energy levels below the "ground" state corresponding to fractional quantum numbers[119],

18.) the observation of continuum state emission of Cs^{2+} and Ar^{2+} at 53.3 nm and 45.6 nm, respectively, with the absence of the other corresponding Rydberg series of lines from these species which confirmed the resonant nonradiative energy transfer of 27.2 eV from atomic hydrogen to the either Cs or Ar^+ catalyst[120],

19.) the spectroscopic observation of the predicted hydride ion $H^-(1/2)$ of hydrogen catalysis by either Cs or Ar^+ catalyst at 407 nm corresponding to its predicted binding energy of 3.05 eV[121],

20.) the observation of characteristic emission from K^{3+} which confirmed the resonant nonradiative energy transfer of $3 \cdot 27.2\ eV$ from atomic hydrogen to atomic K[122],

21.) the spectroscopic observation of the predicted $H^-(1/4)$ ion of hydrogen catalysis by K catalyst at 110 nm corresponding to its predicted binding energy of 11.2 eV[123],

22.) the observation of characteristic emission from Rb^{2+} which confirmed the resonant nonradiative energy transfer of 27.2 eV from atomic hydrogen to Rb^+[124],

23.) the spectroscopic observation of the predicted $H^-(1/2)$ ion of hydrogen catalysis by Rb^+ catalyst at 407 nm corresponding to its predicted binding energy of 3.05 eV[125],

---

[118] Reference Nos. 11-13, 15-16, 20, 24, 27, 32, 39, 42, 46-47, 51-52, 54-55, 57, 72, 81, 89, 91-93
[119] Reference Nos. 28, 33-36, 50, 63, 67, 71, 73, 75-76, 78, 86-87, 90, 92, 93
[120] Reference Nos. 24, 39, 51, 54-55, 57, 91
[121] Reference No. 24
[122] Reference Nos. 27, 39, 42, 46, 51, 54-55, 57, 81, 89, 91
[123] Reference Nos. 81, 42, 27
[124] Reference Nos. 32, 39, 42, 46, 51, 54-55, 57, 81, 89, 91
[125] Reference No. 32

24.) the observation of $H^-(1/2)$, the hydride ion catalyst product of K^+ / K^+ or Rb^+, at its predicted binding energy of 3.0468 eV by high resolution visible spectroscopy as a continuum threshold at 4068.2 Å and a series of structures peaks separated from the binding energy by an integer multiple of the fine structure of $H(1/2)$ starting at 4071 Å[126],

25.) the observation that the high resolution visible K^+ / K^+ or Rb^+-H_2 plasma emission spectra in the region of 4995 to 4060 Å matched the predicted bound-free hyperfine structure lines E_{HF} of $H^-(1/2)$ calculated from the electron g factor as $E_{HF} = j^2 3.00213\, X 10^{-5} + 3.0563\, eV$ (j is an integer) for $j = 1$ to $j = 39$ (3.0563 eV to 3.1012 eV—the hydride binding energy peak plus one and five times the spin-pairing energy, respectively) to within a 1 part per 10^4[127],

26.) Rb^+ or $2K^+$ catalysts formed a plasma having strong VUV emission with a stationary inverted Lyman population with an overpopulation sufficient for lasing, and emission from $H^-(1/2)$ was observed at 4071 Å corresponding to its predicted binding energy of 3.0468 eV with the fine structure and its predicted bound-free hyperfine structure lines $E_{HF} = j^2 3.00213\, X 10^{-5} + 3.0563\, eV$ (j is an integer) that matched for $j = 1$ to $j = 37$ to within a 1 part per 10^4[128],

Response to comments on former Attachment #38

Referring to Applicant's publication Ref. [45], R. L. Mills, J. He, P. Ray, B. Dhandapani, X. Chen, "Synthesis and Characterization of a Highly Stable Amorphous Silicon Hydride as the Product of a Catalytic Helium-Hydrogen Plasma Reaction", Int. J. Hydrogen Energy, Vol. 28, No. 12, (2003), pp. 1401-1424.

Hydrogen has only one proton; thus it has the smallest XPS cross section. The peak intensities are predicted to be low. However, H is the only element that does not have any other primary peaks in the high binding energy region. These peaks are much more intense than the peaks in the low-binding energy region. Thus, H can be identified. The time of flight secondary ion mass spectroscopy (ToF-SIMS) identified the coatings as hydride by the large SiH^+ peak in the positive spectrum and the dominant H^- in the negative spectrum. X-ray photoelectron spectroscopy (XPS) identified the H content of the SiH coatings as hydride

---

[126] Reference Nos. 39, 42, 46, 57, 81, 89, 91

[127] Reference Nos. 39, 42, 46, 57, 81, 89, 91

[128] Reference Nos. 39, 42, 46, 51, 54, 55, 57, 81, 89, 91

ions, $H^-(1/4)$, $H^-(1/9)$, and $H^-(1/11)$ corresponding to peaks at 11, 43, and 55 eV, respectively.

Referring to the following section of Ref. [45]:

b. XPS Characterization

The XPS survey spectra of the noncoated cleaned commercial silicon wafer (control) and a nickel foil coated with an $\alpha - SiH$ film and exposed to air for 20 min were obtained over the region $E_b = 0\ eV$ to $1200\ eV$ and are shown in Figures 18 and 19, respectively. The survey spectra permitted the determination of all of the elements present and detected shifts in the binding energies of the *Si* $2p$ peak, which also identifies the presence or absence of SiO_2. The major species identified in the XPS spectrum of the control sample were silicon, oxygen, and carbon. The $\alpha - SiH$ sample contained essentially silicon with negligible oxygen and carbon.

The XPS spectra (96-108 eV) in the region of the *Si* $2p$ peak of the noncoated cleaned commercial silicon wafer and a nickel foil coated with an $\alpha - SiH$ film and exposed to air for 20 min. are shown in Figures 20 and 21, respectively. The XPS spectrum of the control silicon wafer shows a large SiO_2 content at 104 eV as given by Wagner et al. [C. D. Wagner, W. M. Riggs, L. E. Davis, J. F. Moulder, G. E. Mulilenberg (Editor), *Handbook of X-ray Photoelectron Spectroscopy*, Perkin-Elmer Corp., Eden Prairie, Minnesota, (1997)]. In contrast, the $\alpha - SiH$ sample had essentially no SiO_2. In addition, spin-orbital coupling gives rise to a split *Si* $2p$ peak in pure silicon, but this peak changed to a single broad peak upon reaction to form the $\alpha - SiH$ film indicative of amorphous silicon.

The XPS spectrum (96-108 eV) in the region of the *Si* $2p$ peak of a nickel foil coated with an $\alpha - SiH$ film and exposed to air for 48 hours before the XPS analysis is shown in Figure 22. Essentially no SiO_2 was observed at 104 eV demonstrating that the sample was extraordinarily stable to air exposure. Perhaps trace $SiOH$ is present in the region of 102 eV potentially due to less than 100% coverage of the surface with the $\alpha - SiH$ film; rather, some silicon deposition may have occurred. In contrast, the XPS spectrum (96-108 eV) in the region of the *Si* $2p$ peak of the *HF* cleaned silicon wafer exposed to air for 10 min. before XPS analysis was essentially fully covered by partial oxides SiO_x such as $SiOH$. The mixed silicon oxide peak in the region of 101.5-104 eV shown in Figure 23 was essentially the same percentage of the *Si* $2p$ as that of the SiO_2 peak of the uncleaned wafer shown at 104 eV in Figure 20. In addition, the *O* $1s$ peak of the $\alpha - SiH$ film exposed to air for 48 hours shown in Figure 24 was negligible; whereas, that of the *HF* cleaned wafer exposed to air for 10 min. was intense as shown in Figure 25.

The 0-70 eV and the 0-85 eV binding energy region of high resolution XPS spectra of the commercial silicon wafer and a HF cleaned silicon wafer exposed to air for 10 min. before XPS analysis are shown in Figures 26 and 27, respectively. Only a large $O\ 2s$ peak in the low binding energy region was observed in each case. The 0-70 eV binding energy region of a nickel foil coated with an $\alpha - SiH$ film and exposed to air for 20 min. before XPS analysis is shown in Figure 28. By comparison of the $\alpha - SiH$ sample to the controls, novel XPS peaks were identified at 11, 43, and 55 eV. These peaks do not correspond to any of the primary elements, silicon, carbon, or oxygen, shown in the survey scan in Figure 19, wherein the peaks of these elements are given by Wagner et al. [C. D. Wagner, W. M. Riggs, L. E. Davis, J. F. Moulder, G. E. Mulilenberg (Editor), *Handbook of X-ray Photoelectron Spectroscopy*, Perkin-Elmer Corp., Eden Prairie, Minnesota, (1997)]. Hydrogen is the only element which does not have primary element peaks; thus, it is the only candidate to produce the novel peaks and correspond to the H content of the SiH coatings. These peaks closely matched and were assigned to hydride ions, $H^-(1/4)$, $H^-(1/9)$, and $H^-(1/11)$, respectively, given by Eqs (4-5). The novel hydride ions are proposed to form by the catalytic reaction of He^+ with atomic hydrogen and subsequent autocatalytic reactions of $H(1/p)$ to form highly stable silicon hydride products $\alpha - SiH$ comprising $SiH(1/p)$ (p is an integer greater than one in Eqs. (4-5)).

The XPS spectra of the $Si\ 2p$ region were analyzed, and it was found that the $Si\ 2p$ peak was shifted 0.3-0.7 eV for the $\alpha - SiH$ films relative to that of the HF cleaned silicon wafer as shown in Figures 21 and 22 compared to Figure 20. The shift was due to the influence of the hydride ions since no other counter ion peaks were observed as shown by the survey scan, Figure 19. The stability and the intensity of the hydride ion peaks in the low binding energy region were correlated with the shift of the $Si\ 2p$ peaks as shown by the shift of 0.3 eV in Figure 21 compared to a 0.7 eV shift in Figure 22. This provides further evidence of a novel $\alpha - SiH$ film with increased stability due to the novel hydride ions.

These results indicate that the plasma reaction formed a highly stable novel hydrogenated coating; whereas, the control comprised an oxide coating or an ordinary hydrogen terminated silicon surface which rapidly formed an oxide passivation layer. The hydrogen content of the $\alpha - SiH$ coating appears to be novel hydride ions with high binding energies which account for the exceptional air stability.

The additional reported data supports the catalytic reaction and products of the Invention. Specifically, microwave helium-hydrogen plasmas showed extraordinary broadening, and the corresponding extremely high hydrogen-atom temperature of 180 - 210 eV

was observed with the presence of helium ion catalyst only with hydrogen present. Using water bath calorimetry, excess power was observed from the helium-hydrogen plasma compared to control krypton plasma. For a 8.1 W input, the thermal output power of the helium-hydrogen plasma was measured to be 30.0 W corresponding to 21.9 W of excess power in 3 cm^3. The excess power density and energy balance were high, 7.3 W/cm^3 and $-2.9\,X\,10^4\ kJ/mole\,H_2$, respectively.

The energetic plasma reaction was used to synthesize a potentially commercially important product. Nickel substrates were coated by the reaction product of a low pressure microwave discharge plasma of SiH_4 (2.5%)/He (96.6%)/H_2 (0.9%). The ToF-SIMS identified the coatings as hydride by the large SiH^+ peak in the positive spectrum and the dominant H^- in the negative spectrum. XPS identified the H content of the SiH coatings as hydride ions, $H^-(1/4)$, $H^-(1/9)$, and $H^-(1/11)$ corresponding to predicted peaks at 11, 43, and 55 eV, respectively (See the Hydrino Hydride Ion section of Ref. [1]). The novel hydride ions are proposed to form by the catalytic reaction of He^+ with atomic hydrogen and subsequent autocatalytic reactions of $H(1/p)$ to form highly stable silicon hydride products $SiH(1/p)$ (p is an integer greater than one in Eqs. (4-5)) of Ref [R. Mills, "Spectroscopic Identification of a Novel Catalytic Reaction of Atomic Hydrogen and the Hydride Ion Product", Int. J. Hydrogen Energy, Vol. 26, No. 10, (2001), pp. 1041-1058]. The SiH coating was amorphous as indicated by the shape of the $Si\ 2p$ peak and was remarkably stable to air exposure. After a 48 hour exposure to air, essentially no oxygen was observed as evidence by the negligible $O\ 1s$ peak at 531 eV and absence of any SiO_x $Si\ 2p$ peak in the region of 102-104 eV. The highly stable amorphous silicon hydride coating may advance the production of integrated circuits and microdevices by resisting the oxygen passivation of the surface and possibly altering the dielectric constant and band gap to increase device performance.

Water is not present in the plasma. The amorphous silicon layer is formed from a plasma containing silane which is violently explosive on exposure to water vapor. Oxygen and carbon are only present in trace. The survey spectrum and the ToF-SIMS analysis does not show any impurities that explain the peaks in the low binding energy region proposed by the Examiner. The Examiner proposes no specific alternative assignment. This is not good science. The Examiner's credibility is further eroded given his reliance on a argument in which he has erred regarding the Applicant's assignment of the He II line in Table 1 of reference [28], and his presentation of the Solar spectrum as equivalent to that of a pure helium-hydrogen (98/2%) plasma further undermines his scientific credibility.

Response to Arguments "Specifically regarding Attachment #1"

The NASA-funded team conducted independent studies of Balmer line broadening, power balance, and H line inversion on Applicant's plasma. The Applicant's results were replicated demonstrating the utility of the Applicant's Invention.

Specifically, referring to Ref. 44 of the document entitled **Independent Test Results** which is attached:

44. **A. J. Marchese, P. M. Jansson, J. L. Schmalzel, "The BlackLight Rocket Engine", Phase I Final Report, NASA Institute for Advanced Concepts Phase I, May 1-November 30, 2002, http://www.niac.usra.edu/files/studies/final_report/pdf/752Marchese.pdf.**

Rowan University Professors A. J. Marchese, P. M. Jansson, J. L. Schmalzel performed verification studies as visiting researchers at BlackLight Power, Cranbury, NJ. The prior reported results of BlackLight Power, Inc. of extraordinarily broadened atomic hydrogen lines, population inversion, lower-energy hydrogen lines, and excess power measured by water bath calorimetry were replicated. The application of the energetic hydrogen to propulsion was studied.

Specifically, the data supporting hydrinos was replicated. See

i.) BlackLight Process Theory (pp. 10-12) which gives the theoretical energy levels for hydrinos and the catalytic reaction to form hydrinos,

ii.) Unique Hydrogen Line Broadening in Low Pressure Microwave Water Plasmas (pp. 25-27, particularly Fig. 21) which shows that in the same microwave cavity driven at the same power, the temperature of the hydrogen atoms in the microwave plasma where the hydrino reaction was active was 50 times that of the control based on the spectroscopic line widths,

iii.) Inversion of the Line Intensities in Hydrogen Balmer Series (pp. 27-28, particularly Fig. 22) which shows for the first time in 40 years of intensive worldwide research that atomic hydrogen population inversion was achieved in a steady state plasma and supports the high power released from the reaction of hydrogen to form hydrinos,

iv.) Novel Vacuum Ultraviolet (VUV) Vibration Spectra of Hydrogen Mixture Plasmas (pp. 28-29, particularly Fig. 23) which shows a novel vibrational series of lines in a helium-hydrogen plasmas at energies higher than any known vibrational series and it identically matches the theoretical prediction of 2 squared times the corresponding vibration of the ordinary hydrogen species, and

v.) Water Bath Calorimetry Experiments Showing Increased Heat Generation (pp. 29-30, particularly Fig. 25) that shows that with exactly the same system and same input power,

the heating of the water reservoir absolutely measured to 1% accuracy was equivalent to 55 to 62 W with the catalyst-hydrogen mixture compared to 40 W in the control without the possibility of the reaction to form hydrinos.

Response to Arguments "Specifically regarding Attachments #46 and #53"

The response to the Balmer line broadening issue raise by the Examiner is covered in **Appendix #2** and at **Appendix d**. The deviations based on Maxwell's equations are fully compliant with electromagnetic theory and special relativity; whereas, QM has serious problems as discussed in:

94. R. L. Mills, "The Nature of the Chemical Bond Revisited and an Alternative Maxwellian Approach", J. Phys. D, submitted.
80. R. L. Mills, The Fallacy of Feynman's Argument on the Stability of the Hydrogen Atom According to Quantum Mechanics, Foundations of Physics, submitted.
58. R. L. Mills, "Classical Quantum Mechanics", Physics Essays, submitted.
53. R. Mills, "A Maxwellian Approach to Quantum Mechanics Explains the Nature of Free Electrons in Superfluid Helium", Theoretical Chemistry Accounts, submitted.
22. R. Mills, "The Grand Unified Theory of Classical Quantum Mechanics", Global Foundation, Inc. Orbis Scientiae entitled *The Role of Attractive and Repulsive Gravitational Forces in Cosmic Acceleration of Particles The Origin of the Cosmic Gamma Ray Bursts*, (29th Conference on High Energy Physics and Cosmology Since 1964) Dr. Behram N. Kursunoglu, Chairman, December 14-17, 2000, Lago Mar Resort, Fort Lauderdale, FL, Kluwer Academic/Plenum Publishers, New York, pp. 243-258.
21. R. Mills, "The Grand Unified Theory of Classical Quantum Mechanics", Int. J. Hydrogen Energy, Vol. 27, No. 5, (2002), pp. 565-590.
17. R. Mills, "The Nature of Free Electrons in Superfluid Helium--a Test of Quantum Mechanics and a Basis to Review its Foundations and Make a Comparison to Classical Theory", Int. J. Hydrogen Energy, Vol. 26, No. 10, (2001), pp. 1059-1096.
5. R. Mills, "The Hydrogen Atom Revisited", Int. J. of Hydrogen Energy, Vol. 25, Issue 12, December, (2000), pp. 1171-1183.
1. R. Mills, *The Grand Unified Theory of Classical Quantum Mechanics*, September 2001 Edition, BlackLight Power, Inc., Cranbury, New Jersey, Distributed by Amazon.com; July 2003 Edition posted at www.blacklightpower.com.

1. Response to Examiner's Argument that "Applicant's fractional hydrogen levels are

postulated, not derived from first principle"

The derivation from Maxwell's equations for atom hydrogen states having principle energy levels given by

$$E_n = -\frac{e^2}{n^2 8\pi\varepsilon_o a_H} = -\frac{13.598\ eV}{n^2}$$

where

$$n = \frac{1}{2}, \frac{1}{3}, \frac{1}{4}, ..., \frac{1}{p};\quad p \text{ is an integer; } p \le 137$$

is given in Chps. 1-2, 5-6 of Ref. [1]:

1. R. Mills, *The Grand Unified Theory of Classical Quantum Mechanics*, September 2001 Edition, BlackLight Power, Inc., Cranbury, New Jersey, Distributed by Amazon.com; July 2003 Edition posted at www.blacklightpower.com.

Here it is shown that the lower-energy states are equally valid as the excited states, but require a nonradiative energy transfer to cause the transition rather than being spontaneously radiative. The mechanism discussed in **#b**.

2. Response to Examiner's Argument that "Applicant misunderstands all stationary atomic states are non radiative"

The Examiner does not understand QM. The SE and Dirac equations are not electrostatic. The electron is a point particle with kinetic energy implicit in the Hamiltonian as given in QM textbooks such as McQuarrie [D. A. McQuarrie, *Quantum Chemistry*, University Science Books, Mill Valley, CA, (1983)]. In order for the electron to be stationary, it would have to be everywhere at once, traveling at infinite speed, a situation in violation of special relativity, conservation of energy, Maxwell's equations, as well as other first principles. According to the generally accepted Born interpretation of the meaning of the wavefunction, the probability of finding the electron between r, θ, ϕ and $r + dr, \theta + d\theta, \phi + d\phi$ is given by

$$\int \Psi(r,\theta,\phi)\Psi^*(r,\theta,\phi) dr d\theta d\phi$$

The electron IS VIEWED AS A DISCRETE PARTICLE that moves here and there (from $r = 0$ to $r = \infty$), and $\Psi\Psi^*$ gives the time average of this MOTION. The Schrödinger equation possesses terms corresponding to the electron radial and angular kinetic energy which sum with the potential energy to give the total energy. These are necessary conditions for an electron bound by a central field [H. Margenau, G. M. Murphy, *The Mathematics of Chemistry*

and Physics, D. Van Nostrand Company, Inc., New York, (1956), Second Edition, pp. 363-367]. Herman Haus derived a test of radiation based on Maxwell's equations [Haus, H. A., "On the radiation from point charges", American Journal of Physics, 54, (1986), pp. 1126-1129]. Applying Haus's theorem to the point particle that must have radial kinetic energy demonstrates that the Schrödinger solution for the $n = 1$ state of hydrogen is radiative; thus, it violates Maxwell's equations. Since none is observed for the $n = 1$ state, QM is inconsistent with observation. The derivation is shown in the "Schrödinger Wave Functions in Violation of Maxwell's Equations" section of Ref. [1].

So, off course the point electron having a average trajectory given by the probability wave will radiate (taking this interpretation of Ψ among others as discussed by Laloë [F. Laloë, Do we really understand quantum mechanics? Strange correlations, paradoxes, and theorems, Am. J. Phys. 69 (6), June 2001, 655-701). Feynman knew this very well. He attempted to qualitatively remove the radiation using the Heisenberg Uncertainty Principle (HUP). This attempt is shown to be fatally flawed as discussed in depth in Ref. [80]. Here, it is shown that the quantum theories of Bohr, Schrödinger, and Dirac provide no intrinsic stability of the hydrogen atom based on physics. An old argument from Feynman based on the HUP is shown to be internally inconsistent and fatally flawed. This argument further brings to light the many inconsistencies and shortcomings of QM and the intrinsic HUP that have not been reconciled from the days of their inception. The issue of stability to radiation is resolved by CQM, and the solution eliminates the mysteries and intrinsic problems of QM.

The instability of the hydrogen atom with respect to radiation according to Maxwell's equations is discussed in the following references:

94. R. L. Mills, "The Nature of the Chemical Bond Revisited and an Alternative Maxwellian Approach", J. Phys. D, submitted.

80. R. L. Mills, The Fallacy of Feynman's Argument on the Stability of the Hydrogen Atom According to Quantum Mechanics, Foundations of Physics, submitted.

58. R. L. Mills, "Classical Quantum Mechanics", Physics Essays, submitted.

53. R. Mills, "A Maxwellian Approach to Quantum Mechanics Explains the Nature of Free Electrons in Superfluid Helium", Theoretical Chemistry Accounts, submitted.

17. R. Mills, "The Nature of Free Electrons in Superfluid Helium--a Test of Quantum Mechanics and a Basis to Review its Foundations and Make a Comparison to Classical Theory", Int. J. Hydrogen Energy, Vol. 26, No. 10, (2001), pp. 1059-1096.

5. R. Mills, "The Hydrogen Atom Revisited", Int. J. of Hydrogen Energy, Vol. 25, Issue 12, December, (2000), pp. 1171-1183.

1. R. Mills, *The Grand Unified Theory of Classical Quantum Mechanics*, July 2003 Edition posted at www.blacklightpower.com The Schrödinger Wavefunction in Violation of

Maxwell's Equations section, Chp 35.

Also, from Weisskopf [V. F. Weisskopf, Reviews of Modern Physics, Vol. 21, No. 2, (1949), pp. 305-315], "Dirac's quantum electrodynamics gave a more consistent derivation of the results of the correspondence principle, but it also brought about a number of new and serious difficulties." Quantum electrodynamics; 1.) **does not explain nonradiation of bound electrons**; 2.) contains an internal inconsistency with special relativity regarding the classical electron radius—the electron mass corresponding to its electric energy is infinite; 3.) it admits solutions of negative rest mass and negative kinetic energy; 4.) the interaction of the electron with the predicted zero-point field fluctuations leads to infinite kinetic energy and infinite electron mass; 5.) Dirac used the unacceptable states of negative mass for the description of the vacuum; yet, infinities still arise.

The Examiner has not correctly read the Applicant's theory. The exited states are predicted to be radiative as shown in Chp. 6 of Ref. [1]. The instability to radiation arises due to a radial dipole in the spacetime Fourier transform of the current-density function of the excited state. In this case there are nonvanishing Fourier components synchronous with waves traveling at the speed of light. Thus, the states are radiative.

The radial Dirac delta function is stable in the case of an integer central field. The radiation instability is due to the field of the excited state photon at the electron as given in the Instability of Excited States section of Ref. [1]. In this case, the superposition of the field of the proton and the excited state photon is not an integer, rather it is a fraction. Then, spacetime harmonics of $\frac{\omega_n}{c} = k$ or $\frac{\omega_n}{c}\sqrt{\frac{\varepsilon}{\varepsilon_o}} = k$ do exist for which the spacetime Fourier transform of the current density function is nonzero. Thus, radiation is predicted for excited states, but not the n=1 states; even though, the electron function is a radial Dirac delta function in both cases. The radiative condition based on the Fourier transform is given by

H. A. Haus, On the radiation from point charges, *American Journal of Physics*, **54**, 1126–1129 (1986)

J. Daboul and J. H. D. Jensen, Z. Physik, Vol. 265, (1973), pp. 455-478.

T. A. Abbott and D. J. Griffiths, Am. J. Phys., Vol. 53, No. 12, (1985), pp. 1203-1211.

G. Goedecke, Phys. Rev 135B, (1964), p. 281.

P. Pearle, Foundations of Physics, "Absence of radiationless motions of relativistically rigid classical electron", Vol. 7, Nos. 11/12, (1977), pp. 931-945.

In contrast to QM, CQM derives the fully relativistic stability from Maxwell's equations as given in Chp 1 of Ref. [1] and Ref. [58].

3. Response to Examiner's Argument that "Applicant misunderstands why excited states do radiate, but the ground state do not"

The Examiners dipole operator and probabilities waves does nothing to remove the instability with respect to radiation according to Maxwell's equations for a point electron moving in a central coulomb field. Furthermore, the eigenvalues and eigenfunctions are completely arbitrary as shown in the Schrödinger States Below n=1 section of Ref. [17]. In this case, transitions to an infinite number of states lower than the 13.6 eV state are predicted by QM according to the Examiner's nonphysical reasoning. Furthermore, the n=1 state is purely a consequence of a definition in the infinite number of solutions to the Laguerre differential equation. Neither the Schrödinger equation or the Dirac equation solve the atom correctly. The solutions are inconsistent with physicals laws and numerous experimental observations as discussed previously[129].

A summary of the stability result from Maxwell's equations given in the INTRODUCTION section of Ref. [1] follows. The derivations are given in Chp. 6 of Ref. [1].

INSTABILITY OF EXCITED STATES

For the excited (integer quantum) energy states of the hydrogen atom, σ_{photon}, the two-dimensional surface charge due to the "trapped photons" at the orbitsphere, is given by Eqs. (2.6) and (2.11).

$$\sigma_{photon} = \frac{e}{4\pi(r_n)^2}\left[Y_0^0(\theta,\phi) - \frac{1}{n}\left[Y_0^0(\theta,\phi) + \mathrm{Re}\left\{Y_\ell^m(\theta,\phi)e^{i\omega_n t}\right\}\right]\right]\delta(r-r_n) \quad n = 2,3,4,\ldots, \tag{I.59}$$

Whereas, $\sigma_{electron}$, the two-dimensional surface charge of the electron orbitsphere is

$$\sigma_{electron} = \frac{-e}{4\pi(r_n)^2}\left[Y_0^0(\theta,\phi) + \mathrm{Re}\left\{Y_\ell^m(\theta,\phi)e^{i\omega_n t}\right\}\right]\delta(r-r_n) \tag{I.60}$$

The superposition of σ_{photon} (Eq. (I.59)) and $\sigma_{electron}$ (Eq. (I.60)), where the spherical harmonic functions satisfy the conditions given in the Angular Function section, is equivalent to the sum of a radial electric dipole represented by a doublet function and a radial electric monopole represented by a delta function.

$$\sigma_{photon} + \sigma_{electron} = \frac{e}{4\pi(r_n)^2}\left[Y_0^0(\theta,\phi)\dot{\delta}(r-r_n) - \frac{1}{n}Y_0^0(\theta,\phi)\delta(r-r_n) - \left(1+\frac{1}{n}\right)\left[\mathrm{Re}\left\{Y_\ell^m(\theta,\phi)e^{i\omega_n t}\right\}\right]\delta(r-r_n)\right]$$
$$n = 2,3,4,\ldots, \tag{I.61}$$

---

[129] Reference Nos. 1, 5, 17, 53, 58, 80, 94

where

$$\left[+\delta(r-r_n)-\delta(r-r_n)\right]=\dot{\delta}(r-r_n) \tag{I.62}$$

The Fourier transform of the current-density function that follows from the spacetime Fourier transform of Eq. (I.61), the superposition of σ_{photon} (Eq. (I.59)) and $\sigma_{electron}$ (Eq. (I.60)), is

$$K(s,\Theta,\Phi,\omega)=4\pi s_n\omega_n\frac{\cos(2s_nr_n)}{2s_nr_n}\otimes 2\pi\sum_{\upsilon=1}^{\infty}\frac{(-1)^{\upsilon-1}(\pi\sin\Theta)^{2(\upsilon-1)}}{(\upsilon-1)!(\upsilon-1)!}\frac{\Gamma\left(\frac{1}{2}\right)\Gamma\left(\upsilon+\frac{1}{2}\right)}{(\pi\cos\Theta)^{2\upsilon+1}2^{\upsilon+1}}\frac{2\upsilon!}{(\upsilon-1)!}s^{-2\upsilon}$$

$$\otimes 2\pi\sum_{\upsilon=1}^{\infty}\frac{(-1)^{\upsilon-1}(\pi\sin\Phi)^{2(\upsilon-1)}}{(\upsilon-1)!(\upsilon-1)!}\frac{\Gamma\left(\frac{1}{2}\right)\Gamma\left(\upsilon+\frac{1}{2}\right)}{(\pi\cos\Phi)^{2\upsilon+1}2^{\upsilon+1}}\frac{2\upsilon!}{(\upsilon-1)!}s^{-2\upsilon}\frac{1}{4\pi}[\delta(\omega-\omega_n)+\delta(\omega+\omega_n)] \tag{I.63}$$

Consider the radial wave vector of the cosine function of Eq. (I.63). When the radial projection of the velocity is c

$$\mathbf{s}_n\bullet\mathbf{v}_n=\mathbf{s}_n\bullet\mathbf{c}=\omega_n \tag{I.64}$$

the relativistically corrected wavelength is

$$r_n=\lambda_n \tag{I.65}$$

Substitution of Eq. (I.65) into the cosine function does not result in the vanishing of the Fourier transform of the current-density function. Thus, spacetime harmonics of $\frac{\omega_n}{c}=k$ or $\frac{\omega_n}{c}\sqrt{\frac{\varepsilon}{\varepsilon_o}}=k$ do exist for which the Fourier transform of the current-density function is nonzero. An excited state is metastable because it is the sum of nonradiative (stable) and radiative (unstable) components and de-excites with a transition probability given by the ratio of the power to the energy of the transition [Jackson, J. D., Classical Electrodynamics, Second Edition, John Wiley & Sons, New York, (1975), pp. 758-763].

STABILITY OF "GROUND" AND HYDRINO STATES

For the below "ground" (fractional quantum) energy states of the hydrogen atom, σ_{photon}, the two-dimensional surface charge due to the "trapped photon" at the electron orbitsphere, is given by Eqs. (5.13) and (2.11).

$$\sigma_{photon}=\frac{e}{4\pi(r_n)^2}\left[Y_0^0(\theta,\phi)-\frac{1}{n}\left[Y_0^0(\theta,\phi)+\mathrm{Re}\left\{Y_\ell^m(\theta,\phi)e^{i\omega_n t}\right\}\right]\right]\delta(r-r_n)\quad n=1,\frac{1}{2},\frac{1}{3},\frac{1}{4},\ldots, \tag{I.66}$$

And, $\sigma_{electron}$, the two-dimensional surface charge of the electron orbitsphere is

$$\sigma_{electron} = \frac{-e}{4\pi(r_n)^2}\left[Y_0^0(\theta,\phi) + \mathrm{Re}\left\{Y_\ell^m(\theta,\phi)e^{i\omega_n t}\right\}\right]\delta(r-r_n) \tag{I.67}$$

The superposition of σ_{photon} (Eq. (I.66)) and $\sigma_{electron}$, (Eq. (I.67)) where the spherical harmonic functions satisfy the conditions given in the Angular Function section is a radial electric monopole represented by a delta function.

$$\sigma_{photon} + \sigma_{electron} = \frac{-e}{4\pi(r_n)^2}\left[\frac{1}{n}Y_0^0(\theta,\phi) + \left(1+\frac{1}{n}\right)\mathrm{Re}\left\{Y_\ell^m(\theta,\phi)e^{i\omega_n t}\right\}\right]\delta(r-r_n) \quad n = 1,\frac{1}{2},\frac{1}{3},\frac{1}{4},\ldots, \tag{I.68}$$

As given in the Spacetime Fourier Transform of the Electron Function section of Ref. [1], the radial delta function does not possess spacetime Fourier components synchronous with waves traveling at the speed of light (Eqs. (I.19-I.21)). Thus, the below "ground" (fractional quantum) energy states of the hydrogen atom are stable. The "ground" ($n = 1$ quantum) energy state is just the first of the nonradiative states of the hydrogen atom; thus, it is the state to which excited states decay.

A summary of the stability derivation based on the Haus condition given in Chp. 1 of Ref. [1] is

Nonradiation Based on the Spacetime Fourier Transform of the Electron Current

Although an accelerated *point* particle radiates, an *extended distribution* modeled as a superposition of accelerating charges does not have to radiate. The spacetime Fourier transform of the current-density function is

$$K(s,\Theta,\Phi,\omega) = 4\pi\omega_n \frac{\sin(2sr_n)}{2sr_n} \otimes 2\pi\sum_{\upsilon=1}^{\infty} \frac{(-1)^{\upsilon-1}(\pi\sin\Theta)^{2(\upsilon-1)}}{(\upsilon-1)!(\upsilon-1)!} \frac{\Gamma\left(\frac{1}{2}\right)\Gamma\left(\upsilon+\frac{1}{2}\right)}{(\pi\cos\Theta)^{2\upsilon+1}2^{\upsilon+1}} \frac{2\upsilon!}{(\upsilon-1)!} s^{-2\upsilon}$$

$$\otimes 2\pi\sum_{\upsilon=1}^{\infty} \frac{(-1)^{\upsilon-1}(\pi\sin\Phi)^{2(\upsilon-1)}}{(\upsilon-1)!(\upsilon-1)!} \frac{\Gamma\left(\frac{1}{2}\right)\Gamma\left(\upsilon+\frac{1}{2}\right)}{(\pi\cos\Phi)^{2\upsilon+1}2^{\upsilon+1}} \frac{2\upsilon!}{(\upsilon-1)!} s^{-2\upsilon} \frac{1}{4\pi}[\delta(\omega-\omega_n)+\delta(\omega+\omega_n)]$$

$$\mathbf{s}_n \bullet \mathbf{v}_n = \mathbf{s}_n \bullet \mathbf{c} = \omega_n$$

The relativistically corrected wavelength is

$$\lambda_n = r_n$$

Spacetime harmonics of $\frac{\omega_n}{c} = k$ or $\frac{\omega_n}{c}\sqrt{\frac{\varepsilon}{\varepsilon_o}}$ for which the Fourier transform of the current-density function is nonzero do not exist. Radiation due to charge motion does not occur in any medium when this condition is met.

Haus, H. A., "On the radiation from point charges", American Journal of Physics, 54, (1986), pp. 1126-1129.

Abbott, T. A., Griffiths, D. J., Am. J. Phys., Vol. 153, No. 12, (1985), pp. 1203-1211.

G. Goedecke, Phys. Rev 135B, (1964), p. 281.

A summary of the stability derivation based on the Poynting Power Vector given in Chp. 1, Appendix I of Ref. [1] is

Nonradiation Based on the Electron Electromagnetic Fields and the Poynting Power Vector

Although an accelerated *point* particle radiates, an *extended distribution* modeled as a superposition of accelerating charges does not have to radiate. The general multipole field solution to Maxwell's equations in a source-free region of empty space with the assumption of a time dependence $e^{i\omega_n t}$ is

$$\begin{aligned}\mathbf{B} &= \sum_{\ell,m}\left[a_E(\ell,m)f_\ell(kr)\mathbf{X}_{\ell.m} - \frac{i}{k}a_M(\ell,m)\nabla\times g_\ell(kr)\mathbf{X}_{\ell.m}\right]\\ \mathbf{E} &= \sum_{\ell,m}\left[\frac{i}{k}a_E(\ell,m)\nabla\times f_\ell(kr)\mathbf{X}_{\ell.m} + a_M(\ell,m)g_\ell(kr)\mathbf{X}_{\ell.m}\right]\end{aligned} \tag{1}$$

For the electron source current comprising a multipole of order (ℓ,m), the far fields are given by

$$\begin{aligned}\mathbf{B} &= -\frac{i}{k}a_M(\ell,m)\nabla\times g_\ell(kr)\mathbf{X}_{\ell.m}\\ \mathbf{E} &= a_M(\ell,m)g_\ell(kr)\mathbf{X}_{\ell.m}\end{aligned} \tag{2}$$

and the time-averaged power radiated per solid angle $\frac{dP(\ell,m)}{d\Omega}$ is

$$\frac{dP(\ell,m)}{d\Omega} = \frac{c}{8\pi k^2}\left|a_M(\ell,m)\right|^2\left|\mathbf{X}_{\ell.m}\right|^2 \tag{3}$$

where $a_M(\ell,m)$ is

$$a_M(\ell,m) = \frac{-ek^2}{c\sqrt{\ell(\ell+1)}}\frac{\omega_n}{2\pi}Nj_\ell(kr_n)\Theta\sin(mks) \tag{4}$$

In the case that k is the lightlike k^0, then $k = \omega_n / c$, in Eq. (4), and Eqs. (2-3) vanishes for

$$s = vT_n = R = r_n = \lambda_n \tag{5}$$

There is no radiation.

4. Response to Examiner's Argument that "Applicant misunderstands the most basic fundamentals of the QM theory"

The Applicant rejects the Schrödinger equation. There is no a priori basis for the SE to be the CORRECT equation of nature. In fact it is not even a true wave equation. In this case, the electron velocity is proportional to the frequency squared; consequently, energy and momentum are not conserved for an inverse-squared central Coulombic force as required. There are many other problems beside infinities, instability with respect to radiation according to Maxwell's equations, and the failure to predict spin as discussed previously[130].

The nonradiation boundary condition of the atom requires that the electron be a solution of the two-dimensional wave equation plus time. The derivation is given in the Spacetime Fourier Transform of the Electron Function section and the Angular Function section of Ref. [1] and Ref. [58]. There is no a priori basis why the electron can not obey this wave equation versus one based on a three-dimensions plus time. The subsequent results given in references [131]are remarkably accurate when compared to the corresponding observed values. Thus, the Examiner's position that the radial Dirac delta function must be a solution of the three-dimensional wave equation is irrelevant.

The Applicant's angular functions are solutions of the wave equation as shown in BOX 1.1. DERIVATION OF THE ROTATIONAL PARAMETERS OF THE ELECTRON FROM A SPECIAL CASE OF THE WAVE EQUATION—THE RIGID ROTOR EQUATION of Ref. [1]. The fully relativistic result is stable with respect to radiation and matches the spectrum of hydrogen to the limit of experimental measurement including the electron g factor, fine structure, and Lamb shift as shown in Chps. 1 and 2 of Ref [1].

The Applicant's approach starts with first principles rather than a postulated equation having probability-wave solutions which have no basis in reality[132]. A summary of Applicant's approach is given in the INTRODUCTION section of Ref [1] and the derivation is given in Chp. 1 of Ref. [1]. A further summary is given in Ref. [58] that follows wherein the reference

---

[130] Reference Nos. 1, 5, 17, 53, 58, 80, 94
[131] Reference Nos. 1, 5, 17, 53, 58, 80, 94
[132] Reference Nos. 1, 5, 17, 53, 58, 80, 94

numbers correspond to those in this journal article:

ONE-ELECTRON ATOMS

One-electron atoms include the hydrogen atom, He^{+}, Li^{2+}, Be^{3+}, and so on. The mass-energy and angular momentum of the electron are constant; this requires that the equation of motion of the electron be temporally and spatially harmonic. Thus, the classical wave equation applies and

$$\left[\nabla^2 - \frac{1}{v^2}\frac{\partial^2}{\partial t^2}\right]\rho(r,\theta,\phi,t) = 0 \tag{2}$$

where $\rho(r,\theta,\phi,t)$ is the time dependent charge density function of the electron in time and space. In general, the wave equation has an infinite number of solutions. To arrive at the solution which represents the electron, a suitable boundary condition must be imposed. It is well known from experiments that each single atomic electron of a given isotope radiates to the same stable state. Thus, the physical boundary condition of nonradiation of the bound electron was imposed on the solution of the wave equation for the time dependent charge density function of the electron [1]. The condition for radiation by a moving point charge given by Haus [10] is that its spacetime Fourier transform does possess components that are synchronous with waves traveling at the speed of light. Conversely, it is proposed that the condition for nonradiation by an ensemble of moving point charges that comprises a current density function is

For non-radiative states, the current-density function must NOT possess spacetime Fourier components that are synchronous with waves traveling at the speed of light.

The time, radial, and angular solutions of the wave equation are separable. The motion is time harmonic with frequency ω_n. A constant angular function is a solution to the wave equation. Solutions of the Schrödinger wave equation comprising a radial function radiate according to Maxwell's equation as shown previously by application of Haus' condition [1]. In fact, it was found that any function which permitted radial motion gave rise to radiation. A radial function which does satisfy the boundary condition is a radial delta function

$$f(r) = \frac{1}{r^2}\delta(r - r_n) \tag{3}$$

This function defines a constant charge density on a spherical shell where $r_n = nr_1$ wherein n is an integer in an excited state as given in the Excited States section, and Eq. (2) becomes the two-dimensional wave equation plus time with separable time and angular functions. Given time harmonic motion and a radial delta function, the relationship

between an allowed radius and the electron wavelength is given by

$$2\pi r_n = \lambda_n \tag{4}$$

where the subscript n is determined during photon absorption as given by Eq. (83). Using the observed de Broglie relationship for the electron mass where the coordinates are spherical,

$$\lambda_n = \frac{h}{p_n} = \frac{h}{m_e v_n} \tag{5}$$

and the magnitude of the velocity for *every* point on the orbitsphere is

$$v_n = \frac{\hbar}{m_e r_n} \tag{6}$$

The sum of the $|\mathbf{L}_i|$, the magnitude of the angular momentum of each infinitesimal point of the orbitsphere of mass m_i, must be constant. The constant is $\hbar$.

$$\sum |\mathbf{L}_i| = \sum |\mathbf{r} \times m_i \mathbf{v}| = m_e r_n \frac{\hbar}{m_e r_n} = \hbar \tag{7}$$

Thus, an electron is a spinning, two-dimensional spherical surface (zero thickness), called an *electron orbitsphere*, that can exist in a bound state at only specified distances from the nucleus as shown in Figure 1. The corresponding current function shown in Figure 2 which gives rise to the phenomenon of *spin* is derived in the "Spin Function" section. (See the Appendix and the Orbitsphere Equation of Motion for $\ell = 0$ of Ref. [1] at Chp. 1.)

Nonconstant functions are also solutions for the angular functions. To be a harmonic solution of the wave equation in spherical coordinates, these angular functions must be spherical harmonic functions [13]. A zero of the spacetime Fourier transform of the product function of two spherical harmonic angular functions, a time harmonic function, and an unknown radial function is sought. The solution for the radial function which satisfies the boundary condition is also a delta function given by Eq. (3). Thus, bound electrons are described by a charge-density (mass-density) function which is the product of a radial delta function, two angular functions (spherical harmonic functions), and a time harmonic function.

$$\rho(r,\theta,\phi,t) = f(r)A(\theta,\phi,t) = \frac{1}{r^2}\delta(r - r_n)A(\theta,\phi,t); \qquad A(\theta,\phi,t) = Y(\theta,\phi)k(t) \tag{8}$$

In these cases, the spherical harmonic functions correspond to a traveling charge density wave confined to the spherical shell which gives rise to the phenomenon of orbital angular momentum. The orbital functions which modulate the constant "spin" function shown graphically in Figure 3 are given in the "Angular Functions" section.

The hydrogen molecule is also solved using the nonradiative boundary condition as given in Chp. 12 of Ref. [1] and in Ref. [94], 94. R. L. Mills, "The Nature of the Chemical

Bond Revisited and an Alternative Maxwellian Approach", J. Phys. D, submitted. Here, there is also no a priori reason why the electron must be a solution of the three dimensional wave equation plus time and can not obey a two dimensional wave equation plus time. Furthermore, in addition to the important result of stability to radiation, several more very important physical results are subsequently realized: 1.) The charge is distributed on a two dimension surface; thus, there is no infinities in the corresponding fields. Infinite fields are simply renormalized in the case of the point-particles of quantum mechanics, but it is physically gratifying that none arise in this case since infinite fields have never been measured or realized in the laboratory. 2.) The hydrogen molecular ion or molecule has finite dimensions rather than extending over all space. From measurements of the resistivity of hydrogen as a function of pressure, the finite dimensions of the hydrogen molecule are evident in the plateau of the resistivity versus pressure curve of metallic hydrogen [W. J. Nellis, "Making Metallic Hydrogen", Scientific American, May, (2000), pp. 84-90]. This is in contradiction to the predictions of quantum probability functions such as an exponential radial distribution in space. 3.) Consistent with experiments, neutral scattering is predicted without violation of special relativity wherein a point must be everywhere at once as required in the QM case. 4.) There is no electron self interaction. The continuous charge-density function is a two-dimensional equipotential energy surface with an electric field that is strictly normal for the elliptic parameter $\xi > 0$ (See Sec. III.) according to Gauss' law and Faraday's law. The relationship between the electric field equation and the electron source charge-density function is given by Maxwell's equation in two dimensions [J. A. Stratton, *Electromagnetic Theory*, McGraw-Hill Book Company, (1941), p. 195; J. D. Jackson, Classical Electrodynamics, Second Edition, John Wiley & Sons, New York, (1975), pp. 17-22].

$$\mathbf{n} \bullet (\mathbf{E}_1 - \mathbf{E}_2) = \frac{\sigma}{\varepsilon_0} \tag{12}$$

where $\mathbf{n}$ is the normal unit vector, $\mathbf{E}_1 = 0$ ($\mathbf{E}_1$ is the electric field inside of the MO), $\mathbf{E}_2$ is the electric field outside of the MO and σ is the surface charge density. This relation shows that only a two-dimensional geometry meets the criterion for a fundamental particle. This is the nonsingularity geometry which is no longer divisible. It is the dimension from which it is not possible to lower dimensionality. In this case, there is no electrostatic self interaction since the corresponding potential is continuous across the surface according to Faraday's law in the electrostatic limit, and the field is discontinuous, normal to the charge according to Gauss' law [J. A. Stratton, *Electromagnetic Theory*, McGraw-Hill Book Company, (1941), p. 195; J. D. Jackson, Classical Electrodynamics, Second Edition, John Wiley & Sons, New York, (1975), pp. 17-22; H. A. Haus, J. R. Melcher, "Electromagnetic Fields and Energy", Department of Electrical engineering and Computer Science, Massachusetts Institute of Technology, (1985),

Sec. 5.3]. 5.) The instability of electron-electron repulsion of molecular hydrogen is eliminated since the central field of the hydrogen molecular ion relative to a second electron at $\xi > 0$ which binds to form the hydrogen molecule is that of a single charge at the foci. 6.) The ellipsoidal MO's allow exact spin pairing over all time which is consistent with experimental observation. This aspect is not possible in the QM model. And, 7.) The ellipsoidal MO's allow for the basis of excited states as fully Maxwellian compliant resonator mode excitations and for the ionization of the electron as a plane wave with the $\hbar$ of angular momentum conserved corresponding to the de Broglie wavelength. Physical predictions match the wave-particle duality nature of the free electron as shown in the Electron in Free Space section of Ref [1].

As given previously[133], a proposed solution based on physical laws and fully compliant with Maxwell's equations solves the parameters of molecular ions and molecules of hydrogen isotopes from the Laplacian in elliptic coordinates in closed form equations with fundamental constants only. The boundary condition of nonradiation requires that the electron be a solution of the two-dimensional wave equation plus time. There is no a priori basis why the electron can not obey this wave equation versus one based on three dimensions plus time. The corresponding Dirac delta function in the elliptic parameter ξ gives the physical representation of the bound electron as a two dimensional equipotential surface of charge (mass) density with time-harmonic motion along a geodesic at each position on the surface. The electron molecular orbitals in this case that do not depend on an exchange integral are truly physical rather than purely mathematical. The closed form solutions of H_2^+, D_2^+, H_2, and D_2 given in Table 1 show that hydrogen species can be solved in closed form with tremendous accuracy using first principles. The observed $\sqrt{\frac{k}{\mu}}$ dependency of vibrational energies on the isotope is obtained without the requirement of any imaginary (experimentally not observed) zero-point vibration.

[133] Reference No. 94

Table 1:

The calculated and experimental parameters of H_2, D_2, H_2^+ and D_2^+.

Parameter	Calculated	Experimental	Eqs.[a]
H_2 Bond Energy	4.478 eV	4.478 eV	12.238
D_2 Bond Energy	4.556 eV	4.556 eV	12.240
H_2^+ Bond Energy	2.654 eV	2.651 eV	12.211
D_2^+ Bond Energy	2.696 eV	2.691 eV	12.213
H_2 Total Energy	31.677 eV	31.675 eV	12.234
D_2 Total Energy	31.760 eV	31.760 eV	12.235
H_2 Ionization Energy	15.425 eV	15.426 eV	12.236
D_2 Ionization Energy	15.463 eV	15.466 eV	12.237
H_2^+ Ionization Energy	16.253 eV	16.250 eV	12.209
D_2^+ Ionization Energy	16.299 eV	16.294 eV	12.210
H_2^+ Magnetic Moment	$9.274\,X10^{-24}\,JT^{-1}$ μ_B	$9.274\,X10^{-24}\,JT^{-1}$ μ_B	14.1-14.7
Absolute H_2 Gas-Phase NMR Shift	-28.0 ppm	-28.0 ppm	12.367
H_2 Internuclear Distance[b]	0.748 Å $\sqrt{2}a_o$	0.741 Å	12.225
D_2 Internuclear Distance[b]	0.748 Å $\sqrt{2}a_o$	0.741 Å	12.225
H_2^+ Internuclear Distance[c]	1.058 Å $2a_o$	1.06 Å	12.198
D_2^+ Internuclear Distance[b]	1.058 Å $2a_o$	1.0559 Å	12.198
H_2 Vibrational Energy	0.517 eV	0.516 eV	12.246
D_2 Vibrational Energy	0.371 eV	0.371 eV	12.248
H_2^+ Vibrational Energy	0.270 eV	0.271 eV	12.219
D_2^+ Vibrational Energy	0.193 eV	0.196 eV	12.221
H_2 J=1 to J=0 Rotational Energy[b]	0.0148 eV	0.01509 eV	14.43
D_2 J=1 to J=0 Rotational Energy[b]	0.00741 eV	0.00755 eV	14.35-14.43
H_2^+ J=1 to J=0 Rotational Energy[c]	0.00740 eV	0.00739 eV	14.47
D_2^+ J=1 to J=0 Rotational Energy[b]	0.00370 eV	0.003723 eV	14.35-14.41, 14.47

[a] R. Mills, *The Grand Unified Theory of Classical Quantum Mechanics*, July 2003 Edition, BlackLight Power, Inc., Cranbury, New Jersey, posted at www.blacklightpower.com.

[b] The internuclear distances are not corrected for the reduction due to $\overline{E}_{osc}$.

[c] The internuclear distances are not corrected for the increase due to $\overline{E}_{osc}$.

5. Response to Examiner's Argument that "Applicant is mistaken in understanding and applying Haus's nonradiative condition"

The Examiner is mistaken in his understanding of $\rho(r,t)$. This is the charge as a function of space and time which gives the current. That is, a time dependent charge corresponds to a current.

From the SPACETIME FOURIER TRANSFORM OF THE ELECTRON FUNCTION section of Chp. 1 of Ref. [1] were the references correspond to those in the reference:

Therefore, the spacetime Fourier transform, $M(s,\Theta,\Phi,\omega)$, is the convolution of Eqs. (1.11), (1.35), (1.36), and (1.37).

$$M(s,\Theta,\Phi,\omega) = 4\pi\mathrm{sinc}(2sr_n)\otimes 2\pi\sum_{\upsilon=1}^{\infty}\frac{(-1)^{\upsilon-1}(\pi\sin\Theta)^{2(\upsilon-1)}}{(\upsilon-1)!(\upsilon-1)!}\frac{\Gamma\left(\frac{1}{2}\right)\Gamma\left(\upsilon+\frac{1}{2}\right)}{(\pi\cos\Theta)^{2\upsilon+1}2^{\upsilon+1}}\frac{2\upsilon!}{(\upsilon-1)!}s^{-2\upsilon}$$

$$\otimes 2\pi\sum_{\upsilon=1}^{\infty}\frac{(-1)^{\upsilon-1}(\pi\sin\Phi)^{2(\upsilon-1)}}{(\upsilon-1)!(\upsilon-1)!}\frac{\Gamma\left(\frac{1}{2}\right)\Gamma\left(\upsilon+\frac{1}{2}\right)}{(\pi\cos\Phi)^{2\upsilon+1}2^{\upsilon+1}}\frac{2\upsilon!}{(\upsilon-1)!}s^{-2\upsilon}\frac{1}{4\pi}[\delta(\omega-\omega_n)+\delta(\omega+\omega_n)] \quad (1.39)$$

The condition for nonradiation of a moving charge-density function is that the spacetime Fourier transform of the **current-density function** must not have waves synchronous with waves traveling at the speed of light, that is synchronous with $\frac{\omega_n}{c}$ or synchronous with $\frac{\omega_n}{c}\sqrt{\frac{\varepsilon}{\varepsilon_o}}$ where e is the dielectric constant of the medium. The Fourier transform of the charge-density function of the orbitsphere (bubble of radius r) is given by Eq. (1.39). In the case of time harmonic motion, the **current-density function** is given by the time derivative of the charge-density function. Thus, the **current-density function** is given by the product of the constant angular velocity and the charge-density function. The Fourier transform of the **current-density function** of the orbitsphere is given by the product of the constant angular velocity and Eq. (1.39). Consider the radial and time parts of, $K_\perp$, the Fourier transform of the current-density function where the angular transforms are not zero:

$$K(s,\Theta,\Phi,\omega) = 4\pi\omega_n \frac{\sin(2sr_n)}{2sr_n} \otimes 2\pi \sum_{\upsilon=1}^{\infty} \frac{(-1)^{\upsilon-1}(\pi\sin\Theta)^{2(\upsilon-1)}}{(\upsilon-1)!(\upsilon-1)!} \frac{\Gamma\left(\frac{1}{2}\right)\Gamma\left(\upsilon+\frac{1}{2}\right)}{(\pi\cos\Theta)^{2\upsilon+1}2^{\upsilon+1}} \frac{2\upsilon!}{(\upsilon-1)!} s^{-2\upsilon}$$

$$\otimes 2\pi \sum_{\upsilon=1}^{\infty} \frac{(-1)^{\upsilon-1}(\pi\sin\Phi)^{2(\upsilon-1)}}{(\upsilon-1)!(\upsilon-1)!} \frac{\Gamma\left(\frac{1}{2}\right)\Gamma\left(\upsilon+\frac{1}{2}\right)}{(\pi\cos\Phi)^{2\upsilon+1}2^{\upsilon+1}} \frac{2\upsilon!}{(\upsilon-1)!} s^{-2\upsilon} \frac{1}{4\pi}[\delta(\omega-\omega_n)+\delta(\omega+\omega_n)] \tag{1.40}$$

For the case that the **current-density function** is constant, the delta function of Eq. (1.40) is replaced by a constant. For time harmonic motion, with angular velocity, ω_n, Eq. (1.40) is nonzero only for $\omega = \omega_n$; thus, $-\infty < s < \infty$ becomes finite only for the corresponding wavenumber, s_n. The relationship between the radius and the wavelength is

$$v_n = \lambda_n f_n \tag{1.41}$$

$$v_n = 2\pi r_n f_n = \lambda_n f_n \tag{1.42}$$

$$2\pi r_n = \lambda_n \tag{1.43}$$

The motion on the orbitsphere is angular; however, a radial component exists due to Special Relativistic effects. Consider the radial wave vector of the sinc function. When the radial projection of the velocity is c

$$\mathbf{s}_n \bullet \mathbf{v}_n = \mathbf{s}_n \bullet \mathbf{c} = \omega_n \tag{1.44}$$

the relativistically corrected wavelength is

$$\lambda_n = r_n \tag{1.45}$$

(i.e. the lab frame motion in the angular direction goes to zero as the velocity approaches the speed of light as given by Eq. (24.15)). The charge-density functions in spherical coordinates plus time are given by Eqs. (1.64-1.65). In the case of Eq. (1.64), the wavelength of Eq. (1.44) is independent of θ; whereas, in the case of Eq. (1.65), the wavelength in Eq. (1.44) is a function of $\sin\theta$. Thus, in the latter case, Eq. (1.45) holds wherein the relationship of wavelength and the radius as a function of θ are given by $r_n \sin\theta = \lambda_n \sin\theta$.

The equipotential, uniform or constant charge-density function (Eq. (1.64)) further comprises a **current pattern** given in the ORBITSPHERE EQUATION OF MOTION FOR $\ell = 0$ section and corresponds to the spin function of the electron. It also corresponds to the nonradiative $n = 1$, $\ell = 0$ state of atomic hydrogen. There is acceleration without radiation. In this case, centripetal acceleration. A static charge distribution exists even though each point on the surface is accelerating along a great circle. Haus' condition predicts no radiation for the entire ensemble.

In cases of orbitals of heavier elements and excited states of one electron atoms and atoms or ions of heavier elements which are not constant as given by Eq. (1.65), the

constant spin function is modulated by a time and spherical harmonic function. The modulation or traveling charge-density wave corresponds to an orbital angular momentum in addition to a spin angular momentum. These states are typically referred to as p, d, f, etc. orbitals and correspond to an ℓ quantum number not equal to zero. Haus' condition also predicts nonradiation for a constant spin function modulated by a time and spherically harmonic orbital function. However, in the case that such a state arises as an excited state by photon absorption, it is radiative due to a radial dipole term in its **current-density function** since it possesses spacetime Fourier transform components synchronous with waves traveling at the speed of light as given in the INSTABILITY OF EXCITED STATES section.

Substitution of Eq. (1.45) into the sinc function results in the vanishing of the entire Fourier transform of the **current-density function**. Thus, spacetime harmonics of $\frac{\omega_n}{c} = k$ or $\frac{\omega_n}{c}\sqrt{\frac{\varepsilon}{\varepsilon_o}} = k$ do not exist for which the Fourier transform of the **current-density function** is nonzero. Radiation due to charge motion does not occur in any medium when this boundary condition is met. Note that the boundary condition for the solution of the radial function of the hydrogen atom with the Schrödinger equation is that $\Psi \to 0$ as $r \to \infty$. Here, however, the boundary condition is derived from Maxwell's equations: For non-radiative states, the **current-density function** must not possess spacetime Fourier components that are synchronous with waves traveling at the speed of light. An alternative derivation which provides acceleration without radiation is given by Abbott [134] Bound electrons are described by a charge-density (mass-density) function which is the product of a radial delta function, Eq. (1.3), two angular functions (spherical harmonic functions), and a time harmonic function. This is a solution of Laplace's Equation. Thus, this radial function implies that allowed states are two-dimensional spherical shells (zero thickness) of charge density (and mass density) at specific radii r_n. These shells are referred to as electron orbitspheres. See Figure 1.1 for a pictorial representation of an orbitsphere.

In addition to demonstrating that the Applicant's theory correctly provides for stability of the n=1 state of the hydrogen atom after Haus [Haus, H. A., "On the radiation from point charges", American Journal of Physics, 54, (1986), pp. 1126-1129] and also after others [Abbott, T. A., Griffiths, D. J., Am. J. Phys., Vol. 153, No. 12, (1985), pp. 1203-1211; G. Goedecke, Phys. Rev 135B, (1964), p. 281], Applicant shows that the electron solutions are

---

[134] Reference No. 11

stable according to the Poynting Power Vector derived from the **current-density functions** as given in Appendix I of Ref. [1]. A summary follows:

Nonradiation Based on the Electron Electromagnetic Fields and the Poynting Power Vector

The general multipole field solution to Maxwell's equations in a source-free region of empty space with the assumption of a time dependence $e^{i\omega_n t}$ is

$$\mathbf{B} = \sum_{\ell,m}\left[a_E(\ell,m) f_\ell(kr)\mathbf{X}_{\ell.m} - \frac{i}{k} a_M(\ell,m)\nabla \times g_\ell(kr)\mathbf{X}_{\ell.m}\right]$$
$$\mathbf{E} = \sum_{\ell,m}\left[\frac{i}{k} a_E(\ell,m)\nabla \times f_\ell(kr)\mathbf{X}_{\ell.m} + a_M(\ell,m) g_\ell(kr)\mathbf{X}_{\ell.m}\right] \quad (1)$$

For the electron source current comprising a multipole of order (ℓ,m), the far fields are given by

$$\mathbf{B} = -\frac{i}{k} a_M(\ell,m)\nabla \times g_\ell(kr)\mathbf{X}_{\ell.m}$$
$$\mathbf{E} = a_M(\ell,m) g_\ell(kr)\mathbf{X}_{\ell.m} \quad (2)$$

and the time-averaged power radiated per solid angle $\frac{dP(\ell,m)}{d\Omega}$ is

$$\frac{dP(\ell,m)}{d\Omega} = \frac{c}{8\pi k^2}\left|a_M(\ell,m)\right|^2 \left|\mathbf{X}_{\ell.m}\right|^2 \quad (3)$$

where $a_M(\ell,m)$ is

$$a_M(\ell,m) = \frac{-ek^2}{c\sqrt{\ell(\ell+1)}} \frac{\omega_n}{2\pi} N j_\ell(kr_n)\Theta \sin(mks) \quad (4)$$

In the case that k is the lightlike k^0, then $k = \omega_n / c$, in Eq. (4), and Eqs. (2-3) vanishes for

$$s = vT_n = R = r_n = \lambda_n \quad (5)$$

There is no radiation.

Of course, the QM solutions are not stable with respect to radiation and violate Maxwell's equations as discussed in Chp. 35 of Ref. [1] and elsewhere[135].

5.(repeated) Response to Examiner's Argument "Applicant is confusing QM eigenfunction with QM wave equation"

The Applicant solves the spin and orbital angular momenta and energies physically

---

[135] Reference Nos. 1, 5, 17, 21, 22, 53, 58, 80, 94

rather than purely mathematically. The distinction between an eigenfunction and a "wavefunction comprised of eigenfunctions" for the solution of the bound electron is due entirely to a mathematical postulate of QM. It has no basis in physics and in fact leads to consequences that are not physically tenable as shown *infra*. In the CQM solutions, the constant function integrates to the charge of an electron and the modulation function integrates to zero where the functions are charge and current density-functions rather than probability waves. They are not squared as required in QM. They are not required to yield the Kroenecker delta as they are in the case of QM. This is a nonphysical and nonsensical consequence of QM since Ψ as a probability wave has no basis in reality as discussed previously in Ref. [1, 5, 17, 21, 22, 53, 58, 80, 94] and by Laloë [F. Laloë, Do we really understand quantum mechanics? Strange correlations, paradoxes, and theorems, Am. J. Phys. 69 (6), June 2001, 655-701]. Furthermore, the Examiner's requirement of taking linear combinations of eigenfunctions to result in a "wavefunction" solution to avoid violating the Uncertainty Principle is internally inconsistent with Examiner's point # **6** wherein the Examiner claims the SE spherical harmonic solutions can not be linear combinations since the Kroenecker delta is not obtained as required since the probability density functions must be squared.

The orbital energy of $Y_0^0(\theta,\phi)$ is zero, but the spin energy is given by Eq. (1.82) of Ref. [1]. The orbital energy of $Y_\ell^m(\theta,\phi)$ has a magnitude given by Eq. (1.95) of Ref. [1] that has a time average of zero since it comprises a spherical and time-harmonic modulation wave of the constant spin function as given by Eq. (1.98) of Ref. [1]. The results agree with experimental observations as shown in Chp. 1 and 2 of Ref. [1]. (Also see **#7** of this Response.)

The QM approach outlined by the Examiner can further be showed to be fatally flawed. For example, as discussed in Ref. [80] for $n = 1$, $\ell = 0$; thus, K_{rot} is **zero** which is impossible since the kinetic energy is $\frac{\hbar^2}{2mr^2}$:

2.) Eq. (3) follows from the Schrödinger equation, not the Bohr theory. In the time independent Schrödinger equation, the kinetic energy of rotation K_{rot} is given by [H. Margenau, G. M. Murphy, *The Mathematics of Chemistry and Physics*, D. Van Nostrand Company, Inc., New York, (1956), Second Edition, pp. 363-367]

$$K_{rot} = \frac{\ell(\ell+1)\hbar^2}{2mr^2} \tag{11}$$

where

$$L = \sqrt{\ell(\ell+1)\hbar^2} \tag{12}$$

is the value of the electron angular momentum L for the state $Y_{lm}(\theta,\phi)$[136]. For the n=1 state, $\ell = 0$; thus, **the angular momentum according to the Schrödinger equation is exactly zero—not $\hbar$**. Furthermore, the kinetic energy of rotation K_{rot} is also **zero**. As a consequence, it is internally inconsistent for Feynman to accept the HUP which arises from the Schrödinger equation on the one hand and that the electron obeys the classical Coulomb law and is bound in an inverse squared Coulomb field on the other. Rather than a kinetic energy of $\frac{\hbar^2}{2mr^2}$ which is added to the Coulomb energy of $-\frac{e^2}{r}$ to get the total energy, exactly zero should be added to the Coulomb energy. This is an inescapable nonsensical result which arises from the SE directly, and it can not be saved by incorrectly assigning the angular momentum as $\hbar$ from the uncertainty relationship. Furthermore, the result that $L = K_{rot}$ **= exactly zero violates the HUP making the argument further internally inconsistent.**

Further nonsensical results arise for the purely mathematical approach of QM promoted by the Examiner. From Ref. [17]:

> For the Schrödinger equation, the kinetic energy of rotation K_{rot} is given by
>
> $$K_{rot} = \frac{\ell(\ell+1)\hbar^2}{2mr^2} \tag{10}$$
>
> where
>
> $$L = \sqrt{\ell(\ell+1)\hbar^2} \tag{11}$$
>
> is the value of the electron angular momentum L for the state $Y_{lm}(\theta,\phi)$.

The POSTULATED Schrödinger Equation Fails to Solve the Hydrogen Atom

---

[136] At page 365 Margenau and Murphy [H. Margenau, G. M. Murphy, *The Mathematics of Chemistry and Physics*, D. Van Nostrand Company, Inc., New York, (1956), Second Edition, pp. 363-367] state

" but with the term $\frac{\ell(\ell+1)\hbar^2}{2mr^2}$ added to the normal potential energy. What is the meaning of that term? In classical mechanics, the energy of a particle moving in three dimensions differs from that of a one-dimensional particle by the kinetic energy of rotation, $\frac{1}{2}mr^2\omega^2$. This is precisely the quantity $\frac{\ell(\ell+1)\hbar^2}{2mr^2}$, for we have seen that $\ell(\ell+1)\hbar^2$ is the *certain* value of the square of the angular momentum for the state Y_ℓ, in classical language $(mr^2\omega^2)^2$ which is divided by $2mr^2$, gives exactly the kinetic energy of rotation."

Correctly.

• In the time independent Schrödinger equation, the kinetic energy of rotation K_{rot} is given by Eq. (10) where the value of the electron angular momentum L for the state $Y_{lm}(\theta,\phi)$ is given by Eq. (11). The Schrödinger equation solutions, Eq. (10) and Eq. (11), predict that the ground state electron has zero angular energy and zero angular momentum, respectively.

• The Schrödinger equation solution, Eq. (11), predicts that the ionized electron may have infinite angular momentum.

• The Schrödinger equation solutions, Eq. (10) and Eq. (11), predict that the excited state rotational energy levels are nondegenerate as a function of the ℓ quantum number even in the absence of an applied magnetic field, and the predicted energy is over six orders of magnitude of the observed nondegenerate energy in the presence of a magnetic field. In the absence of a magnetic field, no preferred direction exists. In this case, the ℓ quantum number is a function of the orientation of the atom with respect to an arbitrary coordinate system. Therefore, the nondegeneracy is nonsensical and violates conservation of angular momentum of the photon.

It is absolutely physically correct and mathematically correct to solve the spin and orbital function independently since there is no a priori reason why they have to be a single eigenfunction or product of eigenfunctions. After all, they are independent physical phenomena. The two dimensional wave equation plus time is given by McQuarrie [McQuarrie, D. A., *Quantum Chemistry*, University Science Books, Mill Valley, CA, (1983), p. 207]. It is mathematically identical to the familiar rigid rotor equation of QM. The electron is confined to two dimensions (θ and ϕ) plus time, and the corresponding wave equation solution is called an electron orbitsphere. Spherical harmonic functions and time harmonic functions are well known solutions of the angular and time components of the two dimensional wave equation plus time, respectively. The solutions appear in McQuarrie [McQuarrie, D. A., *Quantum Chemistry*, University Science Books, Mill Valley, CA, (1983), pp. 206-225]. A constant current function is also a solution of the wave equation. A constant function corresponding to the electron spin function is added to each of the spherical harmonic functions to give the charge (mass) density functions of the electron as a function of time. The integral of a spherical harmonic function over the orbitsphere is zero. The integral of the constant function over the orbitsphere is the total charge (mass) of the electron. These functions comprise the

well known s, p, d, f, etc. electrons or orbitals. In the case that such an electron state arises as an excited state by photon absorption, it is radiative due to a radial dipole term in its current density function since it possesses spacetime Fourier components synchronous with waves traveling at the speed of light as shown in the Instability of the Excited States section of Ref. [1]. (See **Appendix #2** of this Response.)

Eqs. (14-15) of Ref. [58] are well known solutions of the classical wave equation in two dimensions plus time. $Y_\ell^m(\theta,\phi)$ are the spherical harmonic functions with $Y_0^0(\theta,\phi)$ the constant function. The constant charge function corresponds to the spin function with the non constant current function generated by Eqs. (10-11) and shown in Figure 2 of Ref. [58]. The solutions for $\ell \neq 0$ corresponding to charge density waves $Y_\ell^m(\theta,\phi)$ that modulate the constant spin function, $Y_0^0(\theta,\phi)$, are harmonic in space (spherical harmonics), and, in contrast to the spin function, rotate time harmonically at frequency ω_n about the z-axis.

From The INTRODUCTION section of Ref. [1]:

The charge-density functions including the time-function factor are

$\ell = 0$

$$\rho(r,\theta,\phi,t) = \frac{e}{8\pi r^2}[\delta(r-r_n)]\left[Y_0^0(\theta,\phi) + Y_\ell^m(\theta,\phi)\right] \tag{I.17}$$

$\ell \neq 0$

$$\rho(r,\theta,\phi,t) = \frac{e}{4\pi r^2}[\delta(r-r_n)]\left[Y_0^0(\theta,\phi) + \mathrm{Re}\left\{Y_\ell^m(\theta,\phi)e^{i\omega_n t}\right\}\right] \tag{I.18}$$

where $\mathrm{Re}\left\{Y_\ell^m(\theta,\phi)e^{i\omega_n t}\right\} = P_\ell^m(\cos\theta)\cos\left(m\phi + \omega_n' t\right)$ and to keep the form of the spherical harmonic as a traveling wave about the z-axis, $\omega_n' = m\omega_n$.

The spin function of the electron (see Figure 1.1 for the charge function and Figure 1.5A for the current function) corresponds to the nonradiative $n = 1$, $\ell = 0$ state of atomic hydrogen which is well known as an s state or orbital. The constant spin function is modulated by a time and spherical harmonic function as given by Eq. (I.18) and shown in Figure 1.2. The modulation or traveling charge density wave corresponds to an orbital angular momentum in addition to a spin angular momentum. These states are typically referred to as p, d, f, etc. orbitals and correspond to an ℓ quantum number not equal to zero. Application of the condition from Haus [Haus, H. A., "On the radiation from point charges", American Journal of Physics, 54, (1986), pp. 1126-1129] (Eqs, (I.19-I.21)) also predicts nonradiation for a constant spin function modulated by a time and spherically harmonic orbital function. There is acceleration without radiation. (Also see Abbott and

Griffiths and Goedecke [T. A. Abbott and D. J. Griffiths, Am. J. Phys., Vol. 153, No. 12, (1985), pp. 1203-1211; G. Goedecke, Phys. Rev 135B, (1964), p. 281]). Nonradiation is also shown directly via Maxwell's equations in Appendix I: Nonradiation Based on the Electromagnetic Fields and the Poynting Power Vector of Ref. [1]. However, in the case that such a state arises as an excited state by photon absorption, it is radiative due to a radial dipole term in its current density function since it possesses spacetime Fourier transform components synchronous with waves traveling at the speed of light as shown in the Instability of Excited States section of Ref. [1].

As shown in **THE ORBITSPHERE EQUATION OF MOTION FOR $\ell = 0$** section of Ref. [1]:

In the derivation of Eqs. (1.58) and (1.59), the moment of inertia, typically caused by a point particle or a reduced mass, is mr^2. However, for $\ell = 0$, the electron mass and charge are uniformly distributed over the orbitsphere, a two-dimensional, spherical shell. The orbitsphere is *not* analogous to a globe, where $I = \frac{2}{3} mr^2$, spinning about some axis. Each point on the sphere with mass m_i has the same angular velocity (ω_n), the same magnitude of linear velocity (v_n), and the same moment of inertia ($m_i r_n^2$). The motion of each point of the orbitsphere is along a great circle, and the motion of each great circle is correlated with the motion on all other great circles. The magnitude of the velocity is not a function of θ. In contrast, the velocity of a point mass on a spinning globe is a function of θ.

The derivation of the momenta and energies are given in Chp. 1 of Ref. [1]:

ROTATIONAL PARAMETERS OF THE ELECTRON (ANGULAR MOMENTUM, ROTATIONAL ENERGY, AND MOMENT OF INERTIA)

One result of the correlated motion along great circles is that some of the kinetic energy is not counted in the rotational energy. That is, for any spin axis there will be an infinite number of great circles with planes passing through that axis with θ angles other than 90°. All points on any one of these great circles will be moving, but not all of that motion will be part of the rotational energy; only that motion perpendicular to the spin axis will be part of the rotational energy. Thus, the rotational kinetic energy will always be less than the total kinetic energy. Furthermore, the following relationships must hold.

$$E_{rotational} = \frac{1}{2} I\omega^2 \leq \frac{1}{2} m_e v^2 \qquad (1.75)$$

$$I\omega \le \hbar \tag{1.76}$$

$$I \le m_e r^2 \tag{1.77}$$

Furthermore, it is known from the Stern-Gerlach experiment that a beam of silver atoms splits into two components when passed through an inhomogeneous magnetic field. This experiment implies a magnetic moment of one Bohr magneton and an associated angular momentum quantum number of 1/2. Historically, this quantum number is called the spin quantum number, and that designation will be retained. The angular momentum can be thought of arising from a spin component or equivalently an orbital component of the spin. The z-axis projection of the spin angular momentum was derived in the Spin Angular Momentum of the Orbitsphere with $\ell = 0$ section.

$$L_z = I\omega \mathbf{i}_z = \pm\frac{\hbar}{2} \tag{1.78}$$

where ω is given by Eq. (1.55); so,

$\ell = 0$

$$|L_z| = I\frac{\hbar}{m_e r^2} = \frac{\hbar}{2} \tag{1.79}$$

Thus,

$$I_z = I_{spin} = \frac{m_e r_n^2}{2} \tag{1.80}$$

From Eq. (1.51),

$$E_{rotational\ spin} = \frac{1}{2}\left[I_{spin}\omega^2\right] \tag{1.81}$$

From Eqs. (1.55) and (1.80),

$$E_{rotational} = E_{rotational\ spin} = \frac{1}{2}\left[I_{spin}\left(\frac{\hbar}{m_e r_n^2}\right)^2\right] = \frac{1}{2}\left[\frac{m_e r_n^2}{2}\left(\frac{\hbar}{m_e r_n^2}\right)^2\right] = \frac{1}{4}\left[\frac{\hbar^2}{2I_{spin}}\right] \tag{1.82}$$

When $\ell \neq 0$, the spherical harmonic is not a constant and the charge-density function is not uniform over the orbitsphere. Thus, the angular momentum can be thought of arising from a spin component and an orbital component.

Derivation of the Rotational Parameters of the Electron

In the derivation of Eq. (1.59) and its solution for $E_{rotational}$ (Eq. (1.60)), the moment of inertia, I, was assumed by McQuarrie [McQuarrie, D. A., Quantum Chemistry, University Science Books, Mill Valley, CA, (1983), pp. 206-221] to be the moment of inertia of a point particle, mr_n^2. However, the correct equation of the electron is a two dimensional shell with a constant or a constant plus a spherical harmonic angular dependence. In that case, the relationships given by Eqs. (1.75) to (1.77) must hold.

The substitution of NI for I in the rigid rotor problem [McQuarrie, D. A., Quantum

Chemistry, University Science Books, Mill Valley, CA, (1983), pp. 206-221] where N is a constant does not change the form of the previous solution given by Eq. (1.60). However, the result that

$$N = \left[\frac{\ell(\ell+1)}{\ell^2+2\ell+1}\right]^{\frac{1}{2}} < 1 \tag{1.83}$$

derived below gives

$$E_{rotational} = \frac{\hbar^2 \ell(\ell+1)}{2I\left(\ell^2+2\ell+1\right)} \tag{1.84}$$

and gives the moment of inertia of the orbitsphere, $I_{orbital}$, where $\ell \neq 0$ as

$$NI = I_{orbital} = m_e r_n^2 \left[\frac{\ell(\ell+1)}{\left(\ell^2+2\ell+1\right)}\right]^{\frac{1}{2}} \tag{1.85}$$

The solution of Eq. (1.59) for $|\mathbf{L}|$, the magnitude of the orbital angular momentum, is [McQuarrie, D. A., Quantum Chemistry, University Science Books, Mill Valley, CA, (1983), pp. 206-221]

$$|\mathbf{L}| = \hbar\sqrt{\ell(\ell+1)} \tag{1.86}$$

where I of Eq. (1.59) is the moment of inertia of a point charge. It is demonstrated by Eq. (1.57) that the total sum of the magnitudes of the angular momenta of the infinitesimal points of the electron orbitsphere is $\hbar$; therefore, the magnitude of the angular momentum of an electron orbitsphere must be less than $\hbar$, and the moment of inertia must be less than that given by $m_e r_n^2$. For example, the moment of inertia of the uniform spherical shell, I_{RS}, is [Fowles, G. R., Analytical Mechanics, Third Edition, Holt, Rinehart, and Winston, New York, (1977), p. 196]

$$I_{RS} = \frac{2}{3} m r_n^2 \tag{1.87}$$

Thus, Eq. (1.86) must be multiplied by a fraction, $\frac{1}{K}$, to give the correct angular momentum. Given that generally $\mathbf{L}$ is

$$\mathbf{L} = I\omega\mathbf{i}_z \tag{1.88}$$

then

$$I_{orbital}\,\omega\mathbf{i}_z = \hbar\frac{1}{K}\sqrt{\ell(\ell+1)}, \tag{1.89}$$

where ω is given by Eq. (1.55). The orbital moment of inertia, $I_{orbital}$, is

$$I_{orbital} = m_e r_n^2 \frac{1}{K}\sqrt{\ell(\ell+1)} \tag{1.90}$$

The total kinetic energy, T, of the orbitsphere is

$$T = \frac{1}{2} m_e v_n^2 \tag{1.91}$$

Substitution of Eq. (1.56) gives

$$T = \frac{\hbar^2}{2m_e r_n^2} \tag{1.92}$$

$E_{rotational}$ of the rigid shell is given by Eq. (1.51) with I given by Eq. (1.87). $E_{rotational\ \text{orbital}}$ of the orbitsphere is given by Eq. (1.60) multiplied by the fraction $\frac{1}{K^2}$ so that Eqs. (1.75) to (1.77) hold with $I = m_e r_n^2$.

$$E_{rotational\ \text{orbital}} = \frac{\hbar^2}{2I}\left[\frac{\ell(\ell+1)}{K^2}\right] \tag{1.93}$$

Eq. (1.59) can be expressed in terms of the variable x which is substituted for $\cos\theta$. The resulting function $P(x)$ is called Legendre's equation and is a well-known equation in classical physics. It occurs in a variety of problems that are formulated in spherical coordinates. When the power series method of solution is applied to $P(x)$, the series must be truncated in order that the solutions be finite at $x = \pm 1$. The solution to Legendre's equation given by Eq. (1.60) is the maximum term of a series of solutions corresponding to the m and ℓ values [McQuarrie, D. A., Quantum Chemistry, University Science Books, Mill Valley, CA, (1983), pp. 206-221, Pauling, Linus, Wilson, E., Bright, Introduction to Quantum Mechanics with Applications to Chemistry, McGraw-Hill Book Company, New York, (1935), pp. 118-121]. The rotational energy must be normalized by the total number of states-each corresponding to a set of quantum numbers of the power series solution. As demonstrated in the Excited States of the One Electron Atom (Quantization) section, the quantum numbers of the excited states are

$$n = 2,3,4,\ldots$$
$$\ell = 1,2,\ldots,n-1$$
$$m = -\ell, -\ell+1,\ldots,0,\ldots,+\ell$$

In the case of an orbitsphere excited state, each rotational state solution of Eq. (1.59) (Legendre's equation) corresponds to a multipole moment of the charge-density function (Eq. (1.65)). $E_{rotational\ \text{orbital}}$ is normalized by N, the total number of multipole moments. N, the total number of multipole moments where each corresponds to an ℓ and m_ℓ quantum number of an energy level corresponding to a principal quantum number of n is

$$N = \sum_{\ell=0}^{n-1} \sum_{m_\ell=-\ell}^{+\ell} 1 = \sum_{\ell=0}^{n-1} 2\ell+1 = n^2 = (\ell+1)^2 = \ell^2 + 2\ell + 1 \tag{1.94}$$

Thus, K^2 is equal to N given by Eq. (1.94). Substitution of Eq. (1.94) into Eq. (1.93) gives

$$E_{rotational\ \text{orbital}} = \frac{\hbar^2}{2I}\left[\frac{\ell(\ell+1)}{\ell^2+2\ell+1}\right] = \frac{\hbar^2}{2I}\left[\frac{\ell}{\ell+1}\right] \tag{1.95}$$

Substitution of Eq. (1.94) into Eq. (1.90) gives the orbital moment of inertia.

$$I_{orbital} = m_e r_n^2 \left[\frac{\ell(\ell+1)}{\ell^2+2\ell+1} \right]^{\frac{1}{2}} = m_e r_n^2 \sqrt{\frac{\ell}{\ell+1}} \tag{1.96}$$

In the case of the excited states, the orbitsphere charge-density function for $\ell \neq 0$, Eq. (1.65), is the sum of two functions of equal magnitude. $\mathbf{L}_z$, total is given by the sum of the spin and orbital angular momenta. The principal energy levels of the excited states are split when a magnetic field is applied. The energy shifts due to spin and orbital angular momenta are given in the Spin and Orbital Splitting section.

$\ell \neq 0$

$$L_{z\,total} = L_{z\,spin} + L_{z\,orbital} \tag{1.97}$$

Similarly, the orbital rotational energy arises from a spin function (spin angular momentum) modulated by a spherical harmonic angular function (orbital angular momentum). The time-averaged orbital rotational energy is zero; the magnitude is given by Eq. (1.95); the rotational energy due to spin is given by Eq. (1.82); the total kinetic energy is given by Eq. (1.92).

$$\langle E_{rotational\ orbital} \rangle = 0 \tag{1.98}$$

The demonstration that the modulated orbitsphere solutions are solutions of the wave equation appears in Box 1.1.

The Applicant's angular functions are solutions of the wave equation as shown in BOX 1.1. DERIVATION OF THE ROTATIONAL PARAMETERS OF THE ELECTRON FROM A SPECIAL CASE OF THE WAVE EQUATION—THE RIGID ROTOR EQUATION of Ref. [1].

Applicant's physical solutions eliminate the fatal flaws of QM. Spin is given; whereas, the SE fail to give spin. Applicant's solutions are further stable with respect to radiation as shown in Appendix I of Ref. [1] and in Ref. [58]; whereas, those of QM are not as discussed previously[137]. The test of a theory is that it agrees with physics, not mathematical postulates.

Applicant's response to Examiner's Ref. [11] posted to the same hydrino study group in Sept. (2001) is attached. The cited author P. Zimmerman has a publicly stated intention to "stab a knife into the heart of CQM" which is improper behavior for a scientist. Furthermore, his competence is questionable given his many outlandish statements and positions posted to this group such as "conservation of energy as a formal concept is quite modern" [P. Zimmerman post of 5/21/03]. Or his lack of understanding for the basic concepts of Maxwell's equations as summarized in R. Mills post on 5/23/03. The Examiner shows bias and poor judgment in citing material posted to an internet chat group from an arch cynic with a

---

[137] Reference Nos. Chp. 35 of Ref. 1, 5, 17, 21, 22, 53, 58, 80, 94

significant vested interest that he is openly protecting. The material is not peer reviewed which sets a double standard by requiring that the Applicant's work is.

6. Response to Examiner's Argument that "Applicant misunderstands the Uncertainty Principle in QM"

It would be fair to the Applicant if the USPTO assigned an Examiner skilled in Maxwell's equations to this case rather that one biased by QM. The Examiner's condescending statement about the HUP reveals his bias as a QM aficionado due to a significant conflict of interest—specifically defending a paradigm in which the Examiner has based his entire career and livelihood. Professors have taught many outdated concepts and theories that were eventually replaced. Theories advance over time, and the truth is that no one understands QM or the HUP as discussed by Laloë [F. Laloë, Do we really understand quantum mechanics? Strange correlations, paradoxes, and theorems, Am. J. Phys. 69 (6), June 2001, 655-701]. It makes no sense since it depends on Ψ which can not be based in realty as discussed in Ref. [17] and the references therein as well as others[138].

The Examiner is confused about mathematics versus physics. The spherical harmonic functions significantly predate QM. The existence of spherical harmonic functions is not limited to or the equivalent of SE probability-waves. A spherical harmonic distribution of charge that moves as a wave, time harmonically on a spherical surface is a real physical problem that is distinct from the purely mathematical probability-waves envisioned by the Examiner. The Applicant correctly applies solutions of the Laplacian, the wave equation, and Maxwell's equations.

The Examiner's strained argument to avoid a situation wherein $\delta\theta \rightarrow \infty$ further shows the internal inconsistency of QM. An excited state has a single angular momentum and orbital splitting energy for a given ℓ quantum number, not multiple as required by QM in order not to violate the HUP.

The Examiner's requirement of taking linear combinations of eigenfunctions to result in a "wavefunction" solution is internally inconsistent with Examiner's point of **# 5(repeated)** wherein the Examiner claims the SE spherical harmonic solutions can not be linear combinations since the Kroenecker delta is not obtained as required since the probability-density functions must be squared.

The Examiner's use of the HUP further demonstrates that its use in QM is totally internally inconsistent as shown by Feynman's failed attempt to use it to provide a QM basis for

---

[138] Reference Nos. 1, 5, 53, 58, 80, 94

the stability of the hydrogen atom as discussed in Ref. [80]. Other failures of the HUP are discussed in Ref. [80]. For example, it is taught that the HUP is the basis of the wave-particle duality, but that has been proven wrong the an experiment by Durr et. al. [S. Durr, T. Nonn, G. Rempe, Nature, September 3, (1998), Vol. 395, pp. 33-37] as discussed previously[139]. It predicts perpetual motion as discussed in [P. F. Schewe and B. Stein, Physic News Update, The American Institute of Physics Bulletin of Physics News, Number 494, July 17, (2000), A. Allahverdyan and T. Nieuwenhuizen, Phys. Rev. Lett., Vol. 85, No. 9, August 28, (2000), pp. 1799-1802] and Ref. [17]. It predicts zero point energy of the vacuum which gives rise to the inescapable prediction of an essentially infinite cosmological constant as discussed previously in Appendix II of Ref. [1] and also Ref. [17]. It also predicts zero point vibration which is not experimentally observed as discussed in Ref. [94]. Other data with far-fetched interpretations based on the HUP such the existence of the same $^{9}Be^{+}$ ion in two places at once, supercurrents flowing in opposite directions at once, and spooky actions at a distance are also explained by first principle laws which demonstrate that the HUP is not a physical principle as discussed in the Foreword section and Chp 37 of Ref. [1] as well as Ref. [80]. Rather it is a misinterpretation of applying the Schwartz Inequality to the wavefunction interpreted as a probability wave [McQuarrie, D. A., *Quantum Chemistry*, University Science Books, Mill Valley, CA, (1983), pp. 135-140]. The mathematical result shows that the electron can have a continuum of momenta and positions in the n=1 state with a continuum of energies simultaneously which can not be physical. This result is independent of error introduced by measurement.

7. Response to Examiner's Argument that "Applicant concept of electron spin is incorrect"

As discussed in **#5** of this Response, the electron is an extended particle, not a point as confused by the Examiner. QM has to rely on a postulated solution since spin (current) in one dimension is nonphysical and nonsensical. CQM solves spin and orbital angular momenta and energies physically. The charge and current density function are solved from Maxwell's equations, not the SE or the Dirac equation. The for p, d, f, etc. orbitals, the spherical harmonic angular functions are charge-density waves on the surface of a spherical shell that modulate the constant, uniform-charged spin function. The time-average rotational energy of the former is zero as given by Eq. (1.98) of Ref. [1]. The rotational energy of the spin function is given by Eq. (1.82) of Ref. [1].

---

[139] Reference Nos. 17, 80, 94

The Applicant's solution for spin is correct in that it agrees, to the limit of experimental observation, with all of the parameters measured on spin and it consistent with all physical laws including Maxwell's equations and special relativity. Applicant does not follow the approach of QM postulates and associated probability waves using an improper wave equation. The SE equation misses spin entirely and the Dirac equation gives rise to many problems as discussed previously[140], and also by others such as Weisskopf [V. F. Weisskopf, Reviews of Modern Physics, Vol. 21, No. 2, (1949), pp. 305-315] discussed in #1 of this Response. The Examiner confuses the mathematical postulates of QM with the Applicant's physical solution.

The electron has a measured magnetic field and corresponding magnetic moment of a Bohr magneton. The field requires a unique current according to Maxwell's equations. The solution is derived from Maxwell's equation in Ref. [58] and Chp 1 of Ref. [1]. where several boundary conditions must be and are satisfied. In the case of the spin function, there is no rotation about an axis. Rather the current corresponding to spin is generated by a basis set of two orthogonal great circles current loops according to Eqs. (10-11) and is shown in Figure 2 of Ref. [58]. In this case, the velocity is the same for each point. More explicitly, the orbitsphere comprises a two-dimensional spherical shell of moving charge. The corresponding current pattern of the orbitsphere comprises an infinite series of correlated orthogonal great circle current loops. The current pattern (shown in Figure 2 of Ref. [58]) is generated over the surface by two orthogonal sets of an infinite series of nested rotations of two orthogonal great circle current loops where the coordinate axes rotate with the two orthogonal great circles. Each infinitesimal rotation of the infinite series is about the new x-axis and new y-axis which results from the preceding such rotation. For each of the two sets of nested rotations, the angular sum of the rotations about each rotating x-axis and y-axis totals $\sqrt{2}\pi$ radians. The current pattern gives rise to the phenomenon corresponding to the spin quantum number.

From Chp. 1 of Ref. [1]:

The Stern Gerlach experiment demonstrates that the magnetic moment of the electron can only be parallel or antiparallel to an applied magnetic field. In spherical coordinates, this implies a spin quantum number of 1/2 corresponding to an angular momentum on the z-axis of $\frac{\hbar}{2}$. However, the Zeeman splitting energy corresponds to a magnetic moment of μ_B and implies an electron angular momentum on the z-axis of $\hbar$—twice that given by Eq. (1.68-1.71) of Ref. [1].

The orbitsphere with $\ell = 0$ is a shell of negative charge current comprising correlated

---

[140] Reference Nos. 1, 5, 17, 21, 22, 53, 58, 80, 94

charge motion along great circles. The superposition of the vector projection of the orbitsphere angular momentum on the z-axis is $\frac{\hbar}{2}$ with an orthogonal component of $\frac{\hbar}{4}$. As shown in the Orbitsphere Equation of Motion for $\ell = 0$ section of Ref. [1], the application of a magnetic field to the orbitsphere gives rise to a precessing angular momentum vector $\mathbf{S}$ directed from the origin of the orbitsphere at an angle of $\theta = \frac{\pi}{3}$ relative to the applied magnetic field. The precession of $\mathbf{S}$ with an angular momentum of $\hbar$ forms a cone in the nonrotating laboratory frame to give a perpendicular projection of $\mathbf{S}_\perp = \pm\sqrt{\frac{3}{4}}\hbar$ (Eq. (1.74a) of Ref. [1]) and a projection onto the axis of the applied magnetic field of $\mathbf{S}_\parallel = \pm\frac{\hbar}{2}$ (Eq. (1.74b) of Ref. [1]). The superposition of the $\frac{\hbar}{2}$ z-axis component of the orbitsphere angular momentum and the $\frac{\hbar}{2}$ z-axis component of $\mathbf{S}$ gives $\hbar$ corresponding to the observed magnetostatic electron magnetic moment of a Bohr magneton.

In summary:

STERN-GERLACH EXPERIMENT

The Stern-Gerlach experiment implies a magnetic moment of one Bohr magneton and an associated angular momentum quantum number of 1/2 ($s = \frac{1}{2}$; $m_s = \pm\frac{1}{2}$). The superposition of the vector projection of the orbitsphere angular momentum on the z-axis is $\frac{\hbar}{2}$ with an orthogonal component of $\frac{\hbar}{4}$. Excitation of a resonant Larmor precession gives rise to $\hbar$ on an axis $\mathbf{S}$ that precesses about the z-axis called the spin axis at the Larmor frequency at an angle of $\theta = \frac{\pi}{3}$ to give a perpendicular projection of

$$\mathbf{S}_\perp = \hbar \sin\frac{\pi}{3} = \pm\sqrt{\frac{3}{4}}\hbar\,\mathbf{i}_{Y_R}$$

and a projection onto the axis of the applied magnetic field of

$$\mathbf{S}_\parallel = \pm\hbar\cos\frac{\pi}{3} = \pm\frac{\hbar}{2}\,\mathbf{i}_{Z_R}$$

The superposition of the $\frac{\hbar}{2}$ z-axis component of the orbitsphere angular momentum and the $\frac{\hbar}{2}$ z-axis component of $\mathbf{S}$ gives $\hbar$ corresponding to the observed electron magnetic moment of a Bohr magneton, μ_B.

The observed electron parameters are explained physically. Classical laws give 1.) a gyromagnetic ratio of $\frac{e}{2m}$, 2.) a Larmor precession frequency of $\frac{e\mathbf{B}}{2m}$, 3.) the Stern-Gerlach experimental result of quantization of the angular momentum that implies a spin quantum number of 1/2 corresponding to an angular momentum of $\frac{\hbar}{2}$ on the z-axis, and 4.) the observed Zeeman splitting due to a magnetic moment of a Bohr magneton $\mu_B = \frac{e\hbar}{2m_e}$ corresponding to an angular momentum of $\hbar$ on the z-axis. Furthermore, the solution is relativistically invariant as shown in the Special Relativistic Correction to the Ionization Energies section. Dirac originally attempted to solve the bound electron physically with stability with respect to radiation according to Maxwell's equations with the further constraints that it was relativistically invariant and gave rise to electron spin [P. Pearle, Foundations of Physics, "Absence of radiationless motions of relativistically rigid classical electron", Vol. 7, Nos. 11/12, (1977), pp. 931-945]. He was unsuccessful and resorted to the current mathematical probability-wave model that has many problems as discussed in Appendix II: Quantum Electrodynamics (QED) is Purely Mathematical and Has No Basis in Reality of Ref. [1].

The g factor is predicted in the g Factor section of Ref. [1]. It is given in a closed form equation (Eq. (1.192)) that contains the fine structure constant only. The calculated g/2=1.001 159 652 137 (Eq. (1.204) of Ref. [1]). The experimental g/2=1.001 159 652 188 (Eq. (1.205) of Ref. [1]).

The *postulated* QED theory of $\frac{g}{2}$ is based on the determination of the terms of a *postulated* power series in α/π where each *postulated* virtual particle is a source of *postulated* vacuum polarization that gives rise to a *postulated* term. The algorithm involves scores of *postulated* Feynman diagrams corresponding to thousands of matrices with thousands of integrations per matrix requiring decades to reach a consensus on the "appropriate" *postulated* algorithm to remove the intrinsic infinities. The remarkable agreement between Eqs. (1.204) and (1.205) demonstrates that $\frac{g}{2}$ may be derived in closed form from Maxwell's equations in a simple straightforward manner that yields a result with eleven figure agreement with experiment—the limit of the experimental capability of the measurement of the fundamental constants that determine α. In Appendix II: Quantum Electrodynamics is Purely Mathematical and Has No Basis in Reality of Ref. [1], the Maxwellian result is contrasted with the QED algorithm of invoking virtual particles, zero point fluctuations of the vacuum, and negative energy states of the vacuum. Rather than an infinity of radically different QED models, an essential feature is that *Maxwellian solutions are unique.*

Regarding Examiner's statement regarding Applicant's QM allegations, the SE (conventional QM) is not relativistically (Lorentz-) covariant as correctly repeated alleged by the Applicant. Ironically, Dirac originally attempted to solve the bound electron physically with stability with respect to radiation according to Maxwell's equations with the further constraints that it was relativistically invariant and gave rise to electron spin [P. Pearle, Foundations of Physics, "Absence of radiationless motions of relativistically rigid classical electron", Vol. 7, Nos. 11/12, (1977), pp. 931-945.]. He was unsuccessful and resorted to the current mathematical-probability-wave model that has many problems as discussed in Appendix II: Quantum Electrodynamics (QED) is Purely Mathematical and Has No Basis in Reality of Ref. [1]. From Weisskopf [V. F. Weisskopf, Reviews of Modern Physics, Vol. 21, No. 2, (1949), pp. 305-315], "Dirac's quantum electrodynamics gave a more consistent derivation of the results of the correspondence principle, but it also brought about a number of new and serious difficulties." Quantum electrodynamics; 1.) does not explain nonradiation of bound electrons; 2.) contains an internal inconsistency with special relativity regarding the classical electron radius—the electron mass corresponding to its electric energy is infinite; 3.) it admits solutions of negative rest mass and negative kinetic energy; 4.) the interaction of the electron with the predicted zero-point field fluctuations leads to infinite kinetic energy and infinite electron mass; 5.) Dirac used the unacceptable states of negative mass for the description of the vacuum; yet, infinities still arise.

Dirac's postulated relativistic wave equation also leads to the inescapable results that it gives rise to the Klein Paradox and a cosmological constant that is at least 120 orders of magnitude larger than the best observational limit as discussed in Chp. 1, Appendix II of Ref. [1] and previously[141].

8. Response to Examiner's Argument "Applicant's hydrogen wave function is seriously flawed"

The Examiner again incorrectly analyzes Applicant's theory from the perspective of QM. Applicants theory is not based on the SE or Dirac equation. Applicant does not follow the approach of QM postulates and associated probability waves using an improper wave equation. QM gives no basis for the stability of the n=1 state and the instability of excited states as discussed previously[142]. It does not obey Maxwell's equations. In contrast, in Chp. 2 of Ref. [1], CQM gives closed form solutions for the resonant photons and excited state

---

[141] Reference Nos. 5, 17, 21, 33, 53, 58, 80, 94

[142] Reference Nos. 1, 80

electron functions. The free space photon also comprises a radial Dirac delta function, and the angular momentum of the photon given by $\mathbf{m} = \frac{1}{8\pi}\mathrm{Re}[\mathbf{r} \times (\mathbf{E} \times \mathbf{B}^*)] = \hbar$ in the Photon section is conserved for the solutions for the resonant photons and excited state electron functions. It can be demonstrated that the resonance condition between these frequencies is to be satisfied in order to have a net change of the energy field [Mizushima, M., Quantum Mechanics of Atomic Spectra and Atomic Structure, W.A. Benjamin, Inc., New York, (1970), p.17]. In the present case, the correspondence principle holds. That is the change in angular frequency of the electron is equal to the angular frequency of the resonant photon that excites the resonator cavity mode corresponding to the transition, and the energy is given by Planck's equation. The predicted energies, Lamb shift, fine structure splitting, hyperfine structure, resonant line shape, line width, selection rules, etc. are in agreement with observation.

Of course transitions with $\Delta n \neq 0$ are allowed based on Eq. (2.42) of Ref. [1] where excited states are radiative according to Maxwell's equations as given in the Instability of Excited States section of Ref. [1] and the transition probabilities are given by Eq. (2.44) of Ref. [1] which depends on the radius. Furthermore, it is well known that the Stark effect is solved classically.

9. Response to Examiner's Argument that "Applicant's application of Special Relativity theory is incorrect"

It was shown in the Special Relativistic Correction to the Ionization Energies section of Ref. [1] that the electron's motion is tangential to the radius; thus, the electron radius is Lorentzian invariant. That is, for the case that k is the lightlike k^0, with $k = \omega_n / c$, r_n is invariant. It was also shown that this condition determines that the electron's angular momentum of $\hbar$, $\frac{e}{m_e}$ of Eq. (1.99) of Ref. [1], and the electron's magnetic moment of a Bohr magneton μ_B are invariant. In the lab frame, the effect of the relativistic length contraction and time dilation for constant spherical motion is a change in the angle of motion with a corresponding decrease in the electron wavelength. The angular motion becomes projected onto the radial axis which contracts, and the extent of the decrease in the electron wavelength and radius due to the electron motion in the laboratory inertial frame are given by

$$\lambda = 2\pi r' \sqrt{1-\left(\frac{v}{c}\right)^2}\sin\left[\frac{\pi}{2}\left(1-\left(\frac{v}{c}\right)^2\right)^{3/2}\right] + r'\cos\left[\frac{\pi}{2}\left(1-\left(\frac{v}{c}\right)^2\right)^{3/2}\right] \quad (1.248)$$

and

$$r = r'\left[\sqrt{1-\left(\frac{v}{c}\right)^2}\,\sin\left[\frac{\pi}{2}\left(1-\left(\frac{v}{c}\right)^2\right)^{3/2}\right]+\frac{1}{2\pi}\cos\left[\frac{\pi}{2}\left(1-\left(\frac{v}{c}\right)^2\right)^{3/2}\right]\right] \tag{1.249}$$

respectively. Then, the relativist factor γ^* is

$$\gamma^* = \frac{2\pi}{2\pi\sqrt{1-\left(\frac{v}{c}\right)^2}\,\sin\left[\frac{\pi}{2}\left(1-\left(\frac{v}{c}\right)^2\right)^{3/2}\right]+\cos\left[\frac{\pi}{2}\left(1-\left(\frac{v}{c}\right)^2\right)^{3/2}\right]} \tag{1.250}$$

where the velocity is given by Eq. (1.56) of Ref. [1] with the radius given by Eq. (1.223) [1].

Plots of ratio of the radii from Eq. (1.249) of Ref. [1] and the correction to the ionization energy γ^* (Eq. (1.250) of Ref. [1]) as a function of the electron velocity v relative to the speed of light c are given in Figures 1.13 and 1.14, respectively.

Figure 1.13. The normalized radius as a function of v/c due to relativistic contraction.

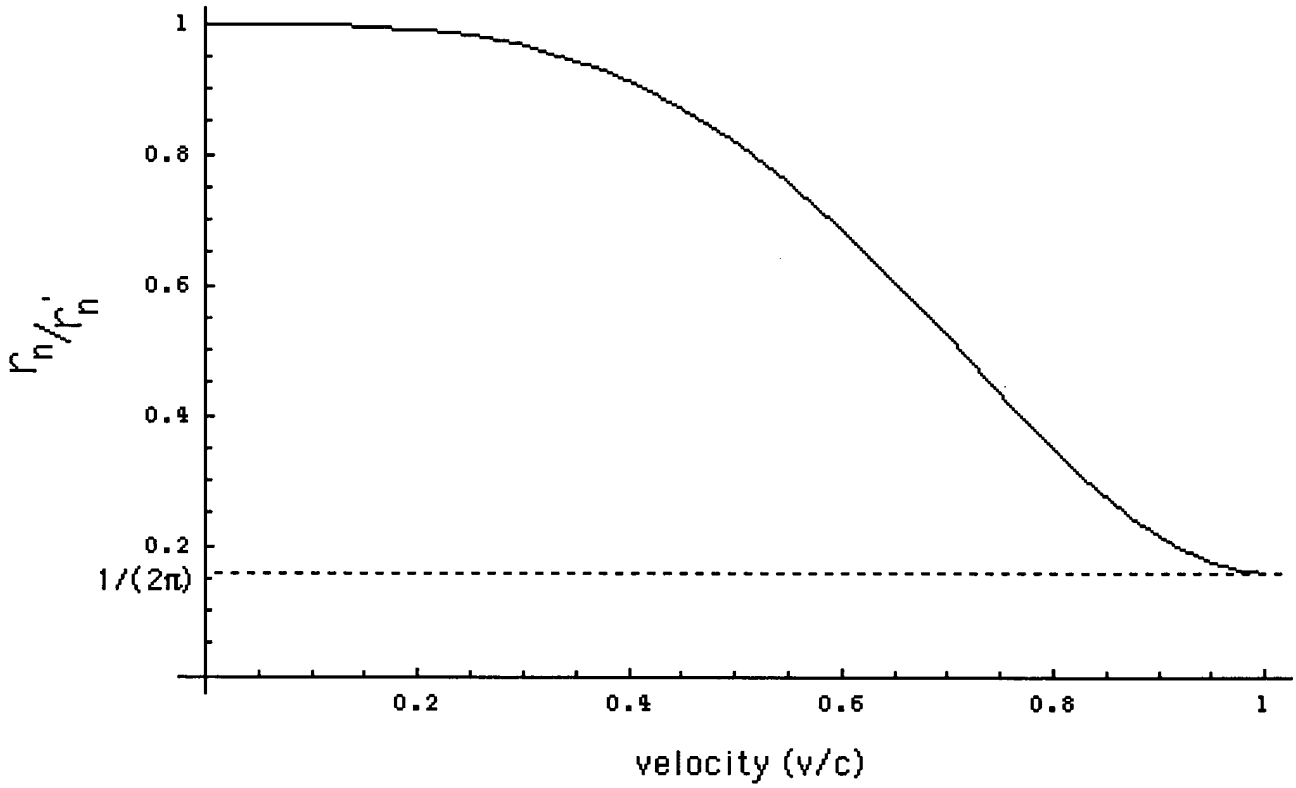

Figure 1.14. The relativistic correction to the one-atom-electron ionization energies as a function of v/c due to relativistic contraction.

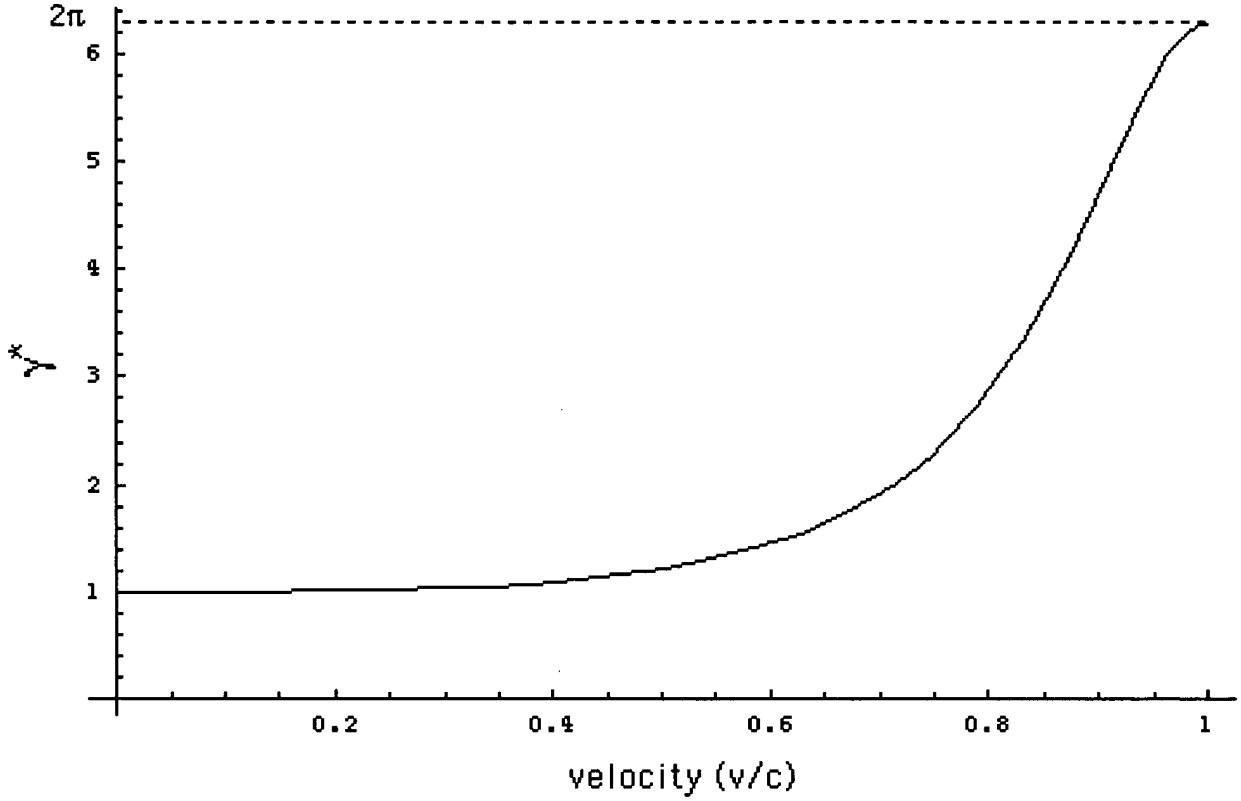

The relativistically corrected one electron ionization energies given by the product of Eqs. (1.233) and (1.250) is

$$E_{ele} = -\gamma^* \frac{Z^2 e^2}{8\pi\varepsilon_o a_0} \frac{\mu}{m_e} = -\gamma^* \frac{\mu}{m_e} Z^2 X 2.1799 X 10^{-18} J = -\gamma^* \frac{\mu}{m_e} Z^2 X 13.606 eV \qquad (1.251)$$

where the reduced mass term μ_e corresponds to the electron-nucleus relativistic correction and is only given by Eq. (1.224) for the hydrogen atom where $Z = 1$. These energies are plotted in Figure 1.15 and are given in Table 1.4.

Figure 1.15. The relativistically corrected one-electron-atom ioinzation energies as a function of the nuclear charge Z.

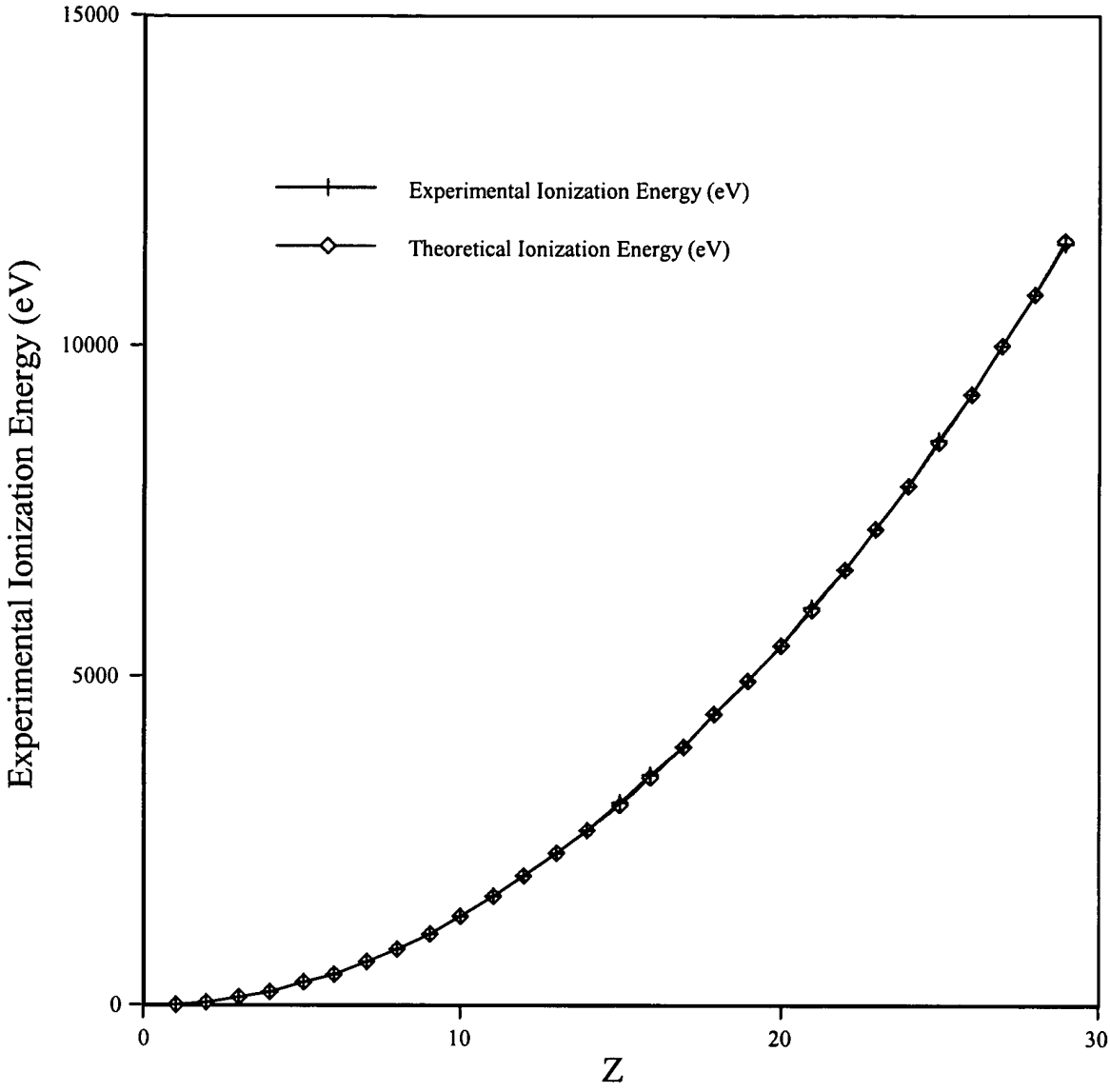

Table 1.4. Relativistically corrected ionization energies for some one-electron atoms.

One e Atom	Z	γ^* Eq. (1.250)	Theoretical Ionization Energies (eV) Eq. (1.251)	Experimental Ionization Energies[a] (eV)	Relative Difference between Experimental and Calculated
H	1	1.000007	13.59849	13.59844	0.00000
He^{+}	2	1.000027	54.40986	54.41778	0.00015
Li^{2+}	3	1.000061	122.43743	122.45429	0.00014
Be^{3+}	4	1.000109	217.68689	217.71865	0.00015
B^{4+}	5	1.000172	340.16647	340.2258	0.00017
C^{5+}	6	1.000251	489.88727	489.99334	0.00022
N^{6+}	7	1.000347	666.86361	667.046	0.00027
O^{7+}	8	1.000461	871.11351	871.4101	0.00034
F^{8+}	9	1.000595	1102.65919	1103.1176	0.00042
Ne^{9+}	10	1.000751	1361.52774	1362.1995	0.00049
Na^{10+}	11	1.000930	1647.75175	1648.702	0.00058
Mg^{11+}	12	1.001135	1961.37017	1962.665	0.00066
Al^{12+}	13	1.001368	2302.42910	2304.141	0.00074
Si^{13+}	14	1.001631	2670.98273	2673.182	0.00082
P^{14+}	15	1.001927	3067.09439	3069.842	0.00090
S^{15+}	16	1.002260	3490.83760	3494.1892	0.00096
Cl^{16+}	17	1.002631	3942.29722	3946.296	0.00101
Ar^{17+}	18	1.003045	4421.57073	4426.2296	0.00105
K^{18+}	19	1.003505	4928.76949	4934.046	0.00107
Ca^{19+}	20	1.004014	5464.02015	5469.864	0.00107
Sc^{20+}	21	1.004577	6027.46611	6033.712	0.00104
Ti^{21+}	22	1.005197	6619.26901	6625.82	0.00099
V^{22+}	23	1.005879	7239.61041	7246.12	0.00090
Cr^{23+}	24	1.006626	7888.69338	7894.81	0.00078
Mn^{24+}	25	1.007444	8566.74431	8571.94	0.00061
Fe^{25+}	26	1.008338	9274.01477	9277.69	0.00040
Co^{26+}	27	1.009311	10010.78335	10012.12	0.00013
Ni^{27+}	28	1.010370	10777.35772	10775.4	-0.00018
Cu^{28+}	29	1.011520	11574.07668	11567.617	-0.00056

[a] From theoretical calculations, interpolation of H isoelectronic and Rydberg series, and experimental data [C. E. Moore, "Ionization Potentials and Ionization Limits Derived from the Analyses of Optical Spectra, Nat. Stand. Ref. Data Ser.-Nat. Bur. Stand. (U.S.), No. 34, 1970; David R. Linde, *CRC Handbook of Chemistry and Physics*, 79 th Edition, CRC Press, Boca Raton, Florida, (1998-9), p. 10-175 to p. 10-177].

The agreement between the experimental and calculated values of Table 1.4 is well within the experimental capability of the spectroscopic determinations including the values at large Z which relies on X-ray spectroscopy. In this case, the experimental capability is three to

four significant figures which is consistent with the last column. The hydrogen atom isoelectronic series is given in Table 1.4 [C. E. Moore, "Ionization Potentials and Ionization Limits Derived from the Analyses of Optical Spectra, Nat. Stand. Ref. Data Ser.-Nat. Bur. Stand. (U.S.), No. 34, 1970; David R. Linde, *CRC Handbook of Chemistry and Physics*, 79 th Edition, CRC Press, Boca Raton, Florida, (1998-9), p. 10-175 to p. 10-177] to much higher precision than the capability of X-ray spectroscopy, but these values are based on theoretical and interpolation techniques rather than data alone. Ionization energies are difficult to determine since the cut-off of the Rydberg series of lines at the ionization energy is often not observed, and the ionization energy must be determined from theoretical calculations, interpolation of H isoelectronic and Rydberg series, as well as direct experimental data.

Similarly, the relativistic ionization energies for two and three electron atoms are given in the Two-Electron Atom and Three-Electron Atom sections of Ref. [1], respectively. It is impossible to use QM to solve such problems in closed equations derived from first principles that contain fundamental constants only.

Applicant's theory is further demonstrated to be in agreement with special relativity based on the success of the predictions for the electron g factor and the fine structure of the hydrogen atom summarized *infra*.

ELECTRON g FACTOR

From Chp. 1 of Ref. [1]:

In contrast to the QM and QED cases (See Appendix II: Quantum Electrodynamics is Purely Mathematical and Has No Basis in Reality), the fourth quantum number arises naturally in CQM as derived in the Electron g Factor section. The Stern-Gerlach experiment implies a magnetic moment of one Bohr magneton and an associated angular momentum quantum number of 1/2. Historically, this quantum number is called the spin quantum number, s ($s = \frac{1}{2}$; $m_s = \pm\frac{1}{2}$). Conservation of angular momentum of the orbitsphere permits a discrete change of its "kinetic angular momentum" ($\mathbf{r} \times m\mathbf{v}$) with respect to the field of $\frac{\hbar}{2}$, and concomitantly the "potential angular momentum" ($\mathbf{r} \times e\mathbf{A}$) must change by $-\frac{\hbar}{2}$. The flux change, ϕ, of the orbitsphere for $r < r_n$ is determined as follows:

$$\Delta\mathbf{L} = \frac{\hbar}{2} - \mathbf{r} \times e\mathbf{A} \tag{I.9}$$

$$= \left[\frac{\hbar}{2} - \frac{e2\pi rA}{2\pi}\right]\hat{z} \tag{I.10}$$

$$= \left[\frac{\hbar}{2} - \frac{e\phi}{2\pi}\right]\hat{z} \tag{I.11}$$

In order that the change of angular momentum, $\Delta\mathbf{L}$, equals zero, ϕ must be $\Phi_0 = \frac{h}{2e}$, the magnetic flux quantum. Thus, to conserve angular momentum in the presence of an applied magnetic field, the orbitsphere magnetic moment can be parallel or antiparallel to an applied field as observed with the Stern-Gerlach experiment, and the flip between orientations is accompanied by the "capture" of the magnetic flux quantum by the orbitsphere. During the spin-flip transition, power must be conserved. Power flow is governed by the Poynting power theorem,

$$\nabla \bullet (\mathbf{E} \times \mathbf{H}) = -\frac{\partial}{\partial t}\left[\frac{1}{2}\mu_o \mathbf{H} \bullet \mathbf{H}\right] - \frac{\partial}{\partial t}\left[\frac{1}{2}\varepsilon_o \mathbf{E} \bullet \mathbf{E}\right] - \mathbf{J} \bullet \mathbf{E} \tag{I.12}$$

Eq. (I.13) derived in the Electron g Factor section gives the total energy of the flip transition which is the sum of the energy of reorientation of the magnetic moment (1st term), the magnetic energy (2nd term), the electric energy (3rd term), and the dissipated energy of a fluxon treading the orbitsphere (4th term), respectively.

$$\Delta E_{mag}^{spin} = 2\left(1 + \frac{\alpha}{2\pi} + \frac{2}{3}\alpha^2\left(\frac{\alpha}{2\pi}\right) - \frac{4}{3}\left(\frac{\alpha}{2\pi}\right)^2\right)\mu_B B \tag{I.13}$$

$$\Delta E_{mag}^{spin} = g\mu_B B \tag{I.14}$$

The spin-flip transition can be considered as involving a magnetic moment of g times that of a Bohr magneton. The g factor is redesignated the fluxon g factor as opposed to the anomalous g factor. The calculated value of $\frac{g}{2}$ is

1.001 159 652 137

The experimental value [R. S. Van Dyck, Jr., P. Schwinberg, H. Dehmelt, "New high precision comparison of electron and positron g factors", Phys. Rev. Lett., Vol. 21, (1987), p. 26-29] of $\frac{g}{2}$ is

1.001 159 652 188(4).

SPIN-ORBITAL COUPLING

Due to 1.) the invariance of each of $\frac{e}{m_e}$ of the electron, the electron angular momentum of $\hbar$, and μ_B from the spin angular and orbital angular momentum, 2.) the condition that flux must be linked by the electron orbitsphere in units of the magnetic flux quantum, and 3.) the maximum projection of the spin angular momentum of the electron onto an axis is $\sqrt{\frac{3}{4}}\hbar$, the magnetic energy term of the electron g-factor gives the spin-orbital coupling energy $E_{s/o}$:

$$E_{s/o} = 2\frac{\alpha}{2\pi}\left(\frac{e\hbar}{2m_e}\right)\frac{\mu_0 e\hbar}{2(2\pi m_e)\left(\frac{r}{2\pi}\right)^3}\sqrt{\frac{3}{4}} = \frac{\alpha\pi\mu_0 e^2\hbar^2}{m_e^2 r^3}\sqrt{\frac{3}{4}} \tag{2.91}$$

For $n = 2$, the radius is $r = 2a_0$, and the predicted energy difference between the $^2P_{3/2}$ and $^2P_{1/2}$ levels of the hydrogen atom is

$$E_{s/o} = \frac{\alpha\pi\mu_0 e^2\hbar^2}{8m_e^2 a_0^3}\sqrt{\frac{3}{4}} \tag{2.92}$$

wherein $\ell = 1$. $E_{s/o}$ may be expressed in terms of the mass energy of the electron.

$$E_{s/o} = \frac{\alpha^5(2\pi)^2}{8}m_e c^2\sqrt{\frac{3}{4}} \tag{2.95}$$

The energy called the fine structure splitting is 10,934.3 *MHz*. The $^2P_{3/2}$ and $^2P_{1/2}$ levels are also split by spin-nuclear and orbital-nuclear coupling. The calculated $^2P_{3/2}$—$^2P_{1/2}$ transition frequency including a transition between hyperfine levels is 10,975.7 *MHz*. The large natural widths of the hydrogen $2p$ levels limits the experimental accuracy. The experimental value of the $^2P_{3/2}$—$^2P_{1/2}$ transition frequency is 10,969.1 *MHz*.

$\frac{e}{m_e}$ is not invariant under QM since the charge is invariant, but the mass is not; so, there are serious problems in applying special relativity to QM. And, QM has many problems calculating the electron g factor as discussed in # 7 of this Response and in Ref. [1]. Infinities arise from the self fields which require arbitrary renormalization algorithms and the so-called physics involves polarization of the vacuum by virtual particles which is not based in reality.

Regarding the Examiner's position that accelerating charge must give rise to radiation. The Examiner misses the point entirely that Applicant solves for the charge and current-density functions of the electron rather than probability-wave functions. And, the electron is an extended particle, not a point particle as is the case in QM (the QM point particle has many problems including the prediction of infinite fields which are nonphysical and have never been observed). In the case that n=1, the Examiner is incorrectly arguing that there is radiation in the magnetostatic and electrostatic case.

From Appendix I of Ref. [1] where the embedded references correspond to those of Appendix I of Ref. [1]:

THE POYNTING POWER VECTOR

A point charge undergoing periodic motion accelerates and as a consequence radiates according to the Larmor formula:

$$P = \frac{1}{4\pi\varepsilon_0}\frac{2e^2}{3c^3}a^2 \tag{1}$$

where e is the charge, a is its acceleration, ε_0 is the permittivity of free space, and c is the speed of light. Although an accelerated *point* particle radiates, an *extended distribution* modeled as a superposition of accelerating charges does not have to radiate[143]. An ensemble of charges, all oscillating at the same frequency, create a radiation pattern with a number of nodes. The same applies to current patterns in phased array antenna design [43]. It is possible to have an infinite number of charges oscillating in such as way as to cause destructive interference or nodes in all directions. The electromagnetic far field is determined from the current distribution in order to obtain the condition, if it exists, that the electron current distribution given by Eq. (6) must satisfy such that the electron does not radiate.

The charge-density functions of the electron orbitsphere in spherical coordinates plus time are given by Eqs. (1.64-1.65). For $\ell = 0$, $N = \frac{-e}{8\pi r_n^2}$, and the charge-density function is

$$\ell = 0$$

$$\rho(r,\theta,\phi,t) = \frac{e}{8\pi r_n^2}[\delta(r-r_n)]\left[Y_0^0(\theta,\phi) + Y_\ell^m(\theta,\phi)\right] \tag{2}$$

The equipotential, uniform or constant charge-density function (Eq. (1.64) and Eq. (2)) further comprises a current pattern given in the ORBITSPHERE EQUATION OF MOTION FOR $\ell = 0$ section. It also corresponds to the nonradiative $n = 1$, $\ell = 0$ state of atomic hydrogen and to the spin function of the electron. The current-density function is given by multiplying Eq. (2) by the constant angular velocity ω_n. There is acceleration without radiation. In this case, centripetal acceleration. A static charge distribution exists

---

[143] Reference Nos. 1, 11, 15, 41-42

even though each point on the surface is accelerating along a great circle. Haus' condition predicts no radiation for the entire ensemble. The same result is trivially predicted from consideration of the fields and the radiated power. Since the current is not time dependent, the fields are given by

$$\nabla \times \mathbf{H} = \mathbf{J} \tag{3}$$

and

$$\nabla \times \mathbf{E} = 0 \tag{4}$$

which are the electrostatic and magnetostatic cases, respectively, with no radiation.

A summary of the stability derivation for p, d, f, etc.. orbitals based on the Haus condition given in Chp. 1 of Ref. [1] is

Nonradiation Based on the Spacetime Fourier Transform of the Electron Current

Although an accelerated *point* particle radiates, an *extended distribution* modeled as a superposition of accelerating charges does not have to radiate. The spacetime Fourier transform of the current-density function is

$$K(s,\Theta,\Phi,\omega) = 4\pi\omega_n \frac{\sin(2sr_n)}{2sr_n} \otimes 2\pi \sum_{\upsilon=1}^{\infty} \frac{(-1)^{\upsilon-1}(\pi\sin\Theta)^{2(\upsilon-1)}}{(\upsilon-1)!(\upsilon-1)!} \frac{\Gamma\left(\frac{1}{2}\right)\Gamma\left(\upsilon+\frac{1}{2}\right)}{(\pi\cos\Theta)^{2\upsilon+1}2^{\upsilon+1}} \frac{2\upsilon!}{(\upsilon-1)!} s^{-2\upsilon}$$

$$\otimes 2\pi \sum_{\upsilon=1}^{\infty} \frac{(-1)^{\upsilon-1}(\pi\sin\Phi)^{2(\upsilon-1)}}{(\upsilon-1)!(\upsilon-1)!} \frac{\Gamma\left(\frac{1}{2}\right)\Gamma\left(\upsilon+\frac{1}{2}\right)}{(\pi\cos\Phi)^{2\upsilon+1}2^{\upsilon+1}} \frac{2\upsilon!}{(\upsilon-1)!} s^{-2\upsilon} \frac{1}{4\pi} [\delta(\omega-\omega_n)+\delta(\omega+\omega_n)]$$

$$\mathbf{s}_n \bullet \mathbf{v}_n = \mathbf{s}_n \bullet \mathbf{c} = \omega_n$$

The relativistically corrected wavelength is

$$\lambda_n = r_n$$

Spacetime harmonics of $\frac{\omega_n}{c} = k$ or $\frac{\omega_n}{c}\sqrt{\frac{\varepsilon}{\varepsilon_o}}$ for which the Fourier transform of the current-density function is nonzero do not exist. Radiation due to charge motion does not occur in any medium when this condition is met.

Haus, H. A., "On the radiation from point charges", American Journal of Physics, 54, (1986),

pp. 1126-1129.

Abbott, T. A., Griffiths, D. J., Am. J. Phys., Vol. 153, No. 12, (1985), pp. 1203-1211.

G. Goedecke, Phys. Rev 135B, (1964), p. 281.

A summary of the stability derivation based on the Poynting Power Vector given in Chp. 1, Appendix I of Ref. [1] is

Nonradiation Based on the Electron Electromagnetic Fields and the Poynting Power Vector

Although an accelerated *point* particle radiates, an *extended distribution* modeled as a superposition of accelerating charges does not have to radiate. The general multipole field solution to Maxwell's equations in a source-free region of empty space with the assumption of a time dependence $e^{i\omega_n t}$ is

$$\begin{aligned}\mathbf{B} &= \sum_{\ell,m}\left[a_E(\ell,m)f_\ell(kr)\mathbf{X}_{\ell.m} - \frac{i}{k}a_M(\ell,m)\nabla\times g_\ell(kr)\mathbf{X}_{\ell.m}\right]\\ \mathbf{E} &= \sum_{\ell,m}\left[\frac{i}{k}a_E(\ell,m)\nabla\times f_\ell(kr)\mathbf{X}_{\ell.m} + a_M(\ell,m)g_\ell(kr)\mathbf{X}_{\ell.m}\right]\end{aligned} \tag{1}$$

For the electron source current comprising a multipole of order (ℓ,m), the far fields are given by

$$\begin{aligned}\mathbf{B} &= -\frac{i}{k}a_M(\ell,m)\nabla\times g_\ell(kr)\mathbf{X}_{\ell.m}\\ \mathbf{E} &= a_M(\ell,m)g_\ell(kr)\mathbf{X}_{\ell.m}\end{aligned} \tag{2}$$

and the time-averaged power radiated per solid angle $\frac{dP(\ell,m)}{d\Omega}$ is

$$\frac{dP(\ell,m)}{d\Omega} = \frac{c}{8\pi k^2}\left|a_M(\ell,m)\right|^2\left|\mathbf{X}_{\ell.m}\right|^2 \tag{3}$$

where $a_M(\ell,m)$ is

$$a_M(\ell,m) = \frac{-ek^2}{c\sqrt{\ell(\ell+1)}}\frac{\omega_n}{2\pi}Nj_\ell(kr_n)\Theta\sin(mks) \tag{4}$$

In the case that k is the lightlike k^0, then $k = \omega_n/c$, in Eq. (4), and Eqs. (2-3) vanishes for

$$s = vT_n = R = r_n = \lambda_n \tag{5}$$

There is no radiation.

Regarding FN 2. The relativistic correction to the electron radius is derived in the Special Relativistic Correction to the Ionization Energies section of Chp. 1, Ref. [1]. A

summary of the relativistic correction to the electron radius is:

Special Relativistic Correction to the Electron Radius

The relationship between the electron wavelength and its radius is given by

$$2\pi r = \lambda$$

where λ is the de Broglie wavelength.

The distance along each great circle in the direction of instantaneous motion undergoes length contraction and time dilation. Using a phase matching condition, the wavelengths of the electron and laboratory inertial frames are equated, and the corrected radius is given by

$$r_n = r_n'\left[\sqrt{1-\left(\frac{v}{c}\right)^2}\sin\left[\frac{\pi}{2}\left(1-\left(\frac{v}{c}\right)^2\right)^{3/2}\right]+\frac{1}{2\pi}\cos\left[\frac{\pi}{2}\left(1-\left(\frac{v}{c}\right)^2\right)^{3/2}\right]\right]$$

where the electron velocity is given by

$$v_n = \frac{\hbar}{m_e r_n}$$

$\frac{e}{m_e}$ of the electron, the electron angular momentum of $\hbar$, and μ_B are invariant, but the mass and charge densities increase in the laboratory frame due to the relativistically contracted electron radius. As $v \to c$, $r/r' \to \frac{1}{2\pi}$ and $r = \lambda$.

The Applicant agrees with the Examiner that a valid theory of the hydrogen atom can not be correct if it requires that the electron in the nucleus. Thus QM is fatally flawed as discussed in Ref. [17, 80]. A valid theory can not permit the electron to "spiral into the nucleus". However, an inescapable fact of QM is that the wave function solution of the SE requires that **the electron is in the nucleus**[144]. In fact, the electron must exist in the nucleus since the wave function is a maximum there. This is clearly claimed in the literature as discussed by Karplus to explain the spin-nuclear coupling called Fermi contact interaction for example [M. Karplus and R. N. Porter, *Atoms and Molecules an Introduction for Students of*

[144] Reference Nos. 17, 80

Physical Chemistry, The Benjamin/Cummings Publishing Company, Menlo Park, California, (1970), p. 567]. In fact, the probability density function Ψ^2 has a maximum at the nucleus for the n=1 state, and the nucleus has a finite volume. Griffiths gives the time average that the electron is in the nucleus [D. J. Griffiths, *Introduction to Quantum Mechanics*, Prentice-Hall, (1995), Prob. 4.14]. This situation corresponds to infinite energy using Feynman's correct assertion [145] that the Coulomb potential must apply to the interaction of the electron and the nucleus.

Conclusion

Applicant has more than met the burden for the issuance of a patent based on the overwhelming experimental evidence given in the document entitled "**Lower-Energy Hydrogen Experimental Data**," given that CQM works better than QM and is based on physical laws rather than pure mathematics as given and discussed in:

94. R. L. Mills, "The Nature of the Chemical Bond Revisited and an Alternative Maxwellian Approach", J. Phys. D, submitted.
80. R. L. Mills, The Fallacy of Feynman's Argument on the Stability of the Hydrogen Atom According to Quantum Mechanics, Foundations of Physics, submitted.
58. R. L. Mills, "Classical Quantum Mechanics", Physics Essays, submitted.
53. R. Mills, "A Maxwellian Approach to Quantum Mechanics Explains the Nature of Free Electrons in Superfluid Helium", Theoretical Chemistry Accounts, submitted.
22. R. Mills, "The Grand Unified Theory of Classical Quantum Mechanics", Global Foundation, Inc. Orbis Scientiae entitled *The Role of Attractive and Repulsive Gravitational Forces in Cosmic Acceleration of Particles The Origin of the Cosmic Gamma Ray Bursts*, (29th Conference on High Energy Physics and Cosmology Since 1964) Dr. Behram N. Kursunoglu, Chairman, December 14-17, 2000, Lago Mar Resort, Fort Lauderdale, FL, Kluwer Academic/Plenum Publishers, New York, pp. 243-258.
21. R. Mills, "The Grand Unified Theory of Classical Quantum Mechanics", Int. J. Hydrogen Energy, Vol. 27, No. 5, (2002), pp. 565-590.
17. R. Mills, "The Nature of Free Electrons in Superfluid Helium--a Test of Quantum Mechanics and a Basis to Review its Foundations and Make a Comparison to Classical Theory", Int. J. Hydrogen Energy, Vol. 26, No. 10, (2001), pp. 1059-1096.
5. R. Mills, "The Hydrogen Atom Revisited", Int. J. of Hydrogen Energy, Vol. 25, Issue 12,

---

[145] Reference No. 80

December, (2000), pp. 1171-1183.

1. R. Mills, *The Grand Unified Theory of Classical Quantum Mechanics*, September 2001 Edition, BlackLight Power, Inc., Cranbury, New Jersey, Distributed by Amazon.com; July 2003 Edition posted at www.blacklightpower.com.